
**CELLULAR MODELS TO STUDY
APOA-I RELATED AMYLOIDOSIS:
MECHANISM OF ACTION AND
SEARCH FOR SPECIFIC TARGETS**

Rita Del Giudice

Dottorato in Scienze Biotechnologiche – XXV ciclo
Indirizzo Biotechnologie Molecolari e Industriali
Università di Napoli Federico II





**CELLULAR MODELS TO STUDY
APOA-I RELATED AMYLOIDOSIS:
MECHANISM OF ACTION AND
SEARCH FOR SPECIFIC TARGETS**

Rita Del Giudice

Dottoranda: Rita Del Giudice
Relatore: Prof.ssa Renata Piccoli
Coordinatore: Prof. Giovanni Sanna

A mia madre

INDICE

RIASSUNTO	pag. 1
SUMMARY	pag. 7
ABBREVIATIONS	pag. 9
INTRODUCTION	pag. 11
1. Protein misfolding and diseases	pag. 11
2. Structure of amyloid fibrils	pag. 12
3. The fibrillogenic process	pag. 13
4. Apolipoprotein A-I	pag. 15
4.1 ApoA-I and amyloidosis	pag. 15
4.2 Structural and functional features of the fibrillogenic polypeptide [1-93]ApoA-I	pag. 17
AIMS	pag. 23
MATERIALS AND METHODS	pag. 25
1. Materials	pag. 25
2. Expression and isolation of [1-93]ApoA-I	pag. 25
3. Fibrillar aggregates	pag. 25
4. Cloning	pag. 26
5. Cell culture	pag. 26
6. Cell transfection and lysates preparation	pag. 27
7. Western blot analyses	pag. 27
8. Binding assay	pag. 28
9. Cytotoxicity assay	pag. 28
10. Fluorescence studies	pag. 29
11. Protein degradation analyses	pag. 30
12. Analyses of ApoA-I expression and secretion	pag. 30
13. Isolation of the recombinant full-length proteins	pag. 30
14. Co-immunoprecipitation experimental procedure	pag. 31
15. Quantitative RT-PCR (qRT-PCR) analysis of ANG mRNA	pag. 31
16. Nucleolar fraction preparation	pag. 32
17. EB/AO staining of apoptotic cells	pag. 32
RESULTS	pag. 33
1. MECHANICISTIC STUDIES: Membrane interaction, internalization and intracellular pathway of ApoA-I fibrillogenic polypeptide	pag. 33
1.1 [1-93]ApoA-I specifically binds to cardiomyoblasts	pag. 33
1.2 [1-93]ApoA-I endocytosis in cardiomyoblasts	pag. 34

1.2.1 [1-93]ApoA-I internalization pathways	pag. 36
1.3 The intracellular fate of [1-93]ApoA-I: proteasomal and lysosomal degradation	pag. 39
1. 4 Internalization of [1-93]ApoA-I fibrils in cardiomyoblasts	pag. 40
2. STUDIES ON MOLECULAR TARGETS: Search for molecular partners of the fibrillogenic polypeptide [1-93]ApoA-I	pag. 42
2.1 ATP synthase β -chain	pag. 43
2.2 Nicastrin	pag. 43
2.3 Co-immunoprecipitation as a suitable tool to detect proteins complexes	pag. 44
2.4 Localization of ATP synthase β -chain in H9c2 cells and co-localization with [1-93]ApoA-I	pag. 45
2.5 Co-localization of [1-93]ApoA-I and nicastrin	pag. 45
3. STRUCTURE TO FUNCTION RELATIONSHIP STUDIES: Production of recombinant wild-type ApoA-I and its amyloidogenic full-length variant L174S	pag. 47
3.1 Isolation of the recombinant proteins	pag. 49
3.2 Analysis of lipid content	pag. 49
4. STUDIES ON PROTEINS WITH A POTENTIAL ROLE IN AMYLOID DISEASES: Does angiogenin play a role in ApoA-I related amyloidosis?	pag. 51
4.1 Angiogenin and its role in stress response	pag. 51
4.2 ANG and ApoA-I associated amyloidosis	pag. 52
DISCUSSION	pag. 63
1. Studies on the fibrillogenic polypeptide [1-93]ApoA-I	pag. 63
1.1 The definition of the intracellular pathway of the fibrillogenic polypeptide	pag. 63
1.2 Towards the definition of two molecular partners of [1-93]ApoA-I	pag. 65
2. Studies on the full-length ApoA-I pathogenic variants	pag. 67
2.1 A cell model to produce full-length variants	pag. 67
2.2 Effects of endogeneous ApoA-I full-length variants on cell vulnerability to stress and stress response	pag. 68
BIBLIOGRAPHY	pag. 71
LIST OF PUBLICATIONS, COMMUNICATIONS AND RESEARCH ACTIVITY IN SCIENTIFIC INSTITUTIONS ABROAD	pag. 79

RIASSUNTO

Base scientifica del progetto di ricerca.

Le amiloidosi costituiscono un ampio gruppo di patologie di tipo degenerativo che nascono dall'incapacità di alcune proteine, o peptidi, di assumere o di conservare la loro conformazione nativa, ciò che porta alla formazione di aggregati fibrillari altamente ordinati ed elevato contenuto di struttura β . Queste strutture, generalmente descritte come fibre o placche amiloidi, si accumulano in vari tessuti ed organi causandone il progressivo malfunzionamento.

Tra le patologie amiloidi ad elevato impatto sociale si annoverano il morbo di Parkinson, di Alzheimer e le encefalopatie spongiformi.

Diverse forme di amiloidosi sono indotte da mutazioni del gene codificante l'apolipoproteina A-I (ApoA-I). ApoA-I è la componente proteica più abbondante nelle lipoproteine plasmatiche ad alta densità (HDL), le quali svolgono un ruolo molto importante nel trasporto dei lipidi tra gli organi di sintesi (fegato e intestino) e i tessuti periferici. Oltre a possedere un ruolo strutturale, ApoA-I interagisce con specifici recettori di membrana, al fine di mediare l'attivazione degli enzimi coinvolti nel metabolismo dei lipidi, in particolare del colesterolo.

Le amiloidosi ereditarie associate ad ApoA-I, a carattere autosomico dominante, sono causate da specifiche mutazioni del gene codificante la proteina. Le 19 mutazioni del gene di ApoA-I riscontrate finora nei pazienti affetti da amiloidosi sono tutte presenti su un solo allele (eterozigosi). Si ritiene che tali mutazioni, che si presentano come sostituzioni amminoacidiche, delezioni o *frameshift*, alterino la struttura tridimensionale della proteina, favorendone il distacco dalle HDL e aumentando la flessibilità della regione 80-100, che in assenza di lipidi è esposta al solvente. Ciò rende la proteina mutata suscettibile all'attacco di una proteasi, tuttora non identificata, che determina il rilascio di un polipeptide corrispondente alla regione N-terminale della proteina di lunghezza pari a 90-100 residui amminoacidici. Tale polipeptide, altamente destrutturato, tende ad aggregare portando alla formazione di fibrille amiloidi che si accumulano in maniera preferenziale in alcuni organi e tessuti, secondo il tipo di mutazione presente. La sostituzione del residuo di leucina in posizione 174 con una serina determina una grave forma di amiloidosi localizzata soprattutto a livello cardiaco. Il principale costituente delle fibrille amiloidi estratte dal cuore dei pazienti è il polipeptide corrispondente alla regione 1-93 della proteina.

Gli eventi che portano alla formazione del peptide amiloidogenico e il meccanismo attraverso il quale si generano le fibrille amiloidi sono tutt'oggi sconosciuti. La mancanza di un efficiente sistema di produzione del polipeptide fibrillogeno in forma ricombinante ha reso impossibili per molti anni studi strutturali e funzionali volti all'analisi del meccanismo molecolare della patologia. I molteplici tentativi effettuati in diversi laboratori sono falliti presumibilmente sia per l'elevata destrutturazione del polipeptide, che lo rende bersaglio di proteasi endogene, sia per la sua propensione all'aggregazione. Nel laboratorio dove ho svolto il mio lavoro di dottorato è stato messo a punto un sistema per l'espressione e l'isolamento della forma ricombinante del polipeptide amiloidogenico corrispondente alla regione 1-93 della proteina, denominato [1-93]ApoA-I. Il polipeptide ricombinante è risultato avere le stesse caratteristiche della sua controparte naturale estratta dalle fibrille di un cuore trapiantato: come quello isolato *ex vivo*, il polipeptide ricombinante subisce

transizioni conformazionali verso strutture ricche in α -elica e ha elevata propensione all'aggregazione in tipiche fibrille a struttura β . La disponibilità di un sistema sperimentale utile alla produzione ricombinante del polipeptide fibrillogenico ha aperto la strada all'analisi delle basi molecolari delle amiloidosi da ApoA-I.

Il progetto di ricerca.

Il mio progetto di ricerca si propone come obiettivo l'analisi del meccanismo d'azione delle varianti amiloidogeniche di ApoA-I e del suo polipeptide fibrillogenico, nonché l'analisi dei processi cellulari coinvolti nella patologia e l'identificazione di potenziali interattori intracellulari del polipeptide, quali potenziali bersagli per future strategie terapeutiche direzionate.

Il percorso e il destino intracellulare del polipeptide fibrillogenico.

Durante la mia attività di dottorato mi sono occupata dell'analisi del meccanismo di internalizzazione e del percorso intracellulare del polipeptide fibrillogenico [1-93]ApoA-I in cellule cardiache (linea H9c2).

Il percorso intracellulare del polipeptide [1-93]ApoA-I, in confronto con la proteina ApoA-I nativa, è stato analizzato in cardiomioblasti, dal momento che il cuore costituisce uno degli organi in cui si osserva l'accumulo progressivo degli aggregati fibrillari. Studi di legame ci hanno consentito di dimostrare la presenza sulla membrana di cardiomioblasti di siti specifici di legame per il polipeptide [1-93]ApoA-I, con una costante di affinità pari a $5.9 \pm 0.7 \times 10^{-7}$ M. Mediante esperimenti di microscopia in fluorescenza abbiamo dimostrato che il polipeptide fibrillogenico co-localizza in maniera significativa, seppure parzialmente, con il trasportatore ABCA1, presente sulla membrana dei cardiomioblasti. Risultati analoghi sono stati ottenuti per ApoA-I, ciò che è in accordo con dati recenti che indicano che, nonostante l'associazione parziale della proteina con ABCA1, tale interazione è essenziale per l'internalizzazione della proteina. In seguito al legame con siti specifici sulla membrana cellulare, il polipeptide [1-93]ApoA-I è internalizzato nelle cellule cardiache mediante i processi di endocitosi clatrina-dipendente ed endocitosi mediata dai *lipid rafts*, mentre sembra essere escluso un coinvolgimento della macropinosi. Tali vie di internalizzazione sono solo parzialmente coincidenti con quelle seguite dalla proteina nativa ApoA-I, dal momento che quest'ultima è internalizzata mediante endocitosi clatrina-dipendente e macropinosi, ma non attraverso endocitosi mediata dai *lipid rafts*.

Una volta internalizzato, il polipeptide fibrillogenico, a differenza di quanto osservato per la proteina nativa, non segue il percorso della retro-endocitosi per essere riciclato sulla membrana cellulare, ma è indirizzato al proteosoma e ai lisosomi per la sua degradazione, dal momento che, dopo una incubazione di 24 ore delle cellule con il polipeptide marcato in fluorescenza, si osserva la totale scomparsa del segnale fluorescente. La rapida degradazione del polipeptide è in accordo con l'assenza di un effetto citotossico del polipeptide sui cardiomioblasti. Per quanto riguarda ApoA-I, la persistenza del segnale fluorescente ad essa associata indica che la proteina non subisce una massiva degradazione, sebbene si osservi un forte segnale di co-localizzazione con i lisosomi. Quest'ultimi, ricchi di colesterolo, potrebbero costituire una stazione intracellulare in cui le lipoproteine si caricano di lipidi prima di essere secrete. Infine, abbiamo dimostrato che, a differenza di quanto osservato per [1-93]ApoA-I in forma non aggregata, le fibrille ottenute *in vitro* non sono in grado di essere internalizzate nel compartimento intracellulare.

Questi risultati permettono di ipotizzare che l'internalizzazione del polipeptide fibrillogenico da parte delle cellule bersaglio e la successiva degradazione intracellulare siano un meccanismo di difesa della cellula volto a rallentare il progressivo accumulo extracellulare del polipeptide fibrillogenico, ciò che è in accordo con l'esordio tardivo della patologia.

La ricerca di partner intracellulari del polipeptide fibrillogenico.

Al fine di identificare gli interattori molecolari del polipeptide fibrillogenico [1-93]ApoA-I è stata utilizzata la strategia del *fishing for partners*, in collaborazione con il gruppo di ricerca del Prof. P. Pucci del Dipartimento di Scienze Chimiche. Esperimenti di *GST-pull down* su estratti di proteine di membrana di cardiomioblasti e analisi di spettrometria di massa hanno portato all'identificazione di putativi interattori del polipeptide [1-93]ApoA-I con diversa localizzazione cellulare e diverse funzioni biologiche. Tra esse la catena beta dell'ATP sintasi e la proteina nicastrin sono state scelte per analisi più approfondite, considerando il loro ruolo fisiologico. La catena beta dell'ATP sintasi, una subunità del complesso multi-enzimatico dell'ATP sintasi, è stata infatti recentemente identificata sulla membrana degli epatociti come recettore ad alta affinità di ApoA-I in complesso con le HDL; in particolare, il legame di ApoA-I con tale proteina stimolerebbe l'endocitosi delle HDL nelle cellule bersaglio.

Nicastrin costituisce una subunità essenziale del complesso della γ -secretasi. È l'endopeptidasi che catalizza la proteolisi di proteine integrali di membrana, quali il recettore *notch* e la proteina precursore del peptide β -amiloide, per cui è stato ipotizzato avere un ruolo attivo nella formazione del peptide β -amiloide, responsabile del morbo di Alzheimer.

La validazione dei putativi interattori identificati mediante l'approccio di proteomica funzionale è stata eseguita mediante esperimenti di co-immunoprecipitazione e analisi di microscopia in fluorescenza.

L'esperimento di co-immunoprecipitazione è stato effettuato incubando un estratto di proteine di membrana di cardiomioblasti con il polipeptide marcato con la sonda FITC. Le specie proteiche co-immunoprecipitate in presenza di un anticorpo anti-FITC sono state analizzate mediante Western blotting utilizzando, separatamente, anticorpi diretti contro ciascuno dei due putativi interattori del polipeptide fibrillogenico precedentemente selezionati. L'analisi delle specie co-immunoprecipitate con il polipeptide ha rivelato la presenza sia della catena beta dell'ATP sintasi che della proteina nicastrin, indicando che entrambe le proteine sono interattori del polipeptide [1-93]ApoA-I.

Analisi di microscopia confocale in fluorescenza ci hanno permesso di dimostrare la presenza della forma ectopica della catena beta dell'ATP sintasi sulla membrana dei cardiomioblasti e di rivelare una significativa co-localizzazione tra tale proteina e il polipeptide fibrillogenico. Utilizzando la medesima tecnica, abbiamo dimostrato la co-localizzazione di [1-93]ApoA-I con nicastrin. Tali risultati confermano che la catena beta dell'ATP sintasi e nicastrin, localizzati sulla membrana cellulare dei cardiomioblasti, sono interattori molecolari del polipeptide fibrillogenico [1-93]ApoA-I, e rappresentano il punto di partenza per la progettazione di future strategie terapeutiche direzionate verso specifici bersagli.

Un modello cellulare per la produzione delle varianti patogene di ApoA-I.

Le analisi strutturali e funzionali delle varianti amiloidogeniche di ApoA-I, in confronto con la proteina nativa, costituiscono un passo fondamentale verso la comprensione

delle basi molecolari della patogenesi. Tuttavia, data l'impossibilità dell'isolamento delle forme mutate di ApoA-I dai pazienti affetti da amiloidosi, dovuta alla presenza, nei tessuti e in circolo, sia della proteina mutata che di quella nativa, risulta necessaria la messa a punto di efficienti sistemi di espressione eterologa.

La mia attività di dottorato ha previsto l'espressione ricombinate della variante amiloidogena L174S in cellule di mammifero. Cellule di ovario di criceto (CHO-K1) sono state trasfettate stabilmente con il plasmide recante la sequenza codificante la variante L174S, o la proteina ApoA-I nativa, ciascuna delle due clonata a valle della sequenza codificante il peptide segnale per la secrezione. Una volta ottenuti i cloni stabili, si è analizzata la cinetica di espressione e secrezione delle proteine ricombinanti. Entrambe le proteine sono efficientemente secrete nel terreno di crescita dalle cellule, ma si differenziano per la cinetica di secrezione. Si è poi proceduto all'isolamento della variante L174S e della proteina nativa dal terreno di coltura, mediante un solo passaggio di purificazione, adoperando una cromatografia ad interazione idrofobica. Dal momento che ApoA-I lega con elevata affinità lipidi, in collaborazione con la Dott.ssa A. Amoresano del Dipartimento di Scienze Chimiche, si è analizzato il contenuto lipidico dei campioni isolati. I risultati hanno rivelato per entrambe le specie proteiche la presenza di due tipi di acidi grassi (uno saturo e uno monoinsaturo) legati alle proteine ricombinanti. Sebbene entrambe le proteine risultino essere associate agli stessi acidi grassi, il rapporto molare lipidi:proteina è più elevato nel caso della variante amiloidogena L174S. E' ipotizzabile che tale differenza possa avere un significato fisiologico nello sviluppo della patologia.

La bassa resa delle proteine ricombinanti prodotte in cellule di mammifero non ha però consentito l'ottenimento di quantità adeguate di proteina per studi funzionali e strutturali. Di conseguenza stiamo attualmente approntando un diverso sistema di espressione delle varianti amiloidogeniche di ApoA-I utilizzando ospiti procariotici.

L'effetto di varianti amiloidogeniche di ApoA-I sulla risposta cellulare allo stress e ruolo dell'angiogenina.

Infine, la mia attività di ricerca ha previsto lo studio degli effetti di una variante amiloidogena di ApoA-I, recante la mutazione L75P, sulla fisiologia cellulare e del ruolo dell'angiogenina (ANG) nelle amiloidosi da ApoA-I. Questa parte del mio progetto di dottorato è stata condotta durante il mio soggiorno presso il Molecular Oncology Research Institute (MORI), Tufts Medical Center di Boston, presso il laboratorio del Prof G. F. Hu.

Tale studio parte dall'osservazione che ANG sembra avere un ruolo in alcune malattie neurodegenerative, quali la sclerosi laterale amiotrofica, il morbo di Parkinson e di Alzheimer, caratterizzate dall'accumulo nel sistema nervoso di fibrille amiloidi. Questa osservazione ci ha spinti ad indagare se ANG svolge una funzione chiave anche nelle patologie amiloidi sistemiche e in particolare in quelle associate alle varianti di ApoA-I.

ANG è una ribonucleasi la cui funzione principale è la stimolazione dell'angiogenesi nelle cellule endoteliali. Essa esplica la sua attività angiogenica promuovendo la trascrizione degli rRNA, grazie al legame con le regioni promotrici del DNA ribosomale. Recentemente è stato dimostrato che ANG è in grado, in caso di stress, di attivare un meccanismo di difesa della cellula.

Cellule epatiche (HepG2), deputate fisiologicamente alla produzione di ApoA-I, sono state trasfettate stabilmente con il plasmide recante la sequenza codificante la variante L75P o la proteina ApoA-I nativa, ciascuna delle due clonata a valle della sequenza codificante il peptide segnale per la secrezione. Ottenuti cloni stabili di tali

cellule, l'analisi dell'espressione e della secrezione delle due proteine ricombinanti ha portato all'osservazione che la variante amiloidogena L75P, a differenza della proteina nativa, si accumula prevalentemente nel compartimento intracellulare, suggerendo che, probabilmente a causa della parziale destrutturazione della proteina, il processo di secrezione sia in parte compromesso. Inoltre, le cellule esprimenti la variante amiloidogena hanno mostrato una ridotta vitalità cellulare e livelli intracellulari di ANG inferiori rispetto alle cellule non trasfettate e a quelle esprimenti ApoA-I nativa.

Abbiamo quindi analizzato la risposta cellulare allo stress in seguito a deprivazione di siero. In cellule che esprimono la variante L75P la vitalità cellulare è risultata essere gravemente compromessa; inoltre, si è osservata una significativa differenza nella localizzazione subcellulare di ANG tra cellule esprimenti ApoA-I nativa o la sua variante L75P. Quando le cellule sono cresciute in assenza di siero, infatti, si osserva che ANG è localizzata prevalentemente nel citosol sia nelle cellule non trasfettate che in quelle esprimenti ApoA-I nativa, in accordo con il suo ruolo nella risposta allo stress. Inaspettatamente, nelle cellule esprimenti la variante amiloidogena, ANG è risultata essere localizzata prevalentemente nel nucleo. Inoltre, esperimenti di qRT-PCR hanno indicato che la deprivazione di siero causa un significativo aumento nell'espressione di ANG nelle cellule epatiche non trasfettate o esprimenti ApoA-I nativa, mentre si è osservato solo un lieve incremento nel caso delle cellule esprimenti la variante amiloidogena.

Queste osservazioni rafforzano l'idea che ANG possa svolgere un ruolo nelle amiloidosi da ApoA-I. Per tale motivo sono stati condotti esperimenti finalizzati alla valutazione della vitalità cellulare in presenza di ANG esogena, aggiunta al terreno privo di siero. Tali esperimenti ci hanno consentito di dimostrare che ANG esplica un forte effetto anti-apoptotico su cellule epatiche esprimenti la variante amiloidogena L75P, mentre non si osservano effetti significativi sulle cellule non trasfettate e su quelle esprimenti ApoA-I nativa.

Allo scopo di comprendere il meccanismo secondo cui ANG esplica il suo ruolo protettivo nei confronti delle cellule epatiche esprimenti la variante amiloidogena, sono stati condotti esperimenti utilizzando tre mutanti di ANG, ognuno difettivo per una sola delle funzioni associate ad ANG. Il mutante R33A non è in grado di traslocare al nucleo, K40Q non è enzimaticamente attivo, mentre il mutante R66A è difettivo per il legame al recettore. L'analisi degli effetti di tali mutanti sulla vitalità cellulare suggerisce che per esercitare il suo ruolo protettivo contro lo stress ANG deve aver accesso al citosol, dal momento che l'unico mutante incapace di ripristinare la funzionalità cellulare compromessa dall'assenza di siero è risultato essere quello difettivo nel legame al recettore. Il ruolo protettivo di ANG sembra invece essere indipendente dalla sua attività enzimatica.

Ulteriori esperimenti saranno necessari per chiarire le basi molecolari con cui ANG esplica il suo ruolo protettivo nelle amiloidosi da ApoA-I.

SUMMARY

An increasing number of human diseases is linked to protein misfolding and aggregation in amyloid fibrils. In spite of the extensive research during the last decade, much remains to be learnt on the basis of the molecular mechanism responsible for cell damage. Among the amyloidogenic proteins, 19 mutated versions of apolipoprotein A-I (ApoA-I) have been associated to amyloid diseases. Fibrils are mainly constituted by N-terminal fragments of ApoA-I, about 90-100 residue long. The 93-residue polypeptide, [1-93]ApoA-I, is the main constituent of extracellular cardiac amyloid fibrils. My research activity was aimed at inspecting the molecular mechanisms of the pathology. Therefore, we analyzed binding and intracellular pathway of recombinant [1-93]ApoA-I in cardiac target cells, we identified potential partners and studied the effects of endogenous amyloidogenic variants of ApoA-I on cell physiology. We demonstrated that the fibrillogenic polypeptide recognizes specific binding sites on target cell membranes and partially co-localizes with ABCA1 transporter. Following binding, the polypeptide is internalized mostly by clathrin-mediated endocytosis and by lipid rafts, whereas a macropinocytosis involvement is excluded. Upon internalization, no retro-endocytosis is observed, while the polypeptide is massively degraded by proteasomal and lysosomal machineries. The rapid degradation of the polypeptide, together with the finding that fibrils obtained *in vitro* have no access to the intracellular compartment, are consistent with the absence of cytotoxic effects on cardiac cells. The identification of the molecular partners of a pathogenic protein is a central issue in the comprehension of the molecular bases of the disease. GST pull-down experiments, and protein identification by mass spectrometry, were performed on cardiomyoblasts membrane extracts. This experimental approach provided a list of about 100 potential interactors of the fibrillogenic polypeptide and, among these, the β -chain of ectopic ATP synthase and nicastrin were selected to be analyzed in detail. By co-immunoprecipitation and fluorescent microscopy experiments both proteins were found to interact with the fibrillogenic polypeptide. Interestingly, the former protein is an ApoA-I receptor, the latter has a role in the production of amyloid β peptide, responsible for Alzheimer's disease. Since patients are heterozygous for the mutated ApoA-I gene, the isolation of amyloidogenic variants from sera is impracticable. Thus, we set up a suitable cellular model, consisting in stably transfected CHO-K1 cells, to express ApoA-I amyloidogenic variant L174S. The recombinant protein, efficiently secreted in the culture medium, was isolated following a one-step purification procedure and found to be associated to fatty acids, for which a role in trafficking and secretion may be hypothesized. Finally, we analyzed the effects of an amyloidogenic ApoA-I variant on cell physiology. We obtained hepatic cells stably over-expressing amyloidogenic ApoA-I variant L75P and found that the protein is mostly retained within the cells, rather than secreted, probably because of its partial unfolding. Moreover, reduced cell viability and decreased angiogenin (ANG) levels were detected. When cells were exposed to stress conditions (e.g. serum starvation), cell viability was more severely affected than cells expressing the wild-type protein. Furthermore, ANG levels and its subcellular localization were altered. ANG is known to play a role in cell recovery from stress and, more recently, it has been associated to neurodegenerative diseases, such as Parkinson's, Alzheimer's and Amyotrophic Lateral Sclerosis. Our data suggest a possible role of ANG in ApoA-I related amyloidosis. According to these observations, the addition of exogenous ANG to our cell model was able to restore cell viability. The analysis of a set of ANG loss-of-function mutants allowed us to demonstrate that ANG needs to be internalized into the cells to elicit its protective action against stress.

ABBREVIATIONS

ApoA-I	Apolipoprotein A-I
[1-93]ApoA-I	The fibrillogenic N-terminal 93-residue polypeptide of ApoA-I
ABCA1	Membrane transporter ATP-binding cassette A1
HDL	High density lipoprotein
ANG	Angiogenin
BSA	Bovine serum albumin
SDS-PAGE	Gel-acrylamide electrophoresys in denaturing conditions
FITC	Fluorescein isothiocyanate
TFE	Trifluoroethanol
MTT	3-(4,5-dimethylthiazol-2-yl)-2,5-diphenyltetrazolium bromide
Co-IP	Co-Immunoprecipitation
AFM	Atomic Force Microscopy
qRT-PCR	Quantitative Real Time PCR
EB/AO staining	Ethidium bromide and acridine orange staining

INRODUCTION

1. Protein misfolding and diseases

According to the Anfinsen's principle [1], a polypeptide achieves its biologically active native state by descending to the thermodynamically most favorable conformation, which corresponds to one of thousands of possible conformers.

From this principle derived the structure-function paradigm, claiming that a specific function of a protein is determined by its unique and rigid three-dimensional structure. Although basically correct, recent data indicate that this empirical rule needs to be adapted, as a growing number of proteins adopt, under native conditions and for the same amino acid sequence, different conformations that exist in a dynamic equilibrium [2].

The folding process is subjected to a strict quality control by molecular chaperones and protease machinery. Misfolded proteins are either rescued by chaperones or eliminated by the ubiquitin-proteasome system or lysosome-mediated autophagy [3]. These mechanisms are normally sufficient to prevent the accumulation of misfolded proteins. However, under certain pathological conditions, the capacity of this protein control machinery is exceeded and misfolded proteins accumulate to dangerous levels [4].

These pathological conditions are generally known as *protein misfolding (or protein conformational) diseases* [5,6] because the pathological protein undergoes structural changes that results in self-association, aggregation and tissue deposition, causing severe functional impairment. These structures are generally described as amyloid fibrils or plaques when they accumulate in the extracellular space, whereas the term "intracellular inclusions" has been suggested as more appropriate when fibrils accumulate inside the cell [7].

The diseases can be broadly grouped into neurodegenerative pathologies, in which aggregation occurs in the nervous system, non-neuropathic localized amyloidoses, in which aggregation occurs in a single type of tissue, and non-neuropathic systemic amyloidoses, when aggregation occurs in multiple tissues.

Examples of amyloid diseases with high social impact are the Alzheimer's and Parkinson's diseases, the spongiform encephalopathies, the Huntington's disease, and the amyotrophic lateral sclerosis [8].

To date almost 30 amyloidogenic proteins have been identified [9], some of which are shown in Table I. Although these proteins do not show any sequence or structure homology, they have a common feature: the ability to give rise to amyloid fibrils morphologically identical, characterized by a highly ordered and rigid structure, extremely stable and resistant to proteases [10]. Moreover, an increasing number of proteins with no link to diseases has been found to form, under some conditions *in vitro*, fibrillar aggregates showing morphological, structural and tinctorial properties typical of amyloid fibrils [11]. This finding has led to the idea that the ability to form amyloid structures is a generic property of polypeptide chains, even though the propensity to form such a structure can vary dramatically with sequence. This generic property has been exploited by living systems for specific purposes, as some organisms have been found to convert, during their normal physiological life cycle, one or more of their endogenous proteins into amyloid fibrils that have functional rather than disease-associated properties [12-14].

Disease	Precursor protein	Fibril component
Alzheimer's disease	Amyloid precursor protein	A β -Peptide 1-40 to 1-43
Spongiform encephalopathies	Prion	Prion or fragments thereof
Parkinson's Disease	α -synuclein	α -synuclein
Primary systemic amyloidosis	Immunoglobulin light chain	Intact light chain or fragments
Secondary systemic amyloidosis	Serum amyloid A	Amyloid A (76-residue fragment)
Senile systemic amyloidosis	Transthyretin	Transthyretin or fragments
Amyotrophic lateral sclerosis	Superoxide dismutase 1	Superoxide dismutase 1
Hereditary cerebral amyloid angiopathy	Cystatin C	Cystatin C minus 10 residues
Hemodialysis-related amyloidosis	β 2-Microglobulin	β 2-Microglobulin
Type II diabetes	Islet amyloid polypeptide (IAPP)	Fragment of IAPP
Familial amyloid polyneuropathy III	Apolipoprotein A-I	N-terminal fragments of apolipoprotein A-I
Hereditary non-neuropathic systemic amyloidosis	Lysozyme	Lysozyme or fragments thereof
Injection-localized amyloidosis	Insulin	Insulin
Hereditary renal amyloidosis	Fibrinogen	Fibrinogen fragments

Table I: The most common amyloidoses, the corresponding pathogenic protein precursors and their components detected in the amyloid fibrils.

2. Structure of amyloid fibrils

Despite the large differences in the structures and functions of the proteins and peptides responsible for the differing amyloidoses, amyloid fibrils are surprisingly similar and share basic structural features.

Fibrils can be imaged *in vitro* using transmission electron microscopy (TEM), atomic force microscopy (AFM) or solid state NMR (ssNMR). These techniques revealed that fibrils appear as rigid structures, extended, unbranched, indefinite in length and molecular weight (Fig. 1). Fibrils usually consist of a variable number of protofilaments (typically 2–6), each about 2–5 nm in diameter [15]. Protofilaments twist together to form rope-like fibrils that are typically 7–13 nm wide [16] or associate laterally to form long ribbons that are 2–5 nm thick and up to 30 nm wide [17-19]. X-ray fiber

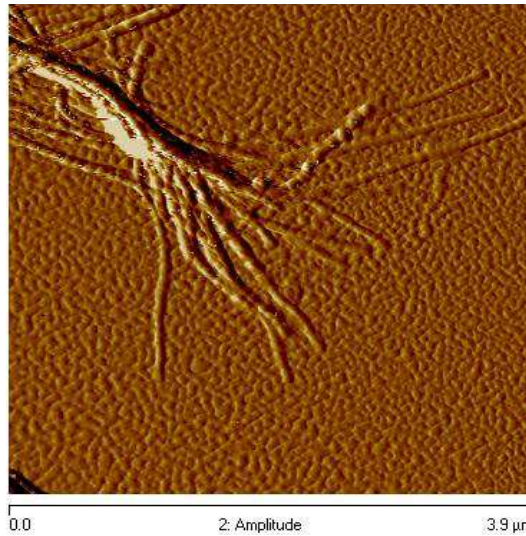


Figure 1: Image of fibrils analyzed by atomic force microscopy.

diffraction has led to the description of the ordered core of the amyloid fibrils as a super-secondary cross-beta structure, where each protofilament results from a double row of beta sheets provided by each monomer, whose strands run parallel to each other and perpendicular to the main fibril axis [20]. Two types of fibrils have been described: fibrils of type 1 are very thin and consist of a single strand, while those of type 2 consist of several strands reaching a diameter of 80-130 Å [21].

Electron microscopy and atomic force analyses have revealed that the amyloidogenic protein is the predominant component of amyloid deposits, but not the only one. Palmitic acid, oleic acid and linoleic acid have been found to be present as constituents of fibrils [22]. Furthermore, amyloid fibrils are often closely associated with sulfur proteoglycans of the extracellular matrix, including glycosaminoglycans (GAGs), which confer rigidity to the fibril structure [23, 24]. Among GAGs, heparan sulphate elicit particular interest as it appears to play an active role in the formation of amyloid fibrils. In fact, it has been reported that this compound promotes the nucleation of fibrils and fibril-fibril association of amyloidogenic proteins [25]. Another ubiquitous component of amyloid deposits is the glycoprotein SAP (serum amyloid P component) [26] which protects amyloid fibrils from degradation by phagocytic cells and proteolytic enzymes [27].

3. The fibrillogenic process

The molecular basis of fibrillogenesis, by which normally soluble polypeptide chains aggregate into insoluble and stable amyloid structures, is not clear yet.

The full elucidation of the protein aggregation process requires the identification of all the conformational states and oligomeric structures adopted by the polypeptide chain during the process and the determination of the thermodynamics and kinetics of all the conformational changes that link these different species. It also implies characterizing each of the transitions at a molecular level and identifying the residues or regions of the sequence that promote the various aggregation steps. The

identification and characterization of oligomers preceding the formation of well defined fibrils is of particular interest because of an increasing awareness that these species are likely to play a critical role in the pathogenesis of protein deposition diseases [28].

It is widely established that amyloid fibrils are formed with nucleation-dependent polymerization (Fig. 2), in which the protein monomer is converted into a fibrillar structure *via* a “nucleated growth” mechanism.

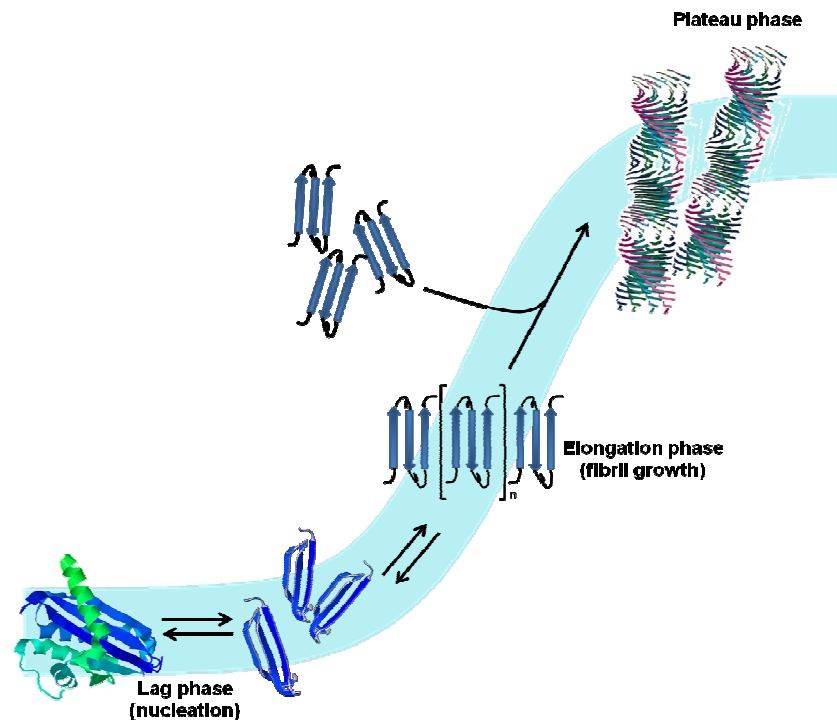


Figure 2: Kinetics of amyloid fibril formation. The process is described by a sigmoidal curve, typical of nucleation-dependent kinetics. Following the rate-limiting step of nucleus formation (lag-phase), aggregate growth proceeds rapidly by further addition of monomers (elongation phase), or other assembly-competent oligomers, to form larger polymers (plateau phase).

During the initial lag phase, corresponding to the phase in which nucleation and aggregation is not observed, the monomers associate to form the so-called "cores" [28], oligomeric forms of β sheets organized in prefibrillar cross, which facilitate the aggregation process. It was also demonstrated that the duration of the lag phase can be greatly reduced by the addition of preformed fibrils or fibril precursors that promote nucleation [29, 30]. In addition, it has been demonstrated that change in experimental conditions, or certain type of mutations, can also reduce the length of the lag phase. The absence of a lag phase, therefore, does not necessarily imply that a nucleated growth mechanism is not operating, but it may simply be that the time required for fibril growth is sufficiently slow relative to the nucleation process and that

the latter is no longer the slowest step in the conversion of a soluble protein into the amyloid state [28].

Once formed, the nucleus grows by extension at one end of the β sheets. This event generates ordered oligomers, called protofibrils, up to 200 nm long with a diameter of 4-10 nm, observable by electron microscopy [31]. The protofibrils grow progressively (polymerization) to form mature fibrils. It was also demonstrated the existence of metastable oligomers of intermediate size between monomers and protofibrils. These protein species have a short half-life and none of them accumulate in significant quantities. An example are the protofilaments, a heterogeneous population of species with high content of β sheets structures. They are considered the forerunners of protofibrils [32].

Two main classes of fibrillogenic proteins have been identified: those with a compact folding in their native state and those that are partially unfolded. In the case of amyloidogenic proteins that are natively folded, destabilizing mutations and/or changes in solution conditions (changes in pH or temperature, or chemical changes) are key factors responsible for the induction of fibrillogenesis, as in the case of β_2 -microglobulin ($A\beta_2M$) or the prion protein APrP [28]. In these cases there is an alteration of the existing balance between the properly folded polypeptide chain and a partially unstructured form, with the increase of the latter protein species characterized by a high tendency to aggregation.

On the other hand, several amyloidogenic proteins or polypeptides are intrinsically disordered. Such proteins include the β -Amyloid peptide ($A\beta$), islet amyloid polypeptide (AIAPP) and α -synuclein [33]. These “natively unfolded” [34] proteins emerged as proteins lacking of almost any secondary structure and were shown to be extremely flexible and disordered under physiological conditions [35]. In some cases, natively folded proteins generate unfolded fragments associated to the amyloid pathology. This may occur when a specific mutation diverts the fate of a globular protein converting it to the precursor of fragments responsible for fibril formation. This is the case of Apolipoprotein A-I (ApoA-I) and its amyloidogenic N-terminal fragment.

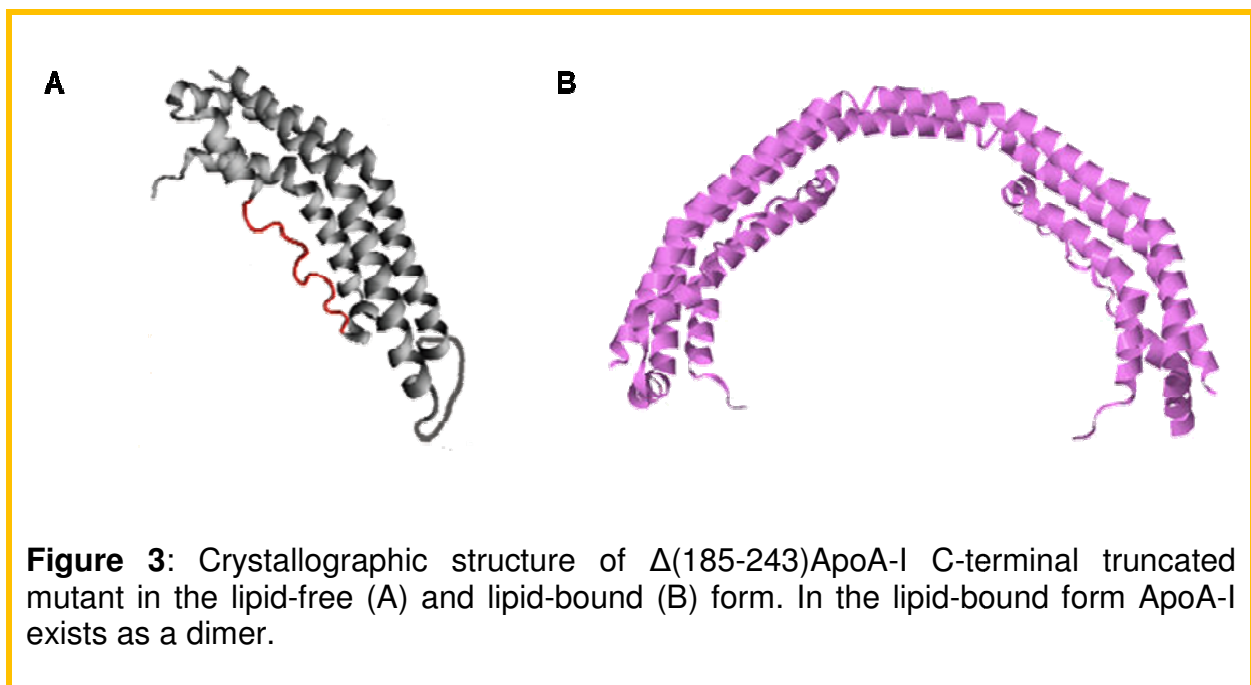
4. Apolipoprotein A-I

ApoA-I, the major structural component of high density lipoprotein (HDL), plays a critical role in lipid metabolism [36], both in delivering cholesterol to steroidogenic tissues and in transporting it from the periphery to the liver for catabolism in the so called reverse cholesterol transport. Therefore, ApoA-I plays an antiatherogenic role *in vivo*, with a protecting effect against cardiovascular diseases [37].

ApoA-I is synthesized by the liver and the intestine as a *pre-pro*-protein. After the cleavage of the *pre*- and *pro*- peptides, the mature protein (28 kDa) is secreted in the plasma, where it is either associated to lipids, or in a lipid-free state (5-10%) [38]. Transcriptional regulation of ApoA-I gene is complex, involving induction by several hormones [39] and inhibition by anti-oxidant molecules [40]. No post translational modifications, like glycosilation or disulfide bonds formation, occur.

During HDL biogenesis, the primary acceptor of cholesterol and phospholipids from macrophages is lipid-free or lipid-poor ApoA-I, containing up to four phospholipid molecules [41]. In this state, ApoA-I is the preferred substrate of the plasma membrane transporter ATP-binding cassette A1 (ABCA1) [42-44]. The conversion of unesterified cholesterol into cholesteryl ester by the enzyme lecithin:cholesterol

acyltransferase (LCAT) is responsible for the conversion of the nascent, discoidal HDL into mature spherical HDL, with ApoA-I representing roughly 70% of HDL protein mass. Circulating HDL are remodelled by the action of proteins and enzymes, such as cholesteryl ester transfer protein [45], LCAT [46], phospholipid transfer protein [47, 48] and hepatic lipase [49]. Plasma HDL remodelling can result in the destabilization of HDL and the release of lipid-free/lipid-poor ApoA-I. Furthermore, the selective uptake of lipids from HDL through scavenger receptor B type 1 (SRB1) can yield lipid-poor ApoA-I [50]. It has been demonstrated that the production of lipid-free/lipid-poor ApoA-I from mature HDL and re-lipidation by ABCA1 is a dynamic process in the arterial wall, which is critical in protecting macrophages from cholesteryl ester accumulation [51]. Nevertheless, the molecular mechanism of the atheroprotective action of ApoA-I, as well as HDL biogenesis, is not fully understood. HDL catabolism requires disassembly of protein and lipid components. While HDL lipid clearance is well described [52], less is known about the catabolism of the HDL protein moiety. Numerous tissue uptake studies support the view that kidneys are the principal site of ApoA-I degradation [53]. The conformational transition from the lipid-free to the lipid-bound state of ApoA-I [51] is made possible by the conformational plasticity of the protein [52]. In fact, different are the structures proposed for ApoA-I as a lipid bound or a lipid-free protein [54, 55]. In the absence of lipids, ApoA-I assumes a compact four-helix bundle structure (Fig. 3A) [55], while, upon lipidation, the amphipathic α -helices substitute protein-protein contacts for protein-lipid interactions (Fig. 3B). This induces the opening of the helical bundle into an extended belt-like α -helix, which wraps around the perimeter of the nascent HDL particle [54]. Therefore, conformational plasticity of full-length ApoA-I is a functionally relevant feature, strictly related to the complex mechanism of its biological action.



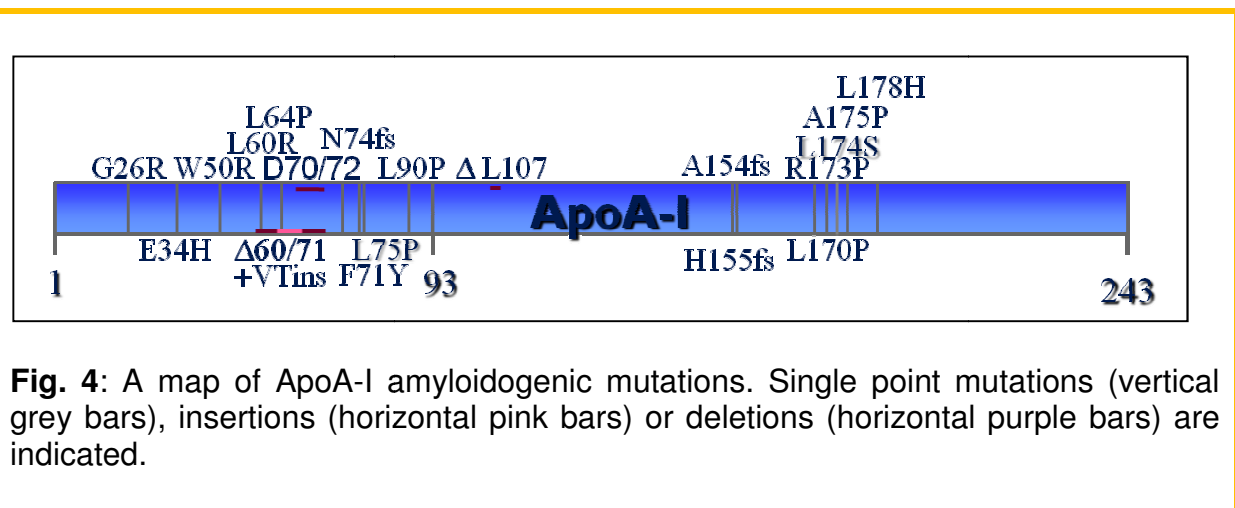
4.1. ApoA-I and amyloidosis

More than 50 naturally occurring ApoA-I variants have been reported, half of them associated with HDL reduced levels [56]. Among them, ApoA-I_{MILANO} variant exerts a protective role against atherosclerosis [57]. Nineteen ApoA-I mutations have been associated with familial systemic amyloidosis, a “gain of function” genetic disease [52], in that new pathological properties are associated to the protein. These variants of ApoA-I are responsible for systemic amyloidoses characterized by aggregate deposition in peripheral organs, such as heart, liver, kidneys, nerves, ovaries or testes, leading to organ damage [58].

Most of the mutants are generated by single point mutations in the 243-amino acid sequence of the native protein, although deletions or deletions/insertions have also been described [59-60]. In Fig. 4 and Table II the map of the nineteen ApoA-I mutations associated to amyloidosis and the affected organs or tissues are indicated for each mutant. For all these variants, amyloid fibrils isolated *ex vivo* were found to be mainly constituted by N-terminal fragments of ApoA-I, 90-100 residue long. Thus, ApoA-I variants represent the precursors of N-terminal fragments of the protein responsible for fibril formation. Twelve of these mutations are present within the N-terminal portion of the protein that is eventually found in fibrils (“internal mutations”), whereas the other mutations occur in positions located outside this region of the polypeptide sequence (“external mutations”) [58, 61]. Although patients are invariably heterozygous for the mutated gene, only the variant isoform was detected in amyloid deposits.

4.2 Structural and functional features of the ApoA-I fibrillogenic polypeptide

The 93-residue fibrillogenic domain of ApoA-I, extracted from amyloid deposits of a patient who underwent heart transplantation for end-stage heart failure, was found to be a natively unfolded protein in water at neutral pH [62].



Mutation	Affected organ or tissue	Ethnic origin
Internal mutations		
G26R	Kidneys, liver, peripheral nerves, GI tract	British, Scandinavian
E34K	Kidneys, liver	Polish
W50R	Kidneys, liver, GI tract	Jewish
L60R	Kidneys, liver, testes, heart	British
L64P	Kidneys, liver	Italian
Δ60-71+ VT ins	Liver	Spanish
Δ70-72	Kidneys, liver, choroid	German
F71Y	Liver, palate	British
N74K frameshift	Kidneys, uterus,, ovaries, pelvic lymph nodes, GI tract	German
L75P	Kidneys, liver, testes	Italian, German, other
L90P	Skin, heart, larynx	French, American
Esternal mutations		
ΔL107	Circulatory sistem	Scandinavian
A154 frameshift	Kidneys	German
H155M frameshift	Kidneys	German
L170P	Larynx	British
R173P	Kidneys, skin, heart, larynx	American, British
L174S	Skin, testes, heart, larynx	Italian, Dutch
A175P	Larynx, testes	British
L178H	Larynx, skin, heart, nerves	French

Table II: The mutations occurring in ApoA-I sequence, associated to amyloid pathology. The affected organs or tissues and the ethnic origins are also indicated.

Acidic conditions (pH 4.0) were able to switch on a complex fibrillogenic pathway, consisting of extensive structural rearrangements of the polypeptide, that shifts from a random coil structure to an unstable helical conformation, and then aggregates into a β -sheet based polymeric structure [63]. Nevertheless, the possibility to analyze the complex fibrillogenic pathway of ApoA-I amyloidogenic polypeptide was very limited so far, due to the low amount available from *in vivo* sources. In the laboratory of Prof. Piccoli, an effective and reliable expression system was set up to produce a recombinant version of 1-93 polypeptide, denoted as [1-93]ApoA-I. The strategy, aimed at protecting the recombinant polypeptide from intracellular degradation, allowed us to obtain a pure and stable product.

The elucidation of the structural properties of the fibrillogenic polypeptide is a central issue in the comprehension of the pathology. To this regard, the identification of structural or environmental factors, able to activate the pathological pathway leading to amyloid fibrils, is of enormous importance to pursue strategies aimed at inhibiting this process. Conformational analyses of the recombinant polypeptide in solution by far-UV CD spectroscopy indicated that in physiological-like conditions the protein is largely unfolded. A pH switch from 7.0 to 4.0 induces a predominant α -helical

structure, through the conversion of the protein from a random coil to a helical/molten globule state. This transition, complete within 2 seconds and fully reversible when the pH is returned to 7.0, is followed by the appearance of a significant β -sheet component. The helical conformers are thought to be key intermediates in the multistep fibrillogenic process. These observations are in good agreement with the behavior of the natural polypeptide isolated from *ex vivo* fibrils [63]. The helical/molten globule intermediate displays a strong propensity to oligomerize, as demonstrated by AFM analyses. [1–93]ApoA-I, in fact, generates typical amyloid fibrils upon incubation at pH 4.0 for lengths of time comparable to those described for the natural polypeptide [61].

Extracellular amyloid deposition *in vivo* takes place in a heterogeneous environment, in which components of the cell membrane and/or the extracellular matrix may have a central role. From a general point of view, the interaction of proteins with biological superstructures, like membranes, may dramatically affect their structural organization. It is known that the interaction of natively folded proteins with groups exposed on a membrane surface often modifies their conformational states [64-66]. On the other hand, unfolded polypeptide chains can gain ordered structures at the membrane surface or inside the bilayer [64]. Conversely, proteins can alter membrane fluidity, and/or permeate the membrane bilayer and can even extract lipids from it [67]. Moreover, it is known that the hydrophobic interior of the plasma membrane can induce structural changes in soluble intrinsically disordered proteins and peptides by favouring secondary structures often leading to aggregate nucleation [68-70, 65, 66]. The well known stability of protein α -helical structures within a membrane lipid bilayer is in line with the concept that the early formation of multimeric species is often promoted by the association of polypeptide molecules through helix-helix interaction. From this point of view, a general mechanism of membrane catalyzed amyloid formation can be envisaged. To this regard, factors able to induce α -helical conformers may accelerate amyloid formation. Conversely, factors able to bind to, and stabilize, helical regions by entrapping the helical intermediates in a minimum energy may slow down the fibrillogenic process.

It is known that the *in vivo* role of ApoA-I is mediated by its interactions with lipids, that are fundamental in the maintenance of the protein native structure, and that the N-terminal region of ApoA-I contributes to lipid binding in the native protein [71, 72]. To this regard, recently the effects of lipids on the propensity of [1-93]ApoA-I to undergo fibrillogenesis was analyzed. It has been found that a lipid environment affects [1-93]ApoA-I aggregation pathway by inducing and stabilizing helical intermediates [73]. Using a multidisciplinary approach, including CD, fluorescence, electrophoretic, and AFM analyses, the effects of a lipid environment on the conformational state and aggregation propensity of [1-93] ApoA-I was investigated. Following addition of the lipid-mimicking detergent Triton X-100, the polypeptide was found to be in a helical state at both pH 8.0 and 6.4, with no conformational transition occurring upon acidification. These helical conformers are stable and do not generate aggregated species, as observed by AFM after 21 days. Similarly, analyses of the effects of cholesterol demonstrated that this natural ApoA-I ligand induces formation of α -helix at physiological concentrations at both pH 8.0 and 6.4 (pathophysiological conditions). The behaviour of [1-93]ApoA-I is in line with that of other amyloidogenic proteins, whose conformations were reported to be strongly affected by the interaction with cholesterol. It is known that cholesterol and sphingolipids are the most abundant molecules of lipid rafts. Amyloid protein precursor (APP) and secretases preferentially localize into ganglioside and cholesterol-rich membrane

microdomains (lipid rafts) [74-76]. Accordingly, it has been proposed that aggregation of soluble A β peptides and APrP is a raft-associated process [75] and that an alteration of cholesterol homeostasis is a shared primary cause of several neurodegenerative diseases [77].

Mechanistic studies with well defined model membranes have shown that natively unfolded polypeptides, upon interaction with surfaces, readily adopt helical structures that represent key intermediates in amyloid formation process [33]. In particular, anionic surfaces and anionic phospholipid-rich membranes can play key roles either in triggering protein fibrillogenesis by acting as conformational catalysts for amyloid fibrils deposition [64], or as inhibitors of fibrillogenesis [77]. In our laboratory has been demonstrated that zwitterionic, positively charged, and negatively charged liposomes affect [1-93]ApoA-I conformation, inducing helical species [73]. These data support the idea that lipids play a key role in [1-93]ApoA-I aggregation *in vivo*.

Nothing is known about the mechanism leading to the release of the fibrillogenic polypeptide from a full-length amyloidogenic variant of ApoA-I, nor in which context the proteolytic cleavage does occur. Nevertheless, the hypothesis can be raised that the fibrillogenic polypeptide is released at the site of fibril deposition, where it accumulates in the extracellular space of target tissues.

Recently, the group of Prof. Piccoli express, isolate and characterize 8 variants of the fibrillogenic polypeptide carrying internal mutations associated to amyloid diseases. This made possible the analysis of the structural and functional properties of the fibrillogenic polypeptides and their relationships, relevant for the comprehension of the disease [78].

These analyses indicated that an amyloidogenic mutation may, or may not, increase the aggregation propensity of the polypeptide. Thus, the paradigm amyloidogenic mutation-increased aggregation propensity has not to be taken as a general rule. Instead, a different scenario was provided by *in silico* analyses. Sequence-based predictions of aggregation propensity and stability of the pathogenic variants of full-length ApoA-I revealed in almost all the variants an increase of conformational fluctuations and chain flexibility in the proximity of the protein region spanning approximately residues 88-110, with the consequent exposure of a putative cleavage site to a proteolytic attack that releases the fibrillogenic moiety [78]. Therefore, all the amyloidogenic mutations occurring at the N-terminal region of ApoA-I have a common feature, that of dramatically affecting the stability of the whole protein, favouring the cleavage that generates the N-terminal fibrillogenic fragment. In addition, some of the mutations increase the aggregation rate of the fibrillogenic polypeptide.

These results are in line with a recent study on the X-ray crystal structure of a C-terminal truncated human ApoA-I, $\Delta(185-243)$ ApoA-I (Fig. 3B), which provided the basis for understanding the impact of amyloidogenic mutations on protein stability [79]. In the crystal structure, lipid free $\Delta(185-243)$ ApoA-I forms a dimer composed of two antiparallel molecules adopting a semi-circular conformation, with a diameter comparable to that of HDL particle. The structure is stabilized by two symmetric four-segment bundles at the opposite ends of the dimer. The Authors propose that the amyloidogenic mutations of ApoA-I lead to fibril formation by destabilizing ApoA-I interaction with lipids, with the consequent formation of lipid poor/free ApoA-I (Fig. 5). Moreover, the presence of a specific amyloidogenic mutation destabilizes the four-helix bundle and the overall protein conformation. As a consequence, region 80-100 is exposed to solvent becoming susceptible to proteolytic cleavage. Segment 44-55

of the protein, with high β -sheet propensity, probably acts as a template for the cross- β -sheet structures of amyloid fibrils.

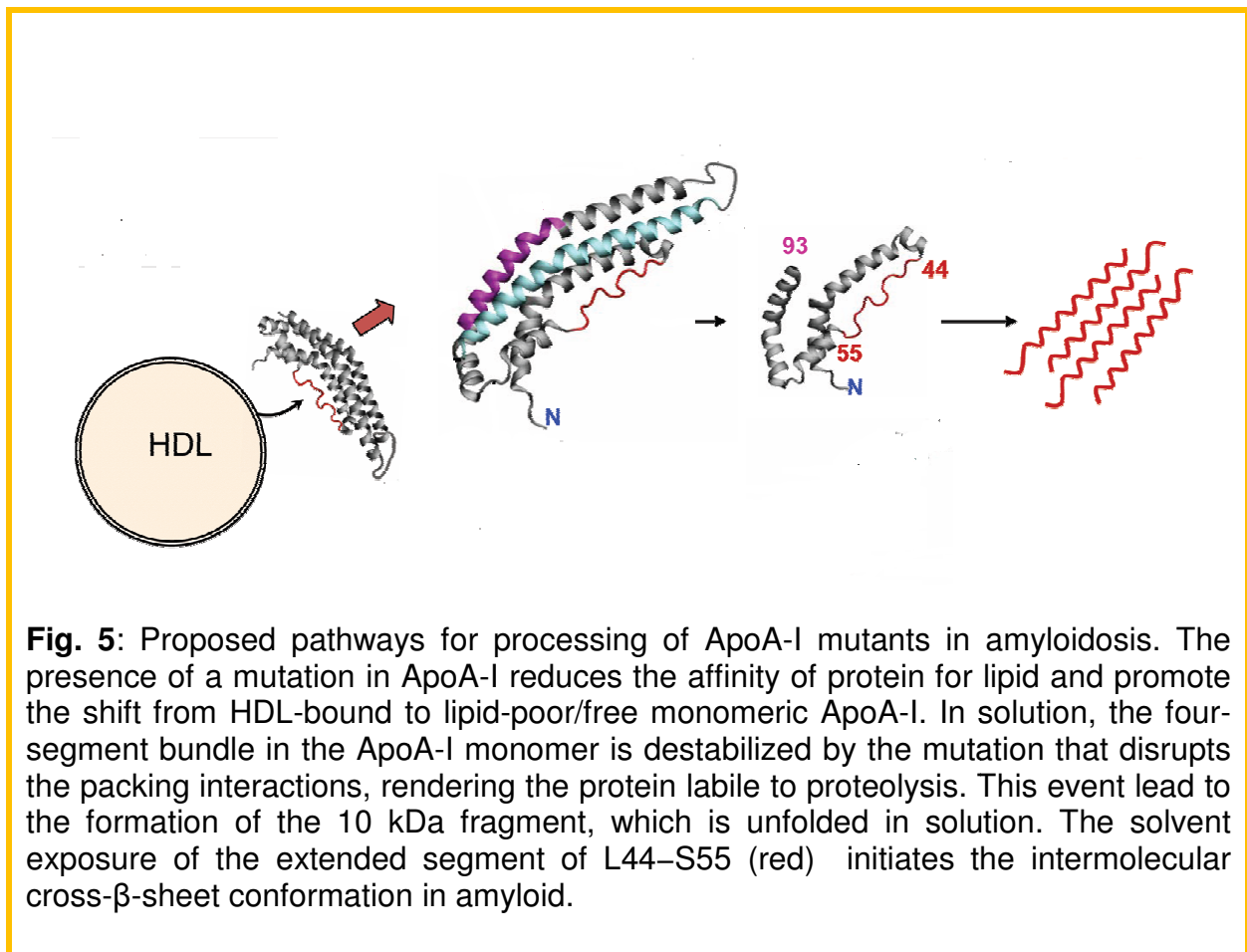


Fig. 5: Proposed pathways for processing of ApoA-I mutants in amyloidosis. The presence of a mutation in ApoA-I reduces the affinity of protein for lipid and promote the shift from HDL-bound to lipid-poor/free monomeric ApoA-I. In solution, the four-segment bundle in the ApoA-I monomer is destabilized by the mutation that disrupts the packing interactions, rendering the protein labile to proteolysis. This event lead to the formation of the 10 kDa fragment, which is unfolded in solution. The solvent exposure of the extended segment of L44–S55 (red) initiates the intermolecular cross- β -sheet conformation in amyloid.

AIMS

My research project is aimed at elucidating the molecular basis of the mechanism of action of naturally occurring mutant forms of Apolipoprotein A-I (ApoA-I) associated to systemic amyloid diseases. From these pathogenic variants, the N-terminal region of the protein (residues 1-93), corresponding to the naturally unfolded polypeptide [1-93]ApoA-I, is released and aggregates generating amyloid fibrils, which accumulate in peripheral tissues (heart, liver) invariably leading to organ failure and death.

The project is aimed at

- elucidating key steps of the mechanism of action of ApoA-I fibrillogenic polypeptide and full-length variants
- identifying intracellular partners of the fibrillogenic polypeptide and cellular processes involved in the development of the disease, as potential therapeutic targets.

The research has been conducted using a double approach:

1. studies on the fibrillogenic polypeptide of ApoA-I
 - elucidation of the mechanism of action of the fibrillogenic polypeptide [1-93]ApoA-I: binding, internalization and intracellular pathway in cardiac target cells
 - search for intracellular partners by a functional proteomic approach
2. studies on the pathogenic variants of ApoA-I
 - setting up of novel cellular models to express ApoA-I pathogenic variants and to study their effects on cell physiology and susceptibility to stress
 - role of angiogenin in stress recovery.

The challenge is that of shedding light on a largely unknown mechanism responsible for the onset and progression of a hereditary devastating disease. The comparison of our results with those reported in the literature for other amyloidogenic proteins or peptides might evidence common traits and suggest potential therapeutic approaches.

Materials and Methods

1. Materials

Anti-human ApoA-I polyclonal antibodies were from DAKO, Denmark. All reagents, ApoA-I, FITC-insulin, transferrin (Tf) and anti-actin polyclonal antibodies were purchased from Sigma-Aldrich (St. Louis, MO). Protein concentration was determined by the BCA assay. LysoTracker Red, goat anti-rabbit and anti-mouse antibodies, conjugated with Texas red or with Bodipy FL were from Molecular Probes. Anti β -catenin antibody was from Santa-Cruz. Anti FITC polyclonal antibodies were from Abcam.

2. Expression and isolation of [1-93]ApoA-I

Recombinant [1-93]ApoA-I, cloned in the expression vector pGEX-4T-3, was expressed in BL21DE3 *E. coli* cells following the procedure described by Di Gaetano et al. (2006) with some modifications [61]. Briefly, bacteria were resuspended in phosphate-buffered saline (PBS) containing 20% sucrose and protease inhibitors (Roche, Germany). Lysates were sonicated, incubated for 30 min at 4°C, and centrifuged. GST-containing species, selected by affinity chromatography, were digested with thrombin to release [1-93]ApoA-I. The recombinant product was isolated by high-performance liquid chromatography (HPLC) reverse phase chromatography on a Ultrapure C8 column (Vydac, Grace, IL, USA) with a gradient of buffer B [90% acetonitrile in 0.1% trifluoroacetic acid (TFA)] in buffer A (0.1% TFA) using a PerkinElmer chromatographic system (Series 200). The final yield of the procedure was estimated to be 2.5 mg/l of bacterial culture. Pure [1–93]ApoA-I was lyophilized and stored at -70°C until use. For experimental purposes, the polypeptide was dissolved in the appropriate buffer and centrifuged before use.

3. Fibrillar aggregates

Fibrillar aggregates were obtained by incubating [1–93]ApoA-I for 2 weeks at 37°C at 0.3 mg/ml protein concentration in 12 mM sodium phosphate buffer, pH 6.4 containing 20% (v/v) trifluoroethanol (TFE). By centrifugation, insoluble aggregates of [1-93]ApoA-I (pellet) were separated from the unaggregated, soluble polypeptide (supernatant). To quantify aggregated [1-93]ApoA-I, the amount of the soluble polypeptide was determined spectrophotometrically and subtracted from the total amount of [1-93]ApoA-I before aggregation. The pellet was dried under N₂ to remove

TFE and resuspended in cell medium to reach the appropriate protein concentration. The suspension of the aggregated species was tested for cytotoxicity.

4. Cloning

Plasmid pBOShApoA1G1S, encoding human ApoA-I, was kindly provided by Prof. L. Pastore [18]. The cDNA encoding ApoA-I variant L174S was obtained by overlap extension PCR mutagenesis using pBOShApoA1G1S as a template. Two couples of primers, reported in Table III, were used (a-b; c-d). The recombinant plasmid carrying the mutated sequence was denoted as pBOSApoA1(L174S). Automated DNA sequencing was performed by Eurofins-MWG (Ebersberg, Germany).

	Mutagenic oligonucleotide
a (F)	5'-GGG GTA CCG AAG GAG GTC CCC CAC GG-3'
b (R)	5'-CGC GGC <u>GCT</u> GCG CTG GCG CAG CTC-3'
c (F)	5'-CAG CGC <u>AGC</u> GCC GCG CGC CTT GAG-3'
d (R)	5'-GCT CTA GAT CTG AGC ACC GGG AAG GG-3'

Table III: oligonucleotides used as primers in the PCR reactions performed to generate the L174S ApoA-I variants. (R) and (F) are reverse and forward primers, respectively; the mutated nucleotide sequences are underlined.

5. Cell culture

Chinese Hamster Ovary (CHO-K1), rat embryos heart myoblasts (H9c2) and human hepatic carcinoma (HepG2) cells were purchased from ATCC. Cells were cultured in Dulbecco's Modified Eagle's Medium (Sigma-Aldrich), supplemented with 10% foetal bovine serum (HyClone) and antibiotics, in a 5% CO₂ humidified atmosphere at 37°C. The growth medium of H9c2 cells was implemented with 2 mM L-glutamine and 2 mM sodium pyruvate. CHO-K1 cells were grown in Dulbecco's modified Eagle's medium (DMEM-F12), supplemented with 10% foetal bovine serum and antibiotics.

6. Cell transfection and lysates preparation

Expression vectors for enhanced green fluorescent protein (pEGFP)-tagged Rab4 [17] and enhanced red fluorescent protein (pmRFP)-tagged Rab5 were kindly provided by Dr Marino Zerial (Max-Planck-Institute, Dresden, Germany). H9c2 cells were transiently transfected with either expression vector by the use of METAFECTENE reagent according to the manufacturer's instructions (Biontex Laboratories GmbH). After 24 h, transfected cells were incubated with the appropriate protein and analyzed. To prepare cell lysates, HepG2 and H9c2 cells were scraped off in PBS, centrifuged at 1,000 g for 10 min and resuspended in lysis buffer (1 mM MgCl₂, 0.25% SDS, 1% Triton X-100 in 10 mM Tris-HCl, pH 7) containing protease inhibitors. Upon 30 min incubation on ice, lysates were centrifuged at 14,000 g for 30 min at 4°C. Supernatants were diluted in loading buffer containing 8 M urea and analyzed, without boiling, by 10% polyacrylamide SDS-PAGE electrophoresis. Protein concentration was determined by BCA assay.

CHO-K1 cells were plated on 6-well culture dishes (1.5×10^5 cells/well) in Dulbecco's modified Eagle's medium (DMEM-F12), supplemented with 10% foetal bovine serum (HyClone) and antibiotics. After 24 h, cells were co-transfected with pSVneo plasmid (0.15 µg), conferring neomycin resistance, and the plasmid encoding either ApoA-I(L174S) or the wild-type protein (1.5 µg). Transfections were performed using Lipofectine (Invitrogen) as described by the manufacturer. After 48 h, cells were grown in the presence of 0.5 mg/ml G418 to select stably transfected clones.

HepG2 cells were plated on 6-well culture dishes (2×10^5 cells/well) in DMEM, supplemented with 10% foetal bovine serum and antibiotics. After 24 h, cells were transfected with the plasmid pRC-rsv conferring neomycin resistance and encoding either wild-type ApoA-I or its amyloidogenic variant carrying the substitution of Leu 75 for Pro (indicated as L75P-ApoA-I). Transfections were performed using Lipofectine as described by the manufacturer. After 48 h, cells were grown in the presence of 0.8 mg/ml G418 to select stably transfected clones.

7. Western blot analyses

For Western blot analyses, following gel electrophoresis, proteins were transferred onto polyvinylidene fluoride (PVDF) membranes (Immobilon-P, Millipore) (25 V, overnight, at 4°C). Membranes were then incubated with the blocking solution (5% BSA in PBS buffer containing 0.1% Tween-20) at RT for 1 h. Following blocking step, membranes were washed with PBS buffer containing 0.1% Tween-20, and incubated at RT for 1 h with one of the following antibodies directed towards: human ApoA-I (dilution 1:500), ATP synthase β-chain (dilution 1:1,000), nicastrin antibodies (dilution 1:1,000), angiogenin (ANG) (1 µg/ml), actin (dilution 1:1,000), B23 (0.3 µg/ml). Membranes were then washed with PBS buffer containing 0.1% Tween-20 and incubated on a shaker for 1 h at RT with goat anti-rabbit or goat anti-mouse

secondary antibodies conjugated to horseradish peroxidase enzyme (HRP). Membranes were then washed with PBS buffer containing 0.1% Tween-20. The detection of immuno-positive species by enzyme-linked chemiluminescence (enhanced chemiluminescence: ECL) was performed according to the manufacturer's instructions (Super Signal®West-Pico Chemiluminescent Substrate, Pierce), using a Phosphoimager (Biorad).

8. Binding assays

Proteins under test (100 µg) were labelled with 1 mCi carrier-free Na¹²⁵I (Amersham) using Iodobeads (Pierce), according to the manufacturer's instructions. Labelled proteins were desalted on PD10 columns (Pharmacia) equilibrated in PBS. The specific activity was about 1.5 µCi/µg. Cells were seeded in 24-well plates at a density of 5x10⁴/well. After 24 h, 200 µl of binding buffer (25 mM Hepes, pH 7.5, 1 mg/ml BSA in DMEM), containing increasing concentrations of the labelled protein under test, were added to the cells. Following 2 h incubation at 4°C, cells were washed three times with PBS containing 0.1% BSA. Bound radioactivity (total binding) was removed by treating cells with 0.7 ml of cold 0.6 M NaCl in PBS for 2 min on ice and measured with a gamma counter (Packard Instrument Co.). Non-specific binding was determined by incubating the cells with the labelled protein in the presence of a 40-fold molar excess of the unlabelled protein. Specific binding was calculated by subtracting non-specific binding from total binding. Affinity constant values (K_d) were calculated according to the Scatchard equation.

9. Cytotoxicity assays

For [1-93]ApoA-I experiments, cells were seeded in 96-well plates (100 µl/well) at a density of 5x10³/well. After 24 h, [1-93]ApoA-I, dissolved in 12 mM sodium phosphate buffer, pH 6.4 (1 mg/ml) and centrifuged to remove insoluble material, was added to the medium to a final concentration of 5 or 10 µM. To test fibrillar aggregates, [1-93]ApoA-I was incubated as described above, and insoluble species were resuspended in cell medium at a final concentration of 5 or 10 µM and added to the cells. Cells were then grown for 72 h at 37°C. Cell viability was assessed by the MTT assay. MTT reagent, dissolved in DMEM without phenol red (Sigma-Aldrich), was added to the cells (100 µl/well) to a final concentration of 0.5 mg/ml. After 4 h at 37°C, the culture medium was removed and the resulting formazan salts were dissolved by the addition of isopropanol containing 0.1 N HCl (100 µl/well). Absorbance values of blue formazan were determined at 570 nm using an automatic plate reader (Microbeta Wallac 1420, Perkin Elmer). Cell survival was expressed as the percentage of viable cells in the presence of the protein under test, with respect to control cells grown in the absence of the protein. Error bars correspond to the s.d. values of three independent experiments.

For the experiments on cell viability in stress conditions in the presence or absence of ANG, cells were seeded in 96-well plates (100 μ l/well) at a density of 3×10^3 /well. After 24 h, cells were grown in complete or serum free medium in the absence or presence of 0.5 μ g/ml wt ANG, or its mutants, for different length of time (24, 48, 72, 96 h). Cell viability was assessed by calculating the number of viable cells by the MTT assay. For each cell line, a calibration curve was obtained by plating increasing number of cells in a multiwell plate (from 0.5×10^3 to 7×10^3 cells) and performing the MTT assay. Error bars correspond to the s.e. values of three independent experiments.

10. Fluorescence studies

Immediately prior to be tested, proteins were dissolved or dialyzed in 0.1 M sodium carbonate, pH 9.0, to a final concentration of 1 mg/ml. Proteins (500 μ g) were conjugated to fluorescein isothiocyanate (FITC), following the manufacturer's protocol (Sigma-Aldrich). A Sephadex G25 column, equilibrated in PBS, was used to separate the unreacted FITC from the conjugate. The same procedure was used to label proteins with rhodamine. Fluorescent fibrillar aggregates of [1-93]ApoA-I were obtained by incubating the FITC-labelled polypeptide as described for the unlabelled polypeptide. Insoluble aggregates were resuspended in cell medium and tested as described below. Cells were seeded on glass coverslips in 24-well plates and grown to semi-confluency. Cells were incubated for the indicated times in complete medium with fluorescent proteins or compounds at the following concentrations: [1-93]ApoA-I (3 μ M), ApoA-I (1 μ M), dextran (5 mg/ml), transferrin (0.5 mg/ml), insulin (0.1 mg/ml). Lysosomes were labelled by adding LysoTracker Red (1:500) to living cells at 37°C. After 40 min, cells were treated with 1 μ g/ml Hoechst 33342 for 10 min at 37°C and washed with PBS. When required, surface bound proteins were stripped with 1 M HEPES, pH 7.5, containing 0.5 M NaCl (HEPES/NaCl) for 5 min. Cells were then fixed for 10 min at RT with 4% paraformaldehyde in PBS.

To inhibit clathrin-dependent endocytosis, cells were pre-incubated in the presence or in the absence of either 100 μ M monodansylcadaverine (MDC) for 30 min, or with 300 μ M sucrose for 15 min. Cells were then incubated for 6 h with the fluorescent protein under test. For immunofluorescence analyses, cells were permeabilized with 0.5% Triton X-100 in PBS (5 min). Cells were then incubated for 30 min with 3% goat serum in PBS to saturate non-specific binding sites. Afterwards, cells were incubated overnight at 4°C with anti-ABCA1 antibodies (1:200), or anti- β -catenin antibody (1:200), and then rinsed with 0.1% Triton X-100 in PBS. Finally, cells were incubated 1 h in the darkness with fluorescent goat anti-rabbit or anti-mouse IgG (1:500). Slides were washed with 0.1% Triton X-100 in PBS and then with PBS, and mounted in 50% glycerol in PBS. Samples were examined using a Leica 6000 UV microscope and a Leica TCS SP5 confocal microscope, equipped with a Leica application suite software. All images were taken under identical conditions.

11. Protein degradation analyses

To inhibit proteasome activity, cells were pre-treated for 4 h at 37°C with 2.5 µM Z-Leu-Leu-Leu-al (MG132), or with 10 µM N-Ac-Leu-Leu-norleucinal (ALLN). Cells were then incubated with the fluorescent protein for the indicated times. Intralysosomal catabolism was inhibited by treating cells with 20 mM ammonium chloride or 100 µM chloroquine. As a control, cells were incubated under the same conditions but in the absence of the inhibitors.

12. Analysis of ApoA-I expression and secretion

Transfected or untransfected CHO-K1 cells were plated on 6-well culture dishes (1×10^5 cells/well) in DMEM-F12. After 24 h, the medium was replaced by HyQSFMCHO and cells were grown in the absence of serum for different lengths of time (24, 48, 72 h). Cells were then counted using the trypan blue exclusion assay. Then, for each sample the cell-conditioned medium and the cell lysate were analysed for the presence of the recombinant protein. To analyse intracellular proteins, 20,000 cells were lysed in 1% NP40 in PBS containing protease inhibitors (Roche, Germany). Upon 30 min incubation on ice, lysates were centrifuged at 14,000 g for 30 min at 4°C. Following the determination of protein content by the BCA assay, 25 µg of proteins were analysed by 15% polyacrylamide SDS-PAGE electrophoresis, followed by Western blotting with anti-ApoA-I antibodies (1:500 dilution). Similarly, aliquots of conditioned medium corresponding to 20,000 cells were analysed for the presence of the recombinant protein.

13. Isolation of the recombinant full-length proteins

Transfected cells were plated at a density of 8×10^4 cells/cm² (corresponding to 2×10^5 cells/ml) in HyQSFMCHO serum-free medium for 72 h (serum-free procedure). The cell-conditioned medium was collected and centrifuged at 1500 rpm for 15 min at room temperature to remove cell debris. Sodium chloride (0.8 M final concentration) was added to the supernatant and the sample was centrifuged at 12000 rpm for 15 min at 4°C to remove insoluble species, filtered and loaded on a hydrophobic chromatography column (1 ml, HiTrap Butyl-S FF, GE Healthcare) following the manufacturer's instructions. Briefly, after loading, the column was washed with 10 volumes of washing buffer (0.8 M sodium chloride in 50 mM sodium phosphate buffer pH 7) to remove unbound proteins; recombinant ApoA-I was then eluted with 20 volumes of 20% isopropanol in 10 mM sodium phosphate buffer. Fractions were analysed by SDS-PAGE on 15% polyacrylamide gels followed by Coomassie staining and Western blotting with anti-ApoA-I antibodies.

For immuno-affinity chromatography, a matrix was generated by linking anti-ApoA-I antibodies to an N-hydroxysuccinimide-activated resin (HiTrap, GE Healthcare)

following the manufacturer's instructions. The column (1 ml) was equilibrated in PBS. After loading, unbound proteins were removed by extensive washing (PBS, 10 volumes) and the recombinant protein was eluted in 0.1 M glycine/HCl buffer, pH 2.7. Reverse phase high-performance liquid chromatography (RP-HPLC) was performed on a Ultrapure C4 column (Vydac, Grace, IL, USA) with a gradient of buffer B (95% acetonitrile, 5% formic acid in 0.05% trifluoroacetic acid) in buffer A (5% formic acid in 0.05% trifluoroacetic acid) using a PerkinElmer chromatographic system (Series 200). Proteins were eluted in 100% buffer B.

14. Co-immunoprecipitation experimental procedure

Rat embryos H9c2 cells ($2 \times 10^4/\text{cm}^2$) were scraped off in PBS, centrifuged at 1,000 g for 10 min, resuspended in lysis buffer (50 mM Tris-HCl pH 7.4 containing 150 mM NaCl, 10% glycerol, 1 mM EDTA) containing protease inhibitors and incubated 10 min on ice. At the end of incubation, 0.025% Triton X-100 was added to the lysis buffer, the sample was incubated at 4°C for 30 min and centrifuged at 3,750 rpm for 30 min. The pellet (cell membranes) was resuspended in lysis buffer and, upon incubation on ice for 10 min, 0.2% N-dodecyl β D-maltoside was added to the sample. After 30 min incubation at 4°C, the sample was centrifuged at 3,750 rpm for 20 min. The protein content of supernatant containing membrane proteins, was determined by using the BCA assay.

In order to remove components potentially interacting with the resin, prior to the co-immunoprecipitation step the sample was pre-cleared by incubating 15 μ l of protein G agarose resin with H9c2 membrane protein extracts (300 μ g) for 30 min at RT. Following centrifugation at 2,000 g for 5 min, the supernatant (i.e. proteins non interacting with the resin) was incubated for 2 h at RT with 15 μ g of fluorescent FITC-labelled [1-93]ApoA-I. A primary antibody, able to specifically recognize FITC molecule, was then added to the sample (150 μ g). Upon 1.5 h incubation at RT, 60 μ l of protein G agarose resin were added to the protein mixture. Following an additional 1.5 h incubation at RT, the sample was centrifuged at 2,000 g for 5 min to remove unbound protein species (supernatant). Multiple washes of the pellet with 100 μ l of PBS were performed in order to remove contaminant protein species. Selected protein complexes were then eluted by the addition of 100 μ l of SDS-PAGE reducing and denaturing loading buffer and analyzed by Western blotting.

15. Quantitative RT-PCR (qRT-PCR) analysis of ANG mRNA

cDNA was synthesized using Quantitect Reverse Transcription kit from 1 μ g of DNase-treated total RNA. Real-time qRT-PCR on cDNAs was carried out using a Light CyclerO 480 SYBR Green I Master with the Light Cycler 480 Detection System (Roche). Cycling conditions were: 95 °C, 5 min; (95 °C, 10 sec; 60 °C, 10 sec) repeated for 40 cycles; 72 °C, 15 sec.

ANG primers used for the PCR were designed using the PrimerDesigner 2.0 software with the following sequences: forward primer, 5'-AGAAGCGGGTGAGAAACAA-3'; reverse primer, 5'-TGTGGCTCGGTACTGGCATG-3', which are complementary to the ANG mRNA (GenBank accession number NG_008717.2), respectively. Actin primer sequences were: forward primer, 5'-ATCACTATTGGCAACGAGC-3'; reverse primer, 5'-GGTCTTTACGGATGTCAACG-3'. The primers were first confirmed for their ability to amplify the correct replicon by RT-PCR. qRT-PCR experiments were performed in triplicate and the results were analyzed using the comparative Ct method normalized against the housekeeping gene ACTIN. The range of ANG expression levels was determined by calculating the standard deviation of the Δ Ct.

16. Nucleolar fraction preparation

Nucleolar fraction was prepared following the method described by Muramatsu and co-workers [80], upon modifications. Briefly, cells were detached by trypsinization, washed extensively with ice-cold PBS and centrifuged at 218 g at 4°C. The cell pellet was resuspended in Buffer A (10 mM Hepes, pH 7.9, 10 mM KCl, 1.5 mM MgCl₂, 0.5 mM DTT) and incubated on ice for 5 min. Cells were homogenized using a tight pestle, while keeping the homogenizer on ice, and centrifuged at 218 g for 5 min at 4°C. The pellet was resuspended in S1 solution (0.25 M sucrose, 10 mM MgCl₂), layered over 3 ml of S2 solution (0.35 M sucrose, 0.5 mM MgCl₂) and centrifuged at 1,430 g for 5 min at 4°C. The pellet was resuspended in S2 solution, sonicated, layered over 3 ml of S3 solution (0.88 M sucrose, 0.5 mM MgCl₂) and centrifuged at 3,000 g for 10 min at 4°C. The pellet, containing the nucleoli, was resuspended with S2 solution, followed by centrifugation at 1,430 g for 5 min at 4°C. Nucleoli were stored at -80°C in S2 solution. To analyse nucleolar proteins, nucleoli were lysed in RIPA buffer (150 mM NaCl, 1% NP40, 0.5% deoxycholate, 0.1% SDS, 50 mM Tris pH 8.0, protease inhibitor cocktail). Upon 30 min incubation on ice, lysates were centrifuged at 1,500 g for 10 min at 4°C. Following the determination of protein content by the BCA assay, 50 µg of proteins were analysed by 4-20% polyacrylamide SDS-PAGE electrophoresis, followed by Western blotting using specific antibodies.

17. EBAO staining of apoptotic cells

The method described by Ribble et al. [81] was followed. Briefly, cells were detached by trypsinization, centrifuged and washed in ice-cold PBS. Cells were resuspended in 50 µl of PBS containing the EB-AO dye mixture (5 µg/ml) for 15 min at 37°C. Stained cells were placed on a clean microscope slide and covered with coverslips. Microscopic images were taken as described above. A total of more than 750 cells were counted for each group.

RESULTS

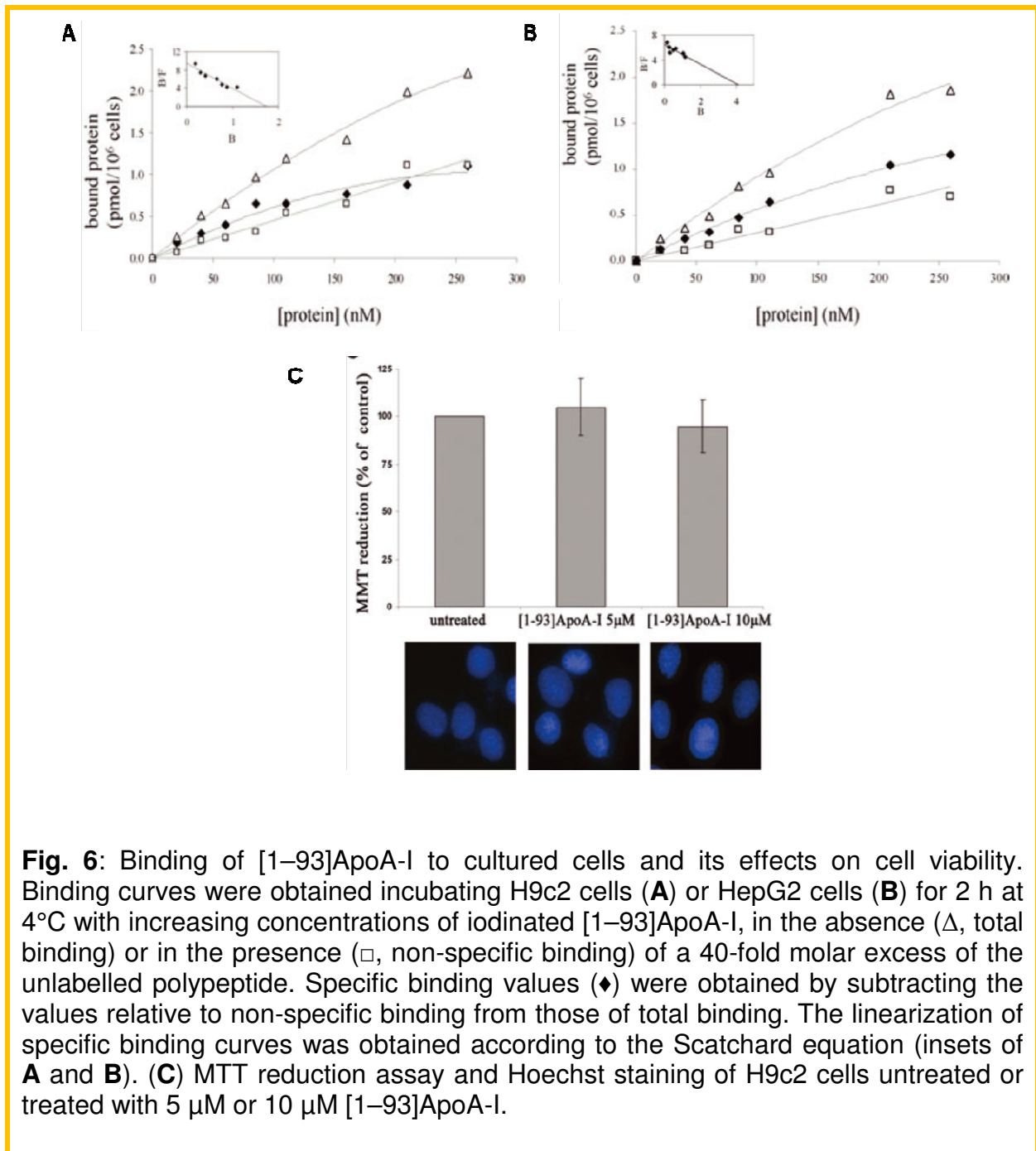
1. MECHANISTIC STUDIES: Membrane interaction, internalization and intracellular pathway of ApoA-I fibrillogenic polypeptide

The molecular mechanism responsible for ApoA-I associated amyloid diseases remains largely unknown. From a general point of view, the elucidation of the cascade of biochemical events triggered by the exposure of cells to fibrillogenic proteins or polypeptides has a primary importance in the comprehension of amyloid diseases. Upon its release, [1-93]ApoA-I is expected to accumulate in the extracellular space. Therefore, the possibility that the fibrillogenic polypeptide of ApoA-I interacts with membranes of target cells and enters the cell compartment, mimicking ApoA-I full-length protein, has to be taken into account. Since in the case of ApoA-I associated amyloidoses the heart is a natural target for aggregate deposition *in vivo*, cardiomyoblasts were chosen as an experimental system to analyze the intracellular pathway of [1-93]ApoA-I in comparison to full-length ApoA-I.

1.1 [1-93]ApoA-I specifically binds to cardiomyoblasts

Binding assays of ¹²⁵I-labelled [1-93]ApoA-I to rat cardiomyoblasts (H9c2) and human hepatocytes (HepG2) were performed to test the ability of [1-93]ApoA-I to recognize and bind specific sites on cell surface. These cell lines are of interest as in ApoA-I associated amyloidoses the heart is a natural target for aggregate deposition *in vivo*, while the liver is the major source of ApoA-I. The binding curves and the linearization of the binding data, according to the Scatchard equation (Fig. 6A and B), indicate that the fibrillogenic fragment is able to bind with high affinity to specific sites on cell surface of both cell lines. In particular, the apparent affinity constants were $5.90 \pm 0.70 \times 10^{-7}$ M and $1.78 \pm 0.26 \times 10^{-7}$ M for H9c2 and HepG2 cells, respectively. These data are comparable to those previously reported for lipid-free ApoA-I binding to other cell lines and are consistent with the finding that region 62-77 of ApoA-I is a membrane binding domain of lipid-free ApoA-I, since the corresponding synthetic peptide binds with high affinity to HepG2 cells [82].

The effects of the fibrillogenic polypeptide on cell viability were then analyzed. H9c2 cells were incubated for 72 h in the presence of 5 or 10 μ M [1-93]ApoA-I and MTT reduction assays were performed to test metabolically active cells. No inhibition of cell viability was observed in treated cells with respect to untreated cells (Fig. 6C). Furthermore, the absence of apoptotic nuclei in treated cells (Fig. 6C) confirmed that the fibrillogenic polypeptide, at least in our experimental conditions, is not cytotoxic for cardiomyoblasts.



1.2 [1-93]ApoA-I endocytosis in cardiomyoblasts

To test whether [1-93]ApoA-I undergoes endocytosis upon interaction with cardiomyoblasts plasma membrane, the fibrillogenic polypeptide was labelled with fluorescein isothiocyanate (FITC). Parallel experiments were performed using labelled full-length ApoA-I. H9c2 cells were incubated for different lengths of time either with the polypeptide or with the full-length protein, cells were then fixed and, after membrane permeabilization, anti-β-catenin antibody was added to the cells to label the plasma membrane compartment. Analyses by fluorescence microscopy after 2 h incubation indicated that the polypeptide is able to bind plasma membrane (Fig. 7A). After 6 h incubation it was found to have been internalized in target cells

(Fig. 7B). Similar results were obtained with labelled ApoA-I. Thus, [1-93]ApoA-I and the full-length protein are able to enter cardiac cells.

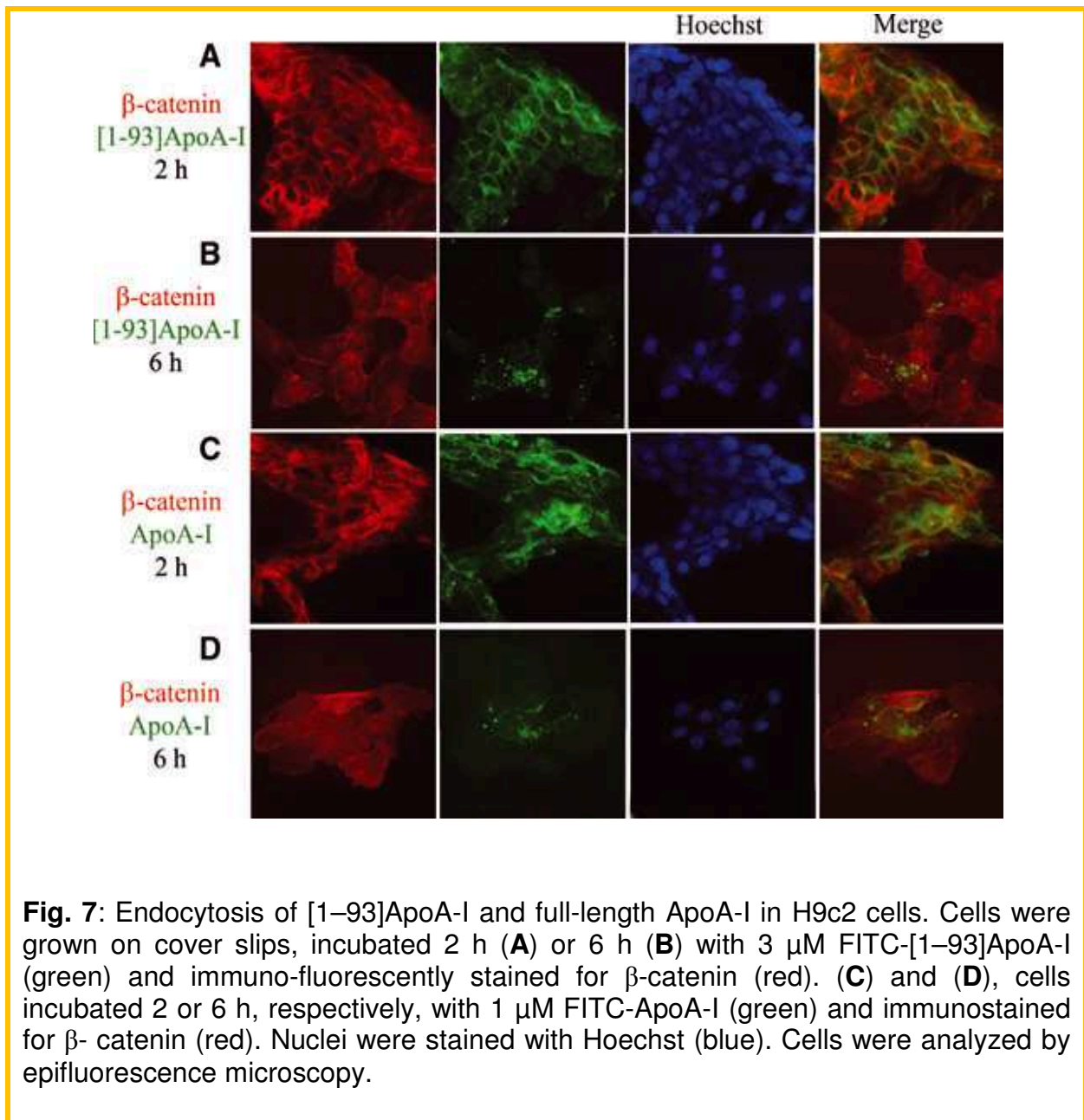


Fig. 7: Endocytosis of [1–93]ApoA-I and full-length ApoA-I in H9c2 cells. Cells were grown on cover slips, incubated 2 h (A) or 6 h (B) with 3 μ M FITC-[1–93]ApoA-I (green) and immuno-fluorescently stained for β -catenin (red). (C) and (D), cells incubated 2 or 6 h, respectively, with 1 μ M FITC-ApoA-I (green) and immunostained for β -catenin (red). Nuclei were stained with Hoechst (blue). Cells were analyzed by epifluorescence microscopy.

It is well known that the plasma membrane is the main site where lipidation of ApoA-I occurs. This process is mediated by the ATP-binding cassette transporter A1 (ABCA1) [83], which allows cellular free cholesterol and phospholipids to be transferred to ApoA-I, leading to the biogenesis of nascent HDL. As ABCA1 transporter plays a central role in ApoA-I membrane binding and lipidation, H9c2 cells were analyzed for the presence of this transporter. H9c2 cell lysates were analyzed by Western blotting with anti-ABCA1 antibodies. As shown in Fig. 8A, an immuno-positive species, with an apparent molecular mass corresponding to that expected for ABCA1 (about 210 kDa), was found to be present in cell extracts prepared from H9c2 (lane 2) and

HepG2 (lane 1) cells, the latter used as a positive control. These results were confirmed by immuno-fluorescence analyses of H9c2 and HepG2 cells with anti-ABCA1 antibodies, that revealed immuno-positive signals in both cell lines (Fig. 8B and C).

Furthermore, to test whether the fibrillogenic polypeptide co-localizes with ABCA1, H9c2 cells were incubated with rhodamine-[1-93]ApoA-I for 2 h. Cells were then fixed and incubated with anti-ABCA1 antibodies to label the transporter. A little co-localization between [1-93]ApoA-I (red signal) and ABCA1 (green signal) was found (Fig. 8D). Similar results were obtained with rhodamine-ApoA-I (Fig. 8E), in agreement with recent reports showing that the majority of cell-associated ApoA-I does not co-localize with ABCA1 [84].

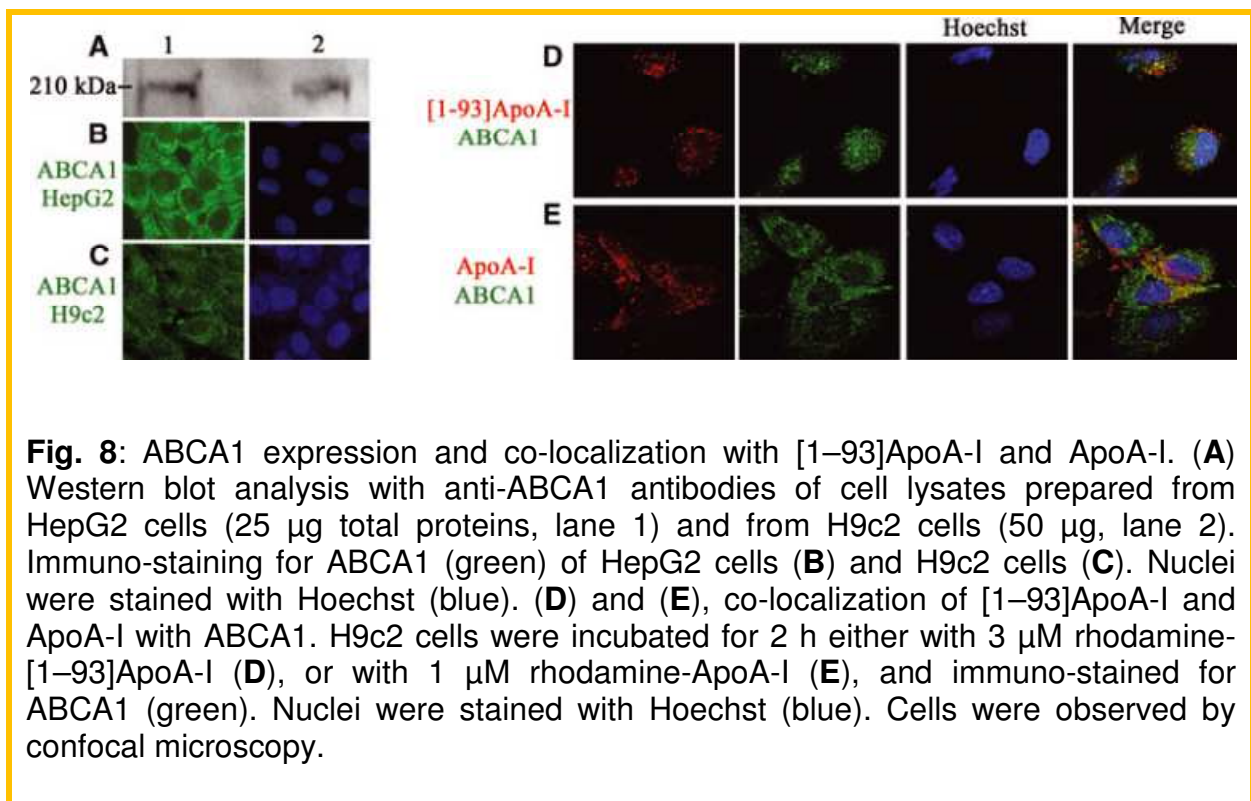


Fig. 8: ABCA1 expression and co-localization with [1–93]ApoA-I and ApoA-I. (A) Western blot analysis with anti-ABCA1 antibodies of cell lysates prepared from HepG2 cells (25 µg total proteins, lane 1) and from H9c2 cells (50 µg, lane 2). Immuno-staining for ABCA1 (green) of HepG2 cells (B) and H9c2 cells (C). Nuclei were stained with Hoechst (blue). (D) and (E), co-localization of [1–93]ApoA-I and ApoA-I with ABCA1. H9c2 cells were incubated for 2 h either with 3 µM rhodamine-[1–93]ApoA-I (D), or with 1 µM rhodamine-ApoA-I (E), and immuno-stained for ABCA1 (green). Nuclei were stained with Hoechst (blue). Cells were observed by confocal microscopy.

1.2.1 [1-93]ApoA-I internalization pathways

The mechanism of [1-93]ApoA-I uptake in cardiomyoblasts has been investigated by analyzing different routes involved in endocytosis.

The involvement of clathrin-coated pits was evaluated using Rab5 as a marker, as this protein regulates vesicular transport from the plasma membrane to the endosomes. H9c2 cells were transiently transfected with Rab5 fused to red fluorescent protein (RFP) and, 24 h after transfection, cells were incubated for 6 h with the FITC-protein under test, in order to allow protein internalization. Co-localization of internalized [1-93]ApoA-I (green signal) with RFP-Rab5 (red signal) was observed (Fig. 9A), indicating that a fraction of the internalized polypeptide is associated to early endosomes. Similar results were obtained when ApoA-I was tested (Fig. 9B). To further confirm that both [1-93]ApoA-I and ApoA-I are internalized in H9c2 cells by clathrin-mediated endocytosis, specific inhibitors of this

internalization pathway, such as monodansylcadaverine (MDC) and sucrose, were used. Upon incubation of H9c2 cells with either MDC or sucrose, the amount of internalized polypeptide, as well as that of the full-length protein, appeared to be reduced, although not fully blocked. This might indicate that in these experimental conditions the endocytic pathway still functions, or, alternately, that endocytosis of [1-93]ApoA-I and ApoA-I does not occur solely *via* clathrin coated pits.

The involvement of lipid rafts in [1-93]ApoA-I endocytosis was then analyzed. To analyze this route of internalization, FITC-insulin was used as a marker. H9c2 cells were incubated with rhodamine-[1-93]ApoA-I in the presence of FITC-insulin for 4 h. Analyses by fluorescence microscopy indicated strong signals of co-localization of [1-93]ApoA-I (red signal) with insulin (green signal), indicating that [1-93]ApoA-I uptake occurs also by lipid rafts (Fig. 9C). On the other hand, when the same experiment was performed with rhodamine-ApoA-I, little co-localization of the full-length protein with FITC-insulin was observed (Fig. 9D) indicating that this route of endocytosis is not predominant for ApoA-I internalization in cardiac cells.

Moreover, since it has been demonstrated that ApoA-I is also internalized by macropinocytosis in other cell lines [85], this internalization route was also tested. H9c2 cells were incubated with rhodamine-[1-93]ApoA-I in the presence of FITC-dextran, as a macropinocytosis marker. A little co-localization was observed between [1-93]ApoA-I (red signal) and dextran (green signal) (Fig. 9E). On the contrary, clear signals of co-localization were detected for ApoA-I (Fig 9F).

As it has been reported that ApoA-I, once internalized, is recycled back to the cell surface [83,86,87], the ability of [1-93]ApoA-I to be recycled to the plasma membrane was analyzed.

To investigate the retroendocytosis pathway, Rab4 was used as a marker, as it directs protein recycling from early endosomes to the plasma membrane. H9c2 cardiomyoblasts were transiently transfected with a vector encoding Rab4 fused to the green fluorescent protein (GFP). 24 h after transfection, cells were incubated with rhodamine-[1-93]ApoA-I, or ApoA-I, for 6 h at 37°C. As shown in Fig. 10A, [1-93]ApoA-I does not co-localize with Rab4-positive endosomal compartments, while significant signals of co-localization were observed for ApoA-I (Fig. 10B).

Taken together, these results clearly indicate that the fibrillogenic polypeptide, once internalized in cardiomyoblasts, is not recycled to the cell membrane, whereas ApoA-I is shuttled back to the plasma membrane to be re-secreted, as described in other cell lines [83, 86, 87].

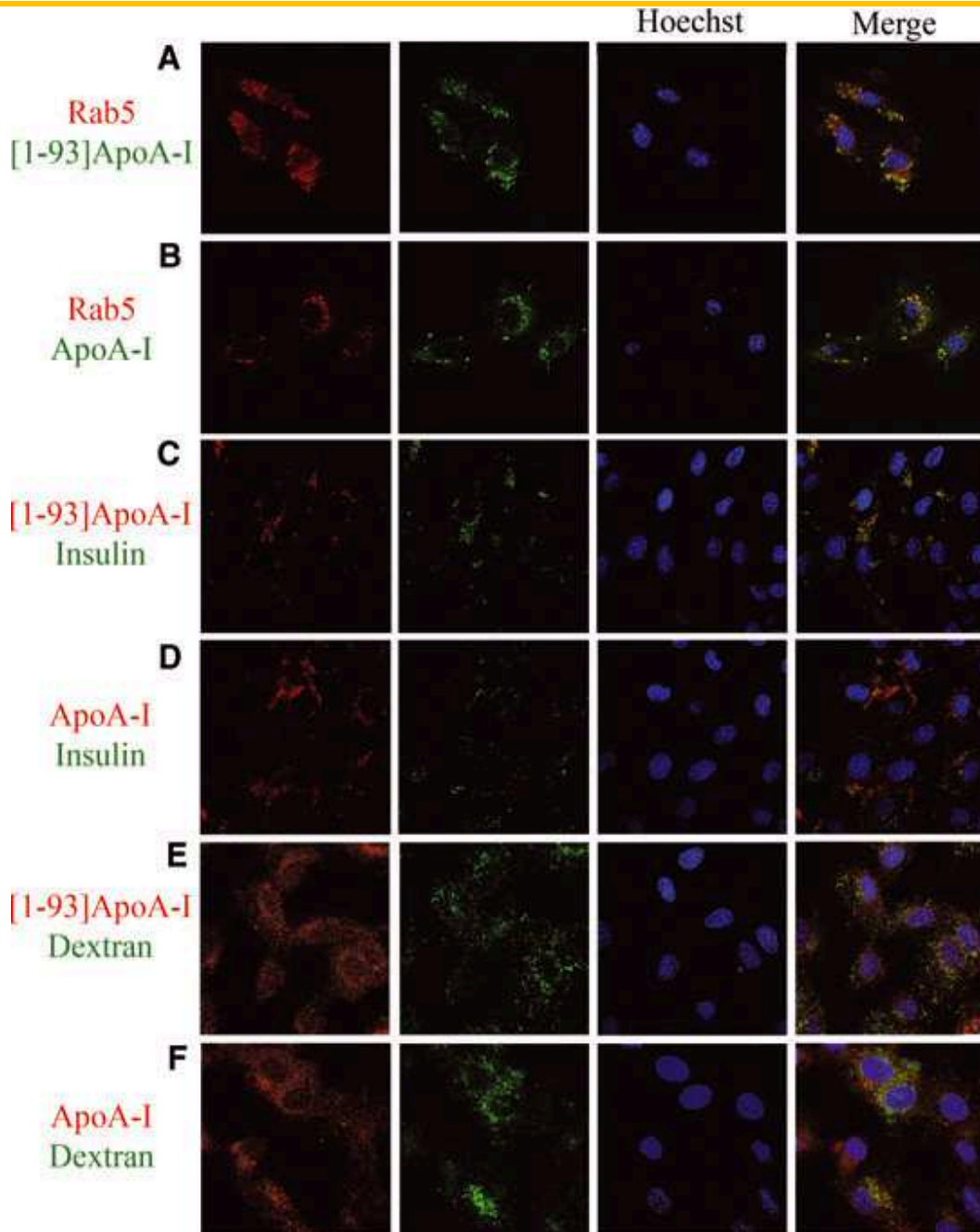
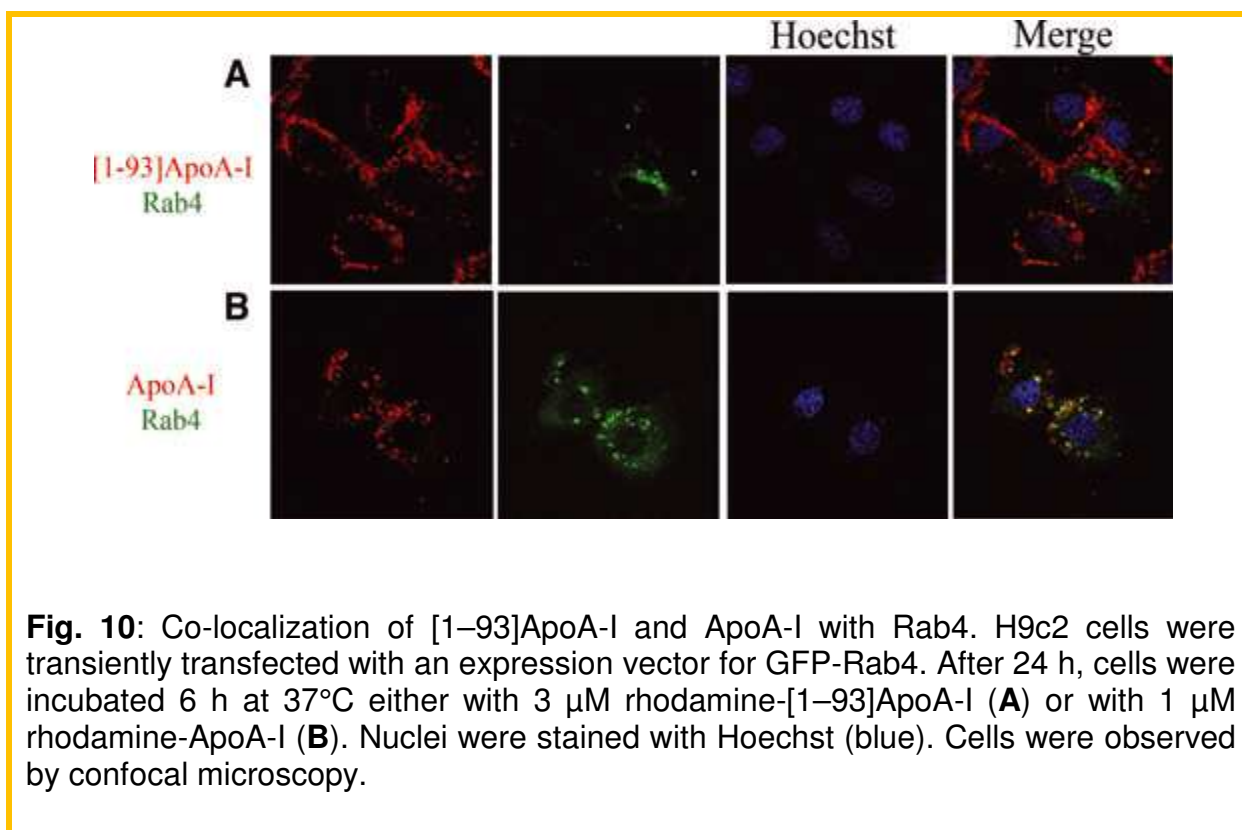


Fig. 9: Analysis of the route of [1–93]ApoA-I and ApoA-I endocytosis in H9c2 cells by confocal microscopy. (A) and (B), clathrin-mediated endocytosis. H9c2 cells were transiently transfected with an expression vector for RFP-Rab5. After 24 h, cells were incubated 6 h at 37°C either with 3 μM FITC-[1–93]ApoA-I (A) or with 1 μM FITC-ApoA-I (B). (C) and (D), lipid rafts-mediated internalization. Cells were incubated 4 h at 37°C either with 3 μM rhodamine-[1–93]ApoA-I (C), or with 1 μM rhodamine-ApoA-I (D), in the presence of FITC insulin (0.1 mg/ml). (E) and (F), macropinocytosis. Cells were incubated 4 h at 37°C either with 3 μM rhodamine- [1–93]ApoA-I (E), or with 1 μM rhodamine-ApoA-I (F), in the presence of FITC dextran (5 mg/ml). Nuclei were stained with Hoechst (blue).



1.3 The intracellular fate of [1-93]ApoA-I: proteasomal and lysosomal degradation

The fate of the internalized polypeptide in cardiomyoblasts was also analyzed. After a prolonged exposure of H9c2 cells to FITC-[1-93]ApoA-I (24 h), the complete disappearance of the intracellular fluorescent signals associated to the polypeptide was observed, suggestive of polypeptide massive degradation (Fig. 11A).

Specific inhibitors of proteasomal and lysosomal activities were used to investigate the degradation pathway of the fibrillogenic polypeptide. When cells were pre-incubated with the proteasome inhibitor MG132, the persistence of [1-93]ApoA-I associated fluorescent signal was observed after 24 h incubation, indicative of proteasome involvement in [1-93]ApoA-I degradation (Fig. 11B). To test whether [1-93]ApoA-I is also targeted to lysosomes, cells were incubated with FITC-[1-93]ApoA-I in the presence of ammonium chloride, an inhibitor of intra-lysosomal catabolism. Following incubation, lysosomes were labelled with LysoTracker red. After incubation for 24 h, a strong fluorescent signal associated to the polypeptide (green signal) was found to co-localize with lysosomes (red signal) (Fig. 11C and D), suggesting that lysosomes play a role in [1-93]ApoA-I catabolism. Different results were obtained instead in the case of full-length ApoA-I, as the protein does not appear to be significantly degraded once internalized (Fig. 11E). This is in agreement with recent reports indicating that in different cell types ApoA-I is not significantly degraded [85]. Moreover, ApoA-I was found to co-localize with lysosomes, in line with reports indicating that lysosomes are an intracellular station of ApoA-I (Fig. 11G and H) [85].

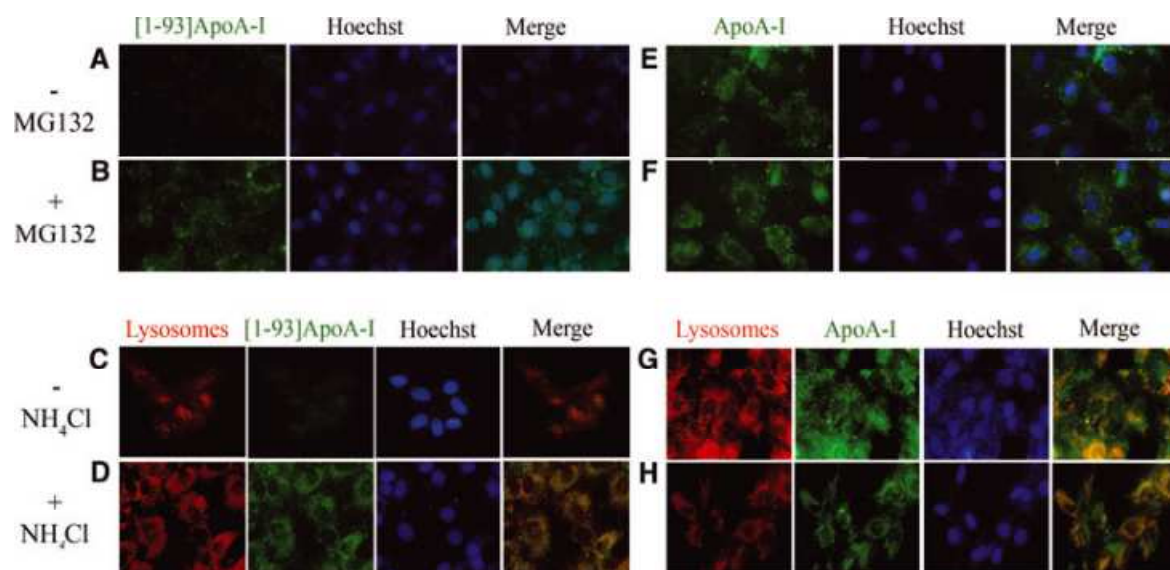


Fig. 11: Analysis of the degradation pathway of [1–93]ApoA-I and ApoA-I in H9c2 cells by epifluorescence microscopy. (A)–(D) [1–93]ApoA-I degradation. Cells were incubated 24 h at 37°C with 3 μ M FITC-[1–93]ApoA-I in the absence (A, C) or in the presence of MG132 (2.5 μ M) (B), or ammonium chloride (100 μ M) (D). (E)–(H), ApoA-I degradation. Cells were incubated for 24 h at 37°C with 1 μ M FITC-ApoA-I, in the absence (E and G) or in the presence of MG132 (F), or ammonium chloride (H). Lysosomes were stained with LysoTracker red. Nuclei were stained with Hoechst (blue).

Taken together, these results indicate that the inhibition of lysosomal or proteasomal activity does not significantly alter the amount of intracellular ApoA-I, whereas both pathways seem to be involved in the degradation of the fibrillogenic polypeptide.

1.4 Internalization of [1-93]ApoA-I fibrils in cardiomyoblasts

Relevant results were obtained when the analyses were extended to the polypeptide in the fibrillar state. [1-93]ApoA-I fibrils were obtained by incubating the polypeptide for 2 weeks at pH 6.4 in the presence of the co-solvent TFE. In collaboration with Dr. A. Relini of University of Genoa, incubated samples were analyzed by AFM microscopy. These analyses showed the presence of fibrils with height of 2.4 ± 0.1 nm and length between 0.4 and 1.5 μ m (Fig. 12A). Fibrils coexist with prefibrillar aggregates, including annular protofibrils and spheroidal aggregates of variable size (height between 3 and 15 nm).

To test the effects of fibrils on cell viability, cardiomyoblasts were incubated for 72 h with 5 or 10 μ M aggregated [1-93]ApoA-I (insoluble species). No inhibition of cell viability was observed by MTT assays in treated cells with respect to untreated cells (Fig. 12B). This was confirmed by the absence of apoptotic nuclei in treated cells (Fig. 12B).

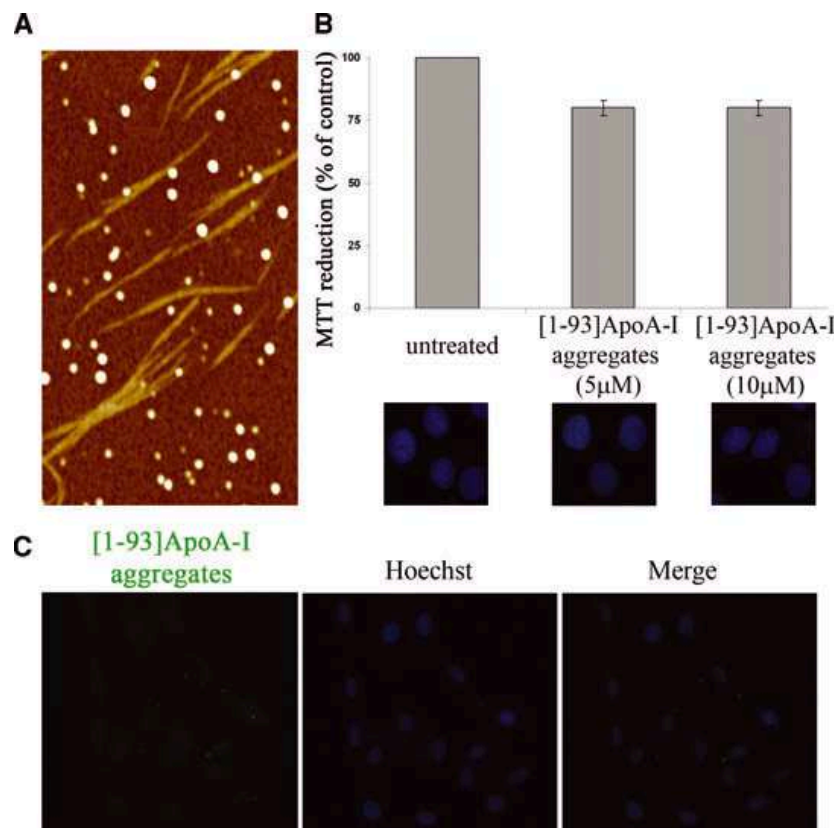


Fig. 12: Analysis of [1–93]ApoA-I fibrils. **(A)** Tapping mode AFM image of aggregated [1–93]ApoA-I. Upon incubation in the aggregating conditions, the whole sample was observed. Fibrils coexist with prefibrillar aggregates; spheroidal aggregates are also found. Scan size 3.0 μm, Z range 10 nm. **(B)** Effects of [1–93]ApoA-I fibrils on cell viability. MTT reduction assay and Hoechst staining of H9c2 cells, untreated or treated with 5 μM or 10 μM [1–93]ApoA-I fibrils, are shown. Error bars indicate standard deviations obtained from three independent experiments. Nuclei images have been acquired at the same magnification. **(C)** Analysis of internalization of [1–93]ApoA-I fibrils in H9c2 cells. Cells were incubated for 6 h with 3 μM FITC-labelled [1–93]ApoA-I fibrils and analyzed by epifluorescence microscopy. Nuclei were stained with Hoechst (blue).

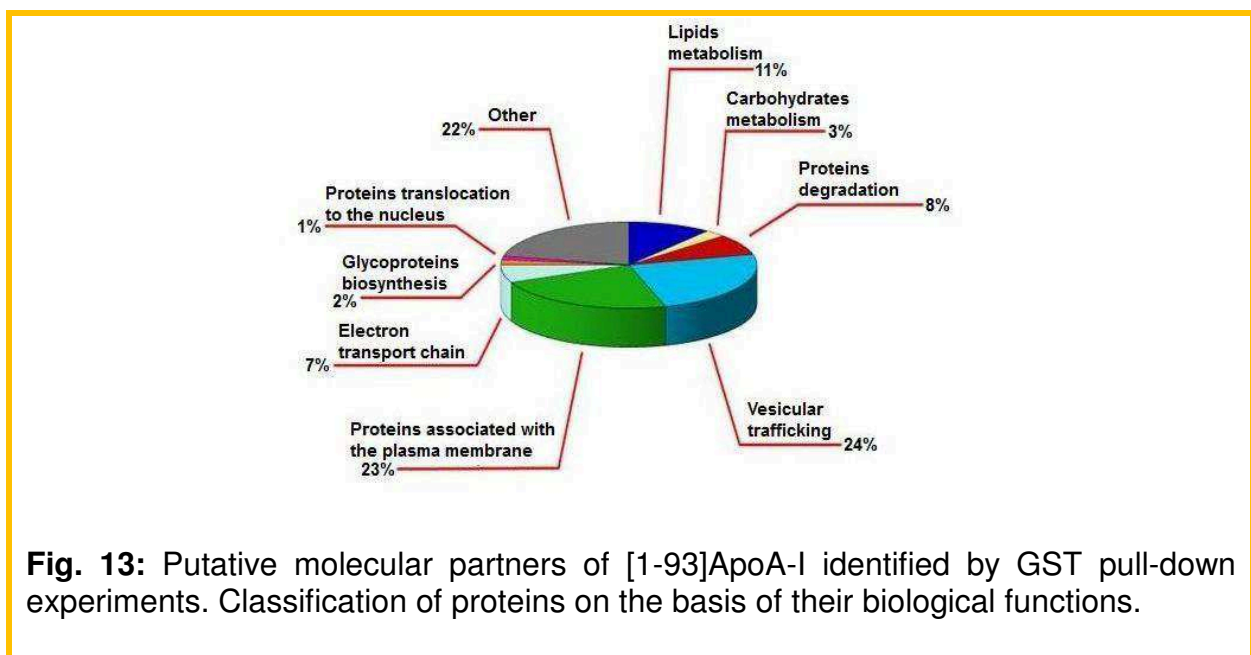
To verify whether the fibrillar material is able to enter the cells, fluorescent fibrils were obtained by incubating FITC-labelled [1-93]ApoA-I under the conditions previously described. H9c2 cells were incubated for 6 h with fluorescent fibrils and then treated with HEPES/NaCl buffer in order to remove polypeptide molecules specifically bound to the extracellular side of the plasma membrane. No fluorescent signals associated to [1-93]ApoA-I fibrils were observed by epifluorescence microscopy analysis (Fig.

12C), demonstrating that no significant internalization of fibrils occurs in cardiomyoblasts.

2. STUDIES ON MOLECULAR TARGETS: Search for molecular partners of the fibrillogenic polypeptide [1-93]ApoA-I

In collaboration with the research group of Prof. P. Pucci, Department of Chemical Sciences, a functional proteomic approach [88, 89] was used to shed light on the molecular basis of ApoA-I associated amyloidoses. This can be achieved by identifying the proteins interacting (interactors) with the fibrillogenic domain of full-length ApoA-I. In order to identify cellular interactors of the fibrillogenic polypeptide, GST pull-down experiments have been conducted by probing proteins extracted from cardiomyoblasts (H9c2 cell line) membrane with the fibrillogenic polypeptide fused to GST (indicated as GST-[1-93]ApoA-I fusion protein). The proteins selected by the bait were identified by mass spectrometry analyses.

This experimental approach provided about 100 potential interactors of the fibrillogenic polypeptide, listed on the basis of their biological function, as well as their subcellular localization (Fig. 13).



A deep analysis of the data bank indicated the presence of several proteins that might play a central role in the mechanism of action of the fibrillogenic polypeptide, such as those that may be involved in its internalization and intracellular transport, or those acting as membrane receptors. Among these putative interactors we selected two proteins to be analyzed in detail: the ATP synthase β -chain and the protein nicastrin.

2.1 ATP synthase β -chain

F₁F₀ ATP synthase, the terminal enzyme of the oxidative phosphorylation pathway, is a complex molecular motor responsible for the large majority of ATP synthesis in all living beings. It is located in the inner membrane of mitochondria, in the thylakoid membrane of chloroplasts in plants, and in the plasma membrane of certain bacteria, where it is part of the so-called "ATP synthasome", in association with an inorganic phosphate (Pi) carrier and with the adenine nucleotide translocase (ANT), which exchanges ADP and ATP.

Interestingly, ATP synthase has been recently detected at the surface of different cell types, wide variety of tumor as well as normal cells. Nevertheless, there is so far no experimental work precisely deciphering the mechanism used by ATP synthase to reach the plasma membrane [90].

Cell surface ATP synthase (namely ecto-F₁-ATPase) expression is related to different biological effects, such as regulation of HDL uptake by hepatocytes, endothelial cell proliferation or antitumor activity of V γ 9/V δ 2 T lymphocytes [90].

An important recent finding is that some components of the F₁ catalytic part of the ATP synthase (also called F₁-ATPase) are expressed as cell surface receptors for apparently unrelated ligands found in the course of studies carried out on cholesterol metabolism, immune mechanisms and angiogenesis [91]. Among these, ATP synthase β -chain was previously identified on the surface of hepatocytes as high-affinity HDL receptor for ApoA-I (K_d = 10⁻⁹ M) [92]. Receptor stimulation by ApoA-I triggers the endocytosis of holo-HDL particles (protein plus lipid) by a mechanism that depends strictly on the generation of ADP [92-94].

Recent results support ApoA-I interaction with endothelial ecto-F₁-ATPase to initiate a signaling pathway contributing to the anti-apoptotic and proliferative effects mediated by HDLs and ApoA-I on endothelial cells [92, 95].

On the basis of this strict correlation between ecto-F₁-ATPase and ApoA-I, it seemed very suggestive to select, within the list of potential interactors of the fibrillogenic polypeptide of ApoA-I, this membrane receptor for further analyses (see below).

2.2 Nicastrin

Nicastrin is an essential subunit of the γ -secretase complex, an endoprotease complex that catalyzes the intramembrane cleavage of integral membrane proteins such as Notch receptors and amyloid precursor protein (APP). It probably represents a stabilizing cofactor required for the assembly of the γ -secretase complex [70, 71]. The complex is composed of a presenilin homodimer (PSEN-1 or PSEN-2), nicastrin (NCSTN), APH-1 (APH-1A or APH-1B) and PEN-2 [96, 97]. Such minimal complex is sufficient for secretase activity, although other components may exist. This complex binds to proteolytic processed C-terminal fragments C83 and C99 of the AD associated amyloid β peptide (A β) [98]. Nicastrin itself is not catalytically active, instead it promotes the maturation and proper trafficking of the other proteins in the complex, all of which undergo significant post-translational modification before becoming active in the cell. Nicastrin has also been identified as a regulator of neprilysin, an enzyme involved in the degradation of A β fragment.

Playing nicastrin an essential role in the mechanism of production of an amyloid peptide, it seemed of interest to inspect its possible involvement in ApoA-I amyloidosis.

2.3 Co-immunoprecipitation as a suitable tool to detect proteins complexes

Co-IP experiments have been performed on cardiomyoblasts membrane extracts, since ATP synthase and nicastrin are membrane proteins.

Membrane protein extracts were incubated with FITC-labelled [1-93]ApoA-I. Following incubation, a primary antibody able to specifically recognize the FITC moiety was added to the sample. Complexes of the fibrillogenic polypeptide with potential partners were selected by a protein G-agarose resin and then eluted with a reducing and denaturing buffer.

First, we verified the presence of the fibrillogenic polypeptide [1-93]ApoA-I in the co-immunoprecipitated protein sample by Western blot analysis with anti-ApoA-I polyclonal antibodies. As shown in Fig. 14, immuno-positive protein species were detected, with a molecular mass corresponding to that of [1-93]ApoA-I.

Protein species co-immunoprecipitated with anti-FITC antibodies, which recognize the fluorescent polypeptide, were then analyzed by Western blotting using antibodies directed towards ATP synthase β -chain or nicastrin.

Western blot analyses performed with anti-ATP synthase β -chain as a primary antibody revealed a unique protein band, whose migration corresponds to a protein with the expected molecular weight of ATP synthase (57 kDa) (Fig. 14, lane 6). A very low immuno-positive signal was detected in the case of unbound material. These observations clearly indicate that ATP synthase β -chain is one of the partners of the fibrillogenic polypeptide of ApoA-I.

The same experiment was then repeated using antibodies directed against nicastrin. First, we analyzed a H9c2 cell lysate for the presence of nicastrin: three immuno-positive protein bands (corresponding to 55, 78 and 95 kDa) were detected (Fig. 14), probably corresponding to three different glycosylated forms. When the co-immunoprecipitated sample was analyzed, the immuno-positive bands corresponding to 55 and 78 kDa were evidenced (see lane 6). These observations strongly suggest that nicastrin is an interactor of the fibrillogenic polypeptide of ApoA-I.

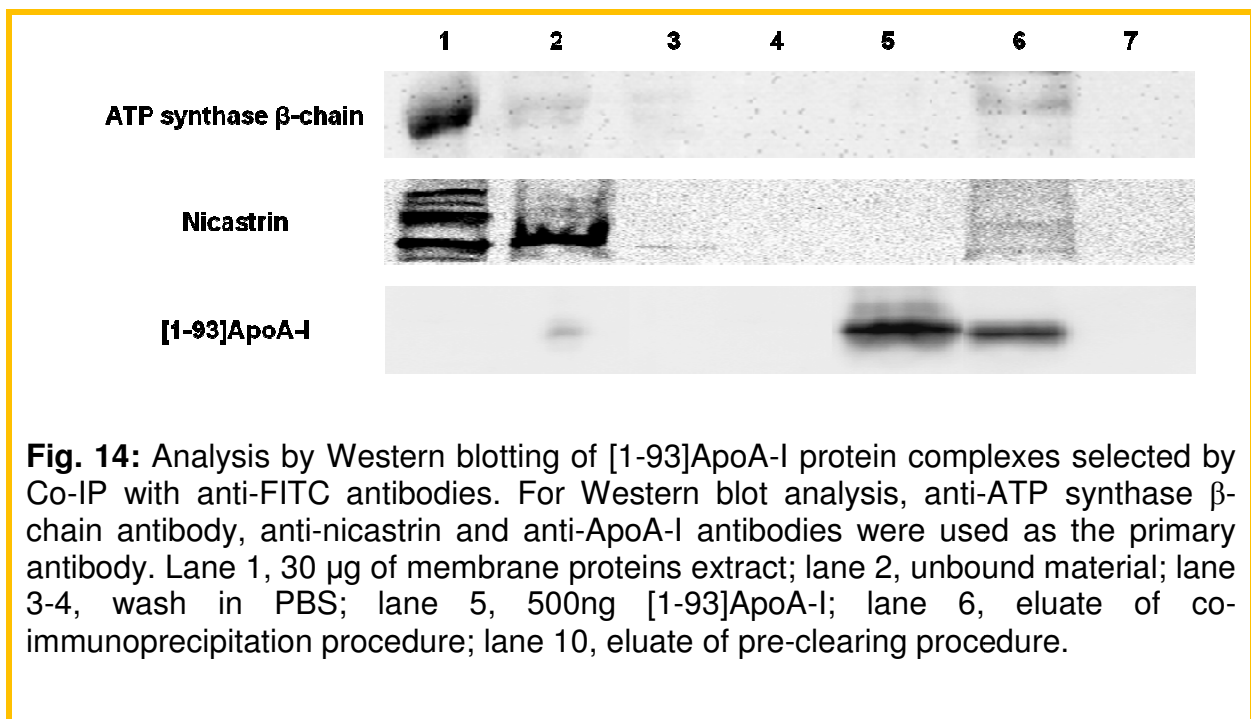


Fig. 14: Analysis by Western blotting of [1-93]ApoA-I protein complexes selected by Co-IP with anti-FITC antibodies. For Western blot analysis, anti-ATP synthase β -chain antibody, anti-nicastrin and anti-ApoA-I antibodies were used as the primary antibody. Lane 1, 30 μ g of membrane proteins extract; lane 2, unbound material; lane 3-4, wash in PBS; lane 5, 500ng [1-93]ApoA-I; lane 6, eluate of co-immunoprecipitation procedure; lane 10, eluate of pre-clearing procedure.

2.4 Localization of ATP synthase β -chain in H9c2 cells and co-localization with [1-93]ApoA-I

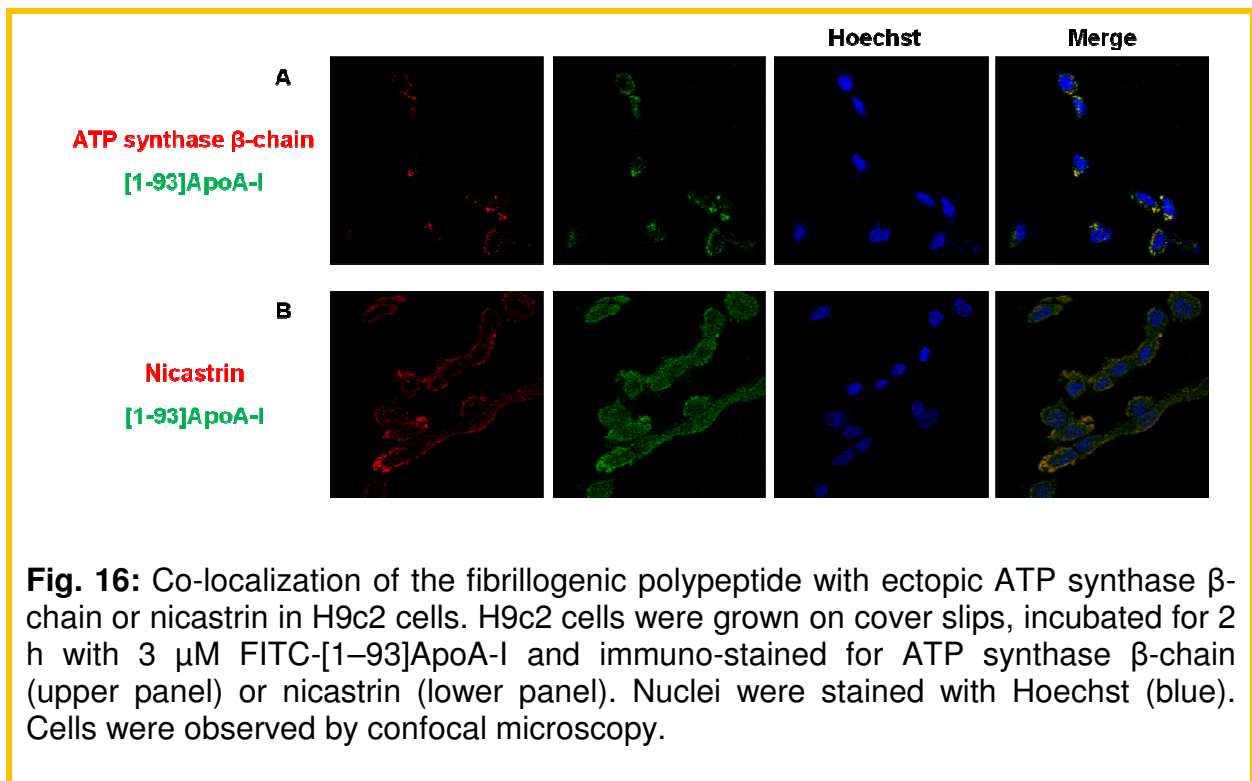
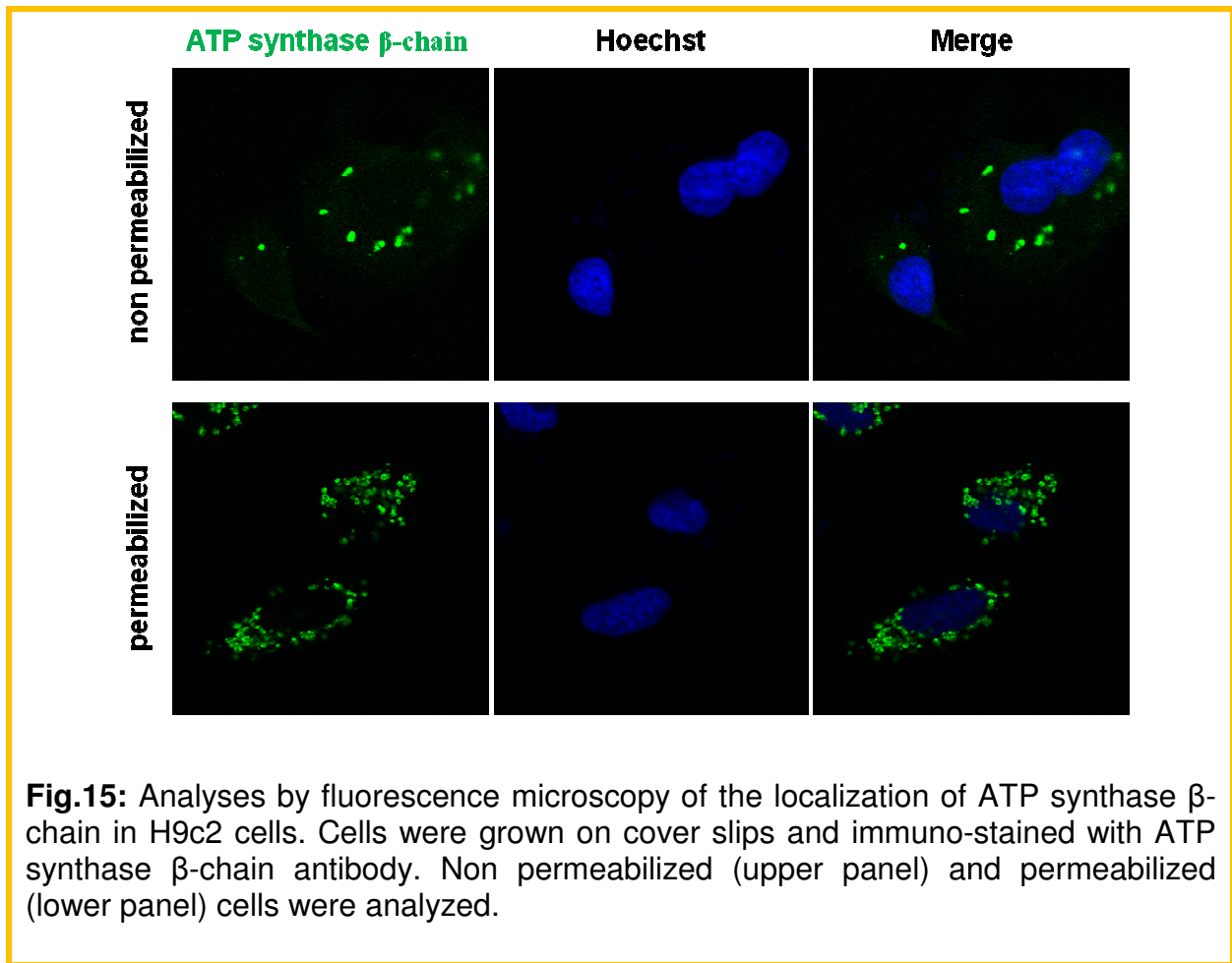
To verify whether ATP synthase β -chain is present at the cell surface of rat embryos H9c2 cardiomyoblasts, immuno-fluorescence analyses of H9c2 cells were performed with anti-ATP synthase β -chain antibody. To this purpose, permeabilized or not permeabilized cells were immuno-stained with anti-ATP synthase β -chain antibody. Immuno-positive signals were clearly evidenced at the plasma membrane of non permeabilized H9c2 cardiomyoblasts (Fig. 15 upper panel). In these experimental conditions, in fact, the primary antibody molecules have no access to the intracellular space and the presence of ATP synthase β -chain on the extracellular surface of plasma membrane can be demonstrated. In the case of permeabilized cells, instead, we found that ATP synthase β -chain was mainly located in the mitochondria (Fig. 15 lower panel), as expected.

Once demonstrated the presence of ATP synthase β -chain on cardiomyoblasts cell membrane, fluorescence microscopy analyses were performed to verify whether the fibrillogenic polypeptide [1-93]ApoA-I co-localizes with ectopic ATP synthase β -chain. H9c2 cells were incubated with FITC-[1-93]ApoA-I for 6 h, fixed and incubated with anti-ATP synthase β -chain. As shown in Fig. 16A, a significant, albeit partial, co-localization of cell membrane associated [1-93]ApoA-I (green) with ectopic ATP synthase β -chain (red) was observed, suggesting a possible interaction of the fibrillogenic polypeptide with the ectopic protein.

Further experiments will be performed to verify whether the two proteins are able to interact directly and to investigate the role of this interaction.

2.5 Co-localization of [1-93]ApoA-I and nicastrin

Fluorescence microscopy analyses were also performed to verify whether the fibrillogenic polypeptide [1-93]ApoA-I co-localizes with nicastrin. To this purpose, cells were treated with the FITC-[1-93]ApoA-I for 6 h at 37°C and, at the end of the incubation, co-localization of the polypeptide and nicastrin was analyzed following a procedure similar to that described for ATP synthase β -chain. In this case, we used antibodies anti-nicastrin as the primary. As shown in Fig. 16B, a significant co-localization of nicastrin (red) with [1-93]ApoA-I (green) was observed, suggesting an interaction of the fibrillogenic polypeptide with nicastrin. Further experiments will be performed to verify whether the two proteins are able to interact directly and to deeply inspect a possible involvement of nicastrin in the proteolytic release of the fibrillogenic polypeptide of ApoA-I.



3. STRUCTURE TO FUNCTION RELATIONSHIP STUDIES: Production of recombinant wild-type ApoA-I and its amyloidogenic full-length variant L174S

Structural and functional analyses of the full-length variants of ApoA-I in comparison to the wild-type protein will greatly contribute to the understanding of the molecular bases of the pathology. Nevertheless, the isolation of the amyloidogenic forms of ApoA-I from patients is impracticable, as all the patients analyzed so far were found to be heterozygous for the mutated gene, thus expressing both the wild-type and the mutated form. Therefore, heterologous expression systems are needed. Nevertheless, with the exception of variants G26R and L178H produced in bacterial cells [99, 100], no reports are available on the production and isolation of ApoA-I amyloidogenic variants.

We set up a system for recombinant expression of the ApoA-I amyloidogenic variant L174S in stably transfected mammalian cells. ApoA-I(L174S) variant carries the substitution of Leu 174 for Ser and is responsible for a severe amyloidosis predominantly involving the heart [63].

Chinese hamster ovary cells (CHO-K1) were stably transfected with a plasmid carrying the cDNA encoding either wild-type ApoA-I or the amyloidogenic variant ApoA-I(L174S). Both recombinant proteins carried at their N-terminus the ApoA-I signal peptide sequence. By growing the cells under antibiotic selection, single, stably transfected clones were isolated and, for each recombinant protein, a single clone was selected for analysis.

First, the kinetics of expression and secretion of the recombinant proteins were analyzed. To this purpose, time course experiments were performed. Cells were grown in complete medium for 24 h, then grown in serum-free medium for up to 72 h. After 24, 48 and 72 h growth, cell lysates were analyzed by Western blotting, using anti-ApoA-I antibodies (Fig. 17A and B, lanes 5-8). Defined amount of pure ApoA-I were analyzed in parallel to generate a reference plot correlating immuno-positive signals to protein amount (Fig. 17A and B, lane 1-4). Endogenous actin, measured with an anti-actin antibody, was used as an internal standard. No significant differences in intracellular protein amount during the time course were detected by densitometric analyses (Fig. 17C).

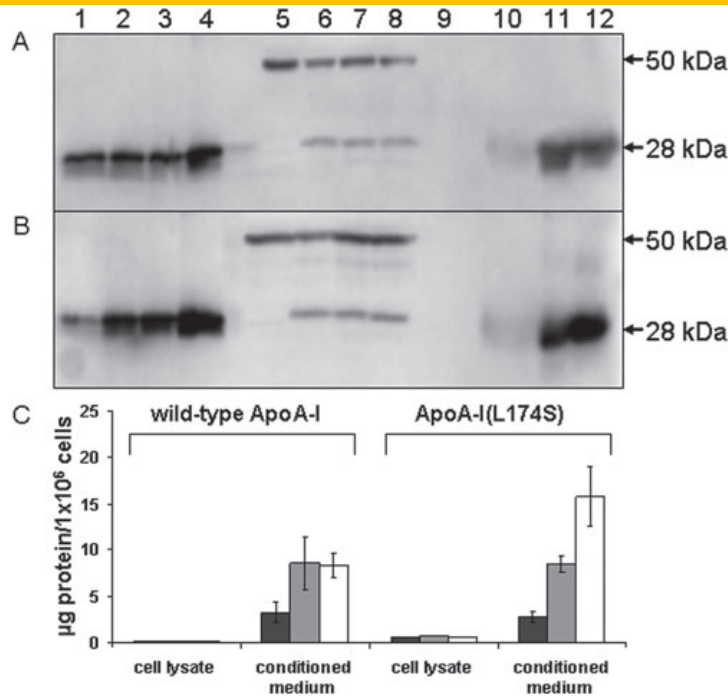


Fig. 17: Analysis of intra- and extracellular levels of recombinant ApoA-I and ApoA-I(L174S) variant in CHO-K1 cells. **(A)** Western blot analysis with anti-ApoA-I antibodies of wild-type ApoA-I. Lanes 1–4, increasing amounts of standard ApoA-I (25, 50, 100, 200 ng); lane 5, lysate of untransfected cells; lanes 6–8, lysates of stably transfected cells at 24, 48, 72 h, respectively; lane 9, cell-conditioned medium of untransfected cells; lanes 10–12, cell-conditioned medium of transfected cells at 24, 48, 72 h, respectively. The upper bands in lanes 5–8 refer to endogenous actin used as an internal standard. **(B)** Western blot analysis with anti-ApoA-I antibodies of ApoA-I(L174S) variant. Samples as in **A**. **(C)** Quantitative analysis of intra- and extracellular recombinant protein levels as a function of time (24 h, black bars; 48 h, grey bars; 72 h, white bars). Protein amounts are expressed as μg of protein/ 1×10^6 cells. The data represent the means \pm SD of protein amounts determined in three independent experiments.

Then, the cell conditioned medium of CHO-K1 clones was analyzed (Fig. 17A and B, lanes 10–12). Densitometric analysis indicated that the maximum level of extracellular wild-type ApoA-I was reached at 48 h, while the amount of ApoA-I(L174S) was found to be increased at 72 h with respect to 48 h (Fig. 17C).

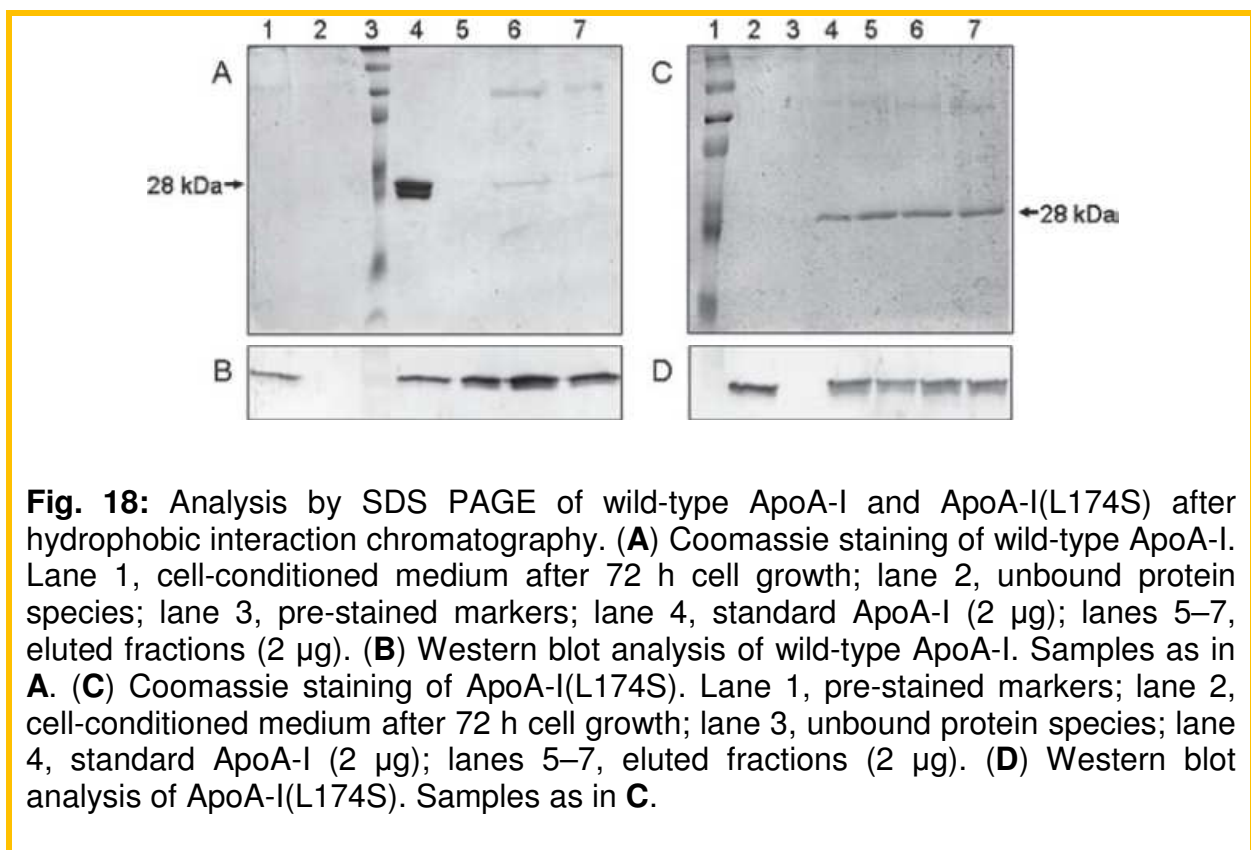
Interestingly, a comparison between the intra and extracellular amount of the recombinant proteins indicated that at any time of cell growth both proteins are mostly secreted by CHO-K1 cells.

The overall data indicate that both proteins are efficiently secreted, although following different kinetics. We estimated that about 5.4 mg/L of wild-type ApoA-I and 4.5 mg/L of the amyloidogenic variant are secreted in 72 h in the culture medium.

3.1 Isolation of the recombinant proteins

To isolate the recombinant proteins, a hydrophobic interaction chromatography was performed. Cells were plated and grown in serum-free medium. After 72 h, the conditioned medium was centrifuged and loaded on a Butyl-S chromatography column, following addition of 0.8 M NaCl. Fractions, eluted with isopropanol 20%, were analyzed by SDS gel electrophoresis followed by Coomassie staining and Western blotting using anti-ApoA-I antibodies (Fig. 18). These analyses revealed that variant L174S was more than 90% pure (Fig. 18C), whereas an additional protein species was observed in wild-type ApoA-I sample (Fig. 18A).

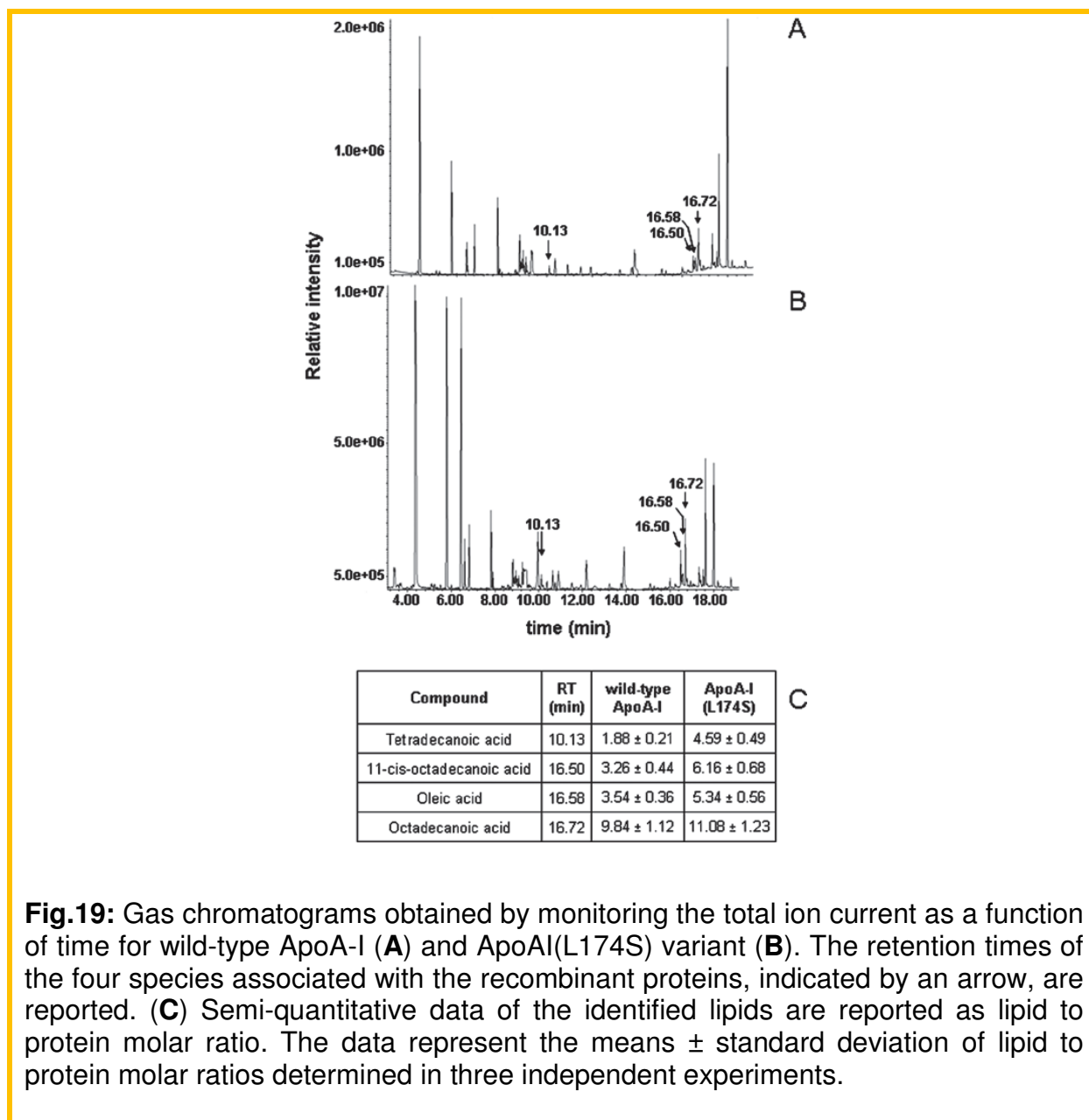
About 0.7 mg of variant ApoA-I(L174S) (\approx 50% yield) and 0.3 mg of wild-type ApoA-I (\approx 20% yield) were obtained from 1L of conditioned medium.



3.2 Analysis of lipid content

Since ApoA-I binds with high affinity lipid molecules, we analyzed the presence of lipids in the isolated protein samples in collaboration with Dr. A. Amoresano, Department of Chemical Sciences. The procedure used consisted in liquid-liquid lipids extraction, lipids derivatization with trimethylsilane, followed by GC-MS analysis (Fig. 19A and B). Either for the wild-type protein and for its variant, the presence of several analytes was revealed (Fig. 19C). We also identified the analytes present in control samples, i.e. an unconditioned medium or a conditioned medium of untransfected cells, both after hydrophobic interaction chromatography. Upon subtraction of species present in the controls, a list of compounds specifically bound

to each recombinant protein was obtained. For both wild-type and mutant proteins, four species were found to be present, identified as oleic acid, stearic acid, cis-11-octadecanoic acid, tetradecanoic acid, with stearic acid as the most abundant (Fig. 19C).



To exclude that these lipids were selected by the hydrophobic chromatography through unspecific interactions with the resin, alternative procedures to isolate the recombinant proteins were used, such as immuno-affinity chromatography, using anti-ApoA-I antibodies covalently bound to a resin, and reverse phase chromatography. The proteins isolated following these procedures were analyzed as previously described. In both cases, no differences in the lipid composition were detected with respect to those reported above. Similar results were obtained when

the proteins eluted from the hydrophobic chromatography were extensively dialyzed prior to be analyzed for the lipid content.

Interestingly, significant differences were appreciated in the relative amount of fatty acids associated to the mutant with respect to the wild-type protein. A semi-quantitative analysis revealed different lipid-to-protein molar ratios for the two proteins, with higher values associated to the variant protein with respect to the wild-type. With the exception of stearic acid, the lipid-to-protein molar ratios calculated for the amyloidogenic variant were significantly higher (1.5 to 2.5-fold) than those determined for wild-type ApoA-I (Fig. 19C).

These findings may be of significance in the development of the pathology. In fact, it has been proposed that amyloidogenic mutations reduce the affinity of ApoA-I for surface lipids of HDL, promoting a shift from HDL-bound to lipid-poor/free ApoA-I. Moreover, other factors have been reported to destabilize HDL assembly, such as an increase of fatty acid content on the surface of HDL, or an increase of triacylglycerol content in the HDL core [79]. Hence, it is likely that the presence of an amyloidogenic mutation in ApoA-I sequence induces a conformational change in the protein structure responsible for a reduced affinity for surface phospholipids of HDL. An extensive comparative study of a pathogenic versus a natural protein represents a key aspect to understand the molecular basis of the pathology.

4. STUDIES ON PROTEINS WITH A POTENTIAL ROLE IN AMYLOID DISEASES: *Does angiogenin play a role in ApoA-I related amyloidosis?*

4.1 Angiogenin and its role in stress response

Angiogenin (ANG) is a 14 kDa ribonuclease (RNase) [101] known to induce angiogenesis in endothelial cells. Although ANG is a small molecule, three distinct function sites including a receptor-binding site, a nuclear localization sequence (NLS) and a catalytic site have been identified.

The growth-stimulating activity of ANG is mediated by its ability to promote rRNA transcription [102, 103], by binding to the promoter region of ribosomal DNA [104]. rRNA transcription is the rate-limiting step in ribosome biogenesis [105], a process required for cell growth as well as maintenance and survival, as proteins are required for all cellular activities. Similarly, ANG-mediated rRNA transcription also plays an important role for cancer cell proliferation in response to genetic and environmental factors [106, 107]

Recent publications have further extended the biological activities of ANG from enabling cell growth and proliferation to sustaining survival under stress conditions [108-111]. Usually, in mammalian cells, stress-induced phosphorylation of eIF2 α inhibits global protein synthesis to conserve anabolic energy for the repair of stress-induced damage.

However, stress-induced translational silence is also observed in cells expressing a non-phosphorylatable eIF2 α mutant (S51A) [112], indicating the existence of a phosphor-eIF2 α independent pathway of translational control. Yamasaki and coworkers demonstrated that this pathway is mediated by a subset of tRNA fragments produced by a specific cleavage at the anticodon loop [108]. This class of small RNA has been designated as tiRNA (tRNA-derived, stress-induced small RNA) and shown to inhibit protein translation in an eIF2 α independent manner. ANG was found to be the RNase that is responsible for this specific cleavage. The

enzymatically inactive ANG variant H13A lost the ability to mediate the production of tiRNA, indicating that the ribonucleolytic activity of ANG is fundamental for its role in stress response [108].

In Fig. 20 the overall mechanism of action of ANG is summarized.

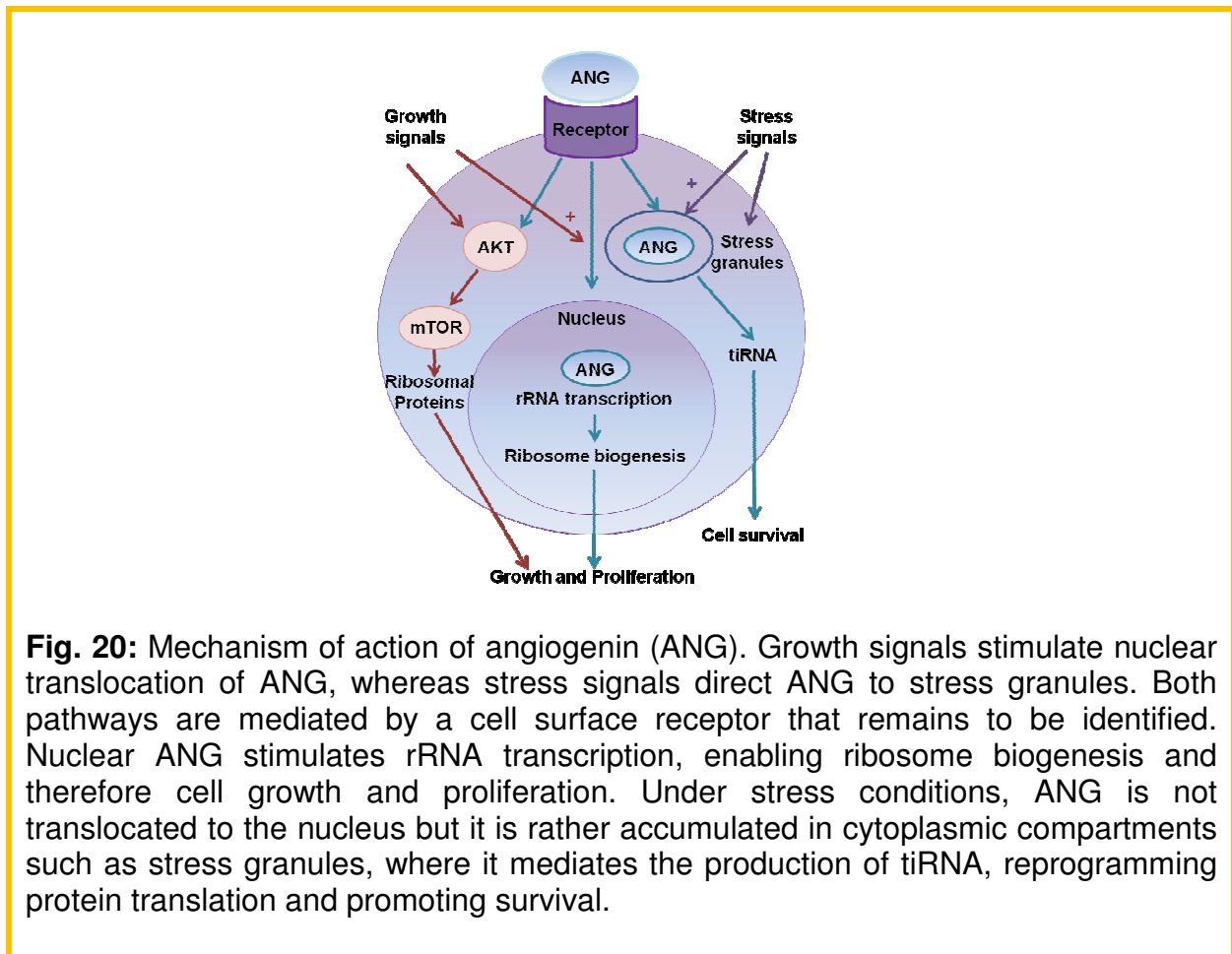


Fig. 20: Mechanism of action of angiogenin (ANG). Growth signals stimulate nuclear translocation of ANG, whereas stress signals direct ANG to stress granules. Both pathways are mediated by a cell surface receptor that remains to be identified. Nuclear ANG stimulates rRNA transcription, enabling ribosome biogenesis and therefore cell growth and proliferation. Under stress conditions, ANG is not translocated to the nucleus but it is rather accumulated in cytoplasmic compartments such as stress granules, where it mediates the production of tiRNA, reprogramming protein translation and promoting survival.

4.2 ANG and ApoA-I associated amyloidosis

Recently, it has been reported that serum ANG levels are dramatically reduced in a transgenic mouse model in which alpha-synuclein, responsible for Parkinson's disease (PD), is over-expressed [113]. Moreover, Kim and co-workers demonstrated that ANG plays a major role in Alzheimer's disease (AD) pathogenesis since they observed a decrease in serum ANG levels in AD patients [114].

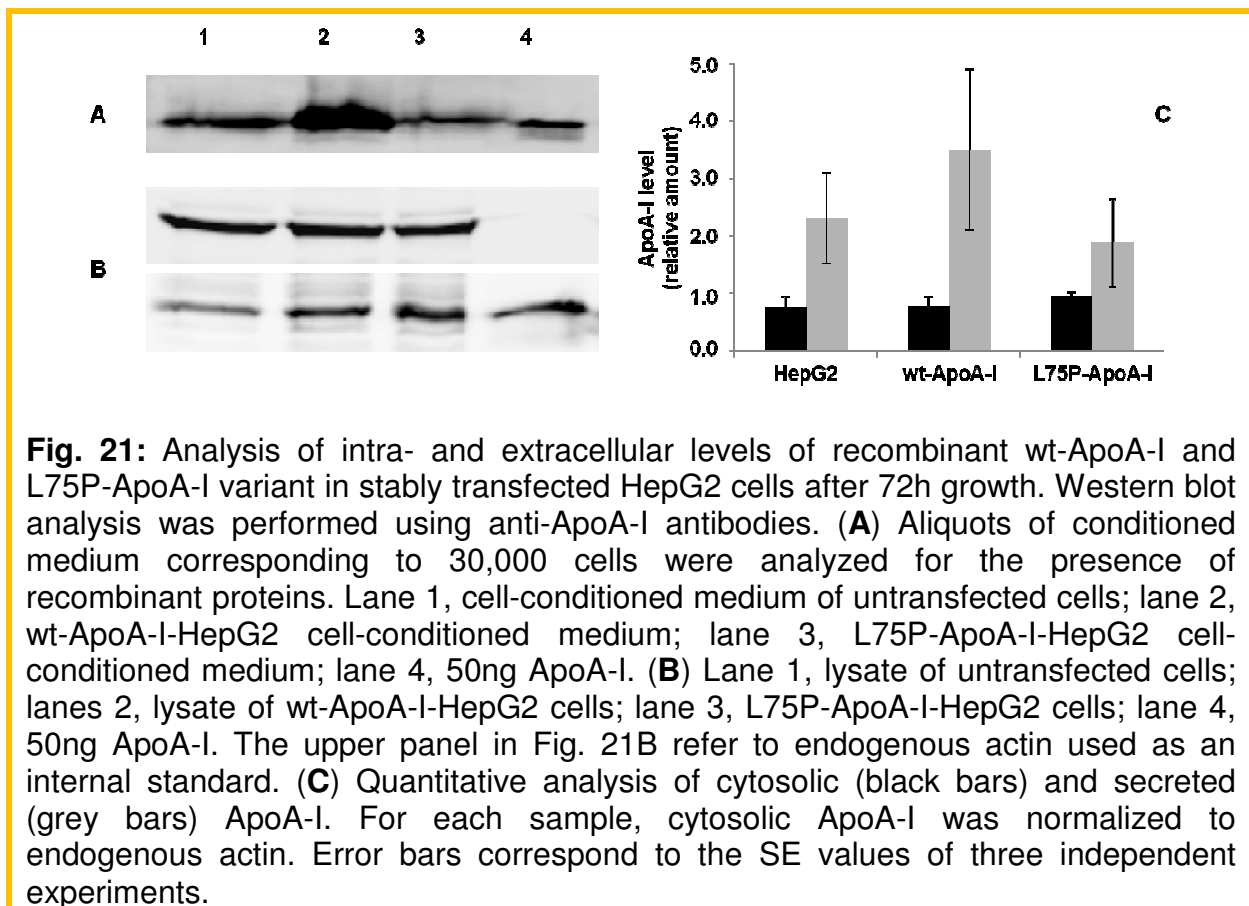
Since fibrillogenesis is a common feature of AD and PD, in which a role of ANG has been envisaged, we questioned if changes in ANG levels may occur also in ApoA-I related amyloidosis.

In this pathology, all the patients analysed so far were found to be heterozygous for the mutated gene, as both the wild-type and the mutated form is expressed, with the latter circulating in plasma at lower levels than the wild-type [52]. An ApoA-I amyloidogenic variant, responsible for preferential deposition of amyloid fibrils in the liver, carries the substitution of Leu 75 for Pro (L75P-ApoA-I). This fibrillogenic variant was used in this study to investigate the role of ANG in ApoA-I related amyloidosis.

As the liver is the main producer of ApoA-I and the major target of L75P-ApoA-I related amyloidosis, human hepatic cells (HepG2) were stably transfected with either plasmid pRC-rsv-ApoAI, carrying the cDNA encoding wild-type ApoA-I, or with plasmid pRC-rsv-L75P-ApoAI, carrying the cDNA encoding the amyloidogenic variant L75P-ApoA-I. By this way, this experimental system mimics patient's heterozygosis as both the wild-type and the mutated form are expressed.

Both recombinant proteins carried at their N-terminus the ApoA-I signal peptide sequence. By growing the cells under antibiotic selection, single, stably transfected clones were isolated; for each recombinant protein a single clone was selected for analyses. Cells stably expressing either recombinant wt-ApoA-I or its amyloidogenic variant L75P are indicated as wt-ApoA-I-HepG2 and L75P-ApoA-I-HepG2 cells, respectively. Wt-ApoA-I-HepG2 cells were used to mimic healthy condition, whereas L75P-ApoA-I-HepG2 cells mimic pathological condition. In all the experiments, untransfected HepG2 cells were used as a control.

After 72 h cell growth, conditioned media and cell lysates were analyzed by Western blotting with an anti-human ApoA-I polyclonal antibody. For both wild-type ApoA-I (wt-ApoA-I) and L75P-ApoA-I transfectants, an immunopositive species with a molecular mass corresponding to that of ApoA-I was observed in the conditioned medium as well as in the lysate (Fig. 21A and B, respectively). Endogenous actin, measured with an anti-actin antibody, was used as an internal standard (Fig. 21, lanes B upper panel). Densitometric analyses (Fig. 21 C) indicated that wt-ApoA-I is efficiently secreted, while a significant amount of L75P-ApoA-I was retained in the cytosol. An immuno-positive band was detected also in untransfected cells (Fig. 21 A and B, lanes 1), confirming that endogenous ApoA-I is expressed in HepG2 cells.



As known, serum provides sustenance for cultured cells as it contains trophic factors; serum withdrawal induces apoptosis in a variety of cells, including HepG2 cells. This type of stress was extensively used as a model to investigate apoptosis regulation [115]. It has been also observed that undifferentiated P19 cells have a very low endogenous ANG levels and undergo apoptosis in the absence of serum [116]. Therefore, serum starvation was used to analyse a possible involvement of ANG in ApoA-I related amyloidosis.

Cells were grown in complete DMEM medium for 24 h, then grown in serum-free medium for 48 h. At the end of incubation, quantitative Real Time PCR (qRT-PCR) was performed and subcellular localization of ANG was analyzed in the presence (growth condition) and absence of serum (serum starvation). In Fig 22 the result of qRT-PCR is shown; the amount of ANG was normalized to the endogenous actin and each ΔCt was then normalized to untransfected HepG2 cells. We observed that in cells expressing the amyloidogenic variant L75P, cultured in growth condition, cellular ANG levels were lower than those of untransfected cells as well as of wt-ApoA-I HepG2 cells, for which the total amount of ANG was comparable (Fig. 22, black bars). For untransfected and wt-ApoA-I-HepG2 cells, a significant increase in ANG levels occurred when the cells were cultured in serum-free medium, while a very slight increase was observed in the case of L75P-ApoA-I-HepG2 cells (Fig. 22, grey bars).

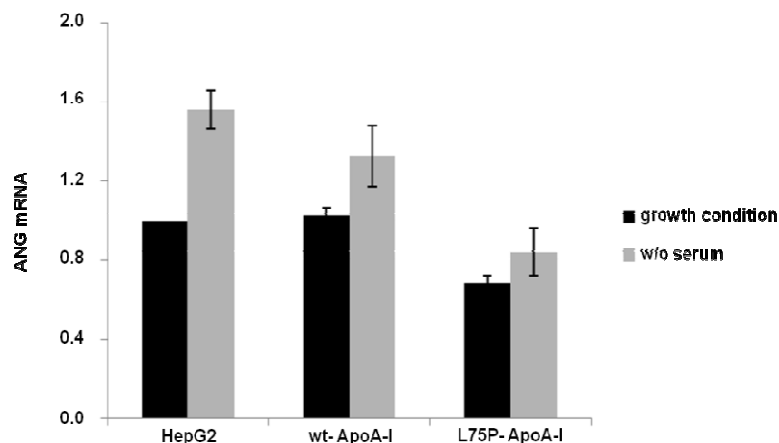
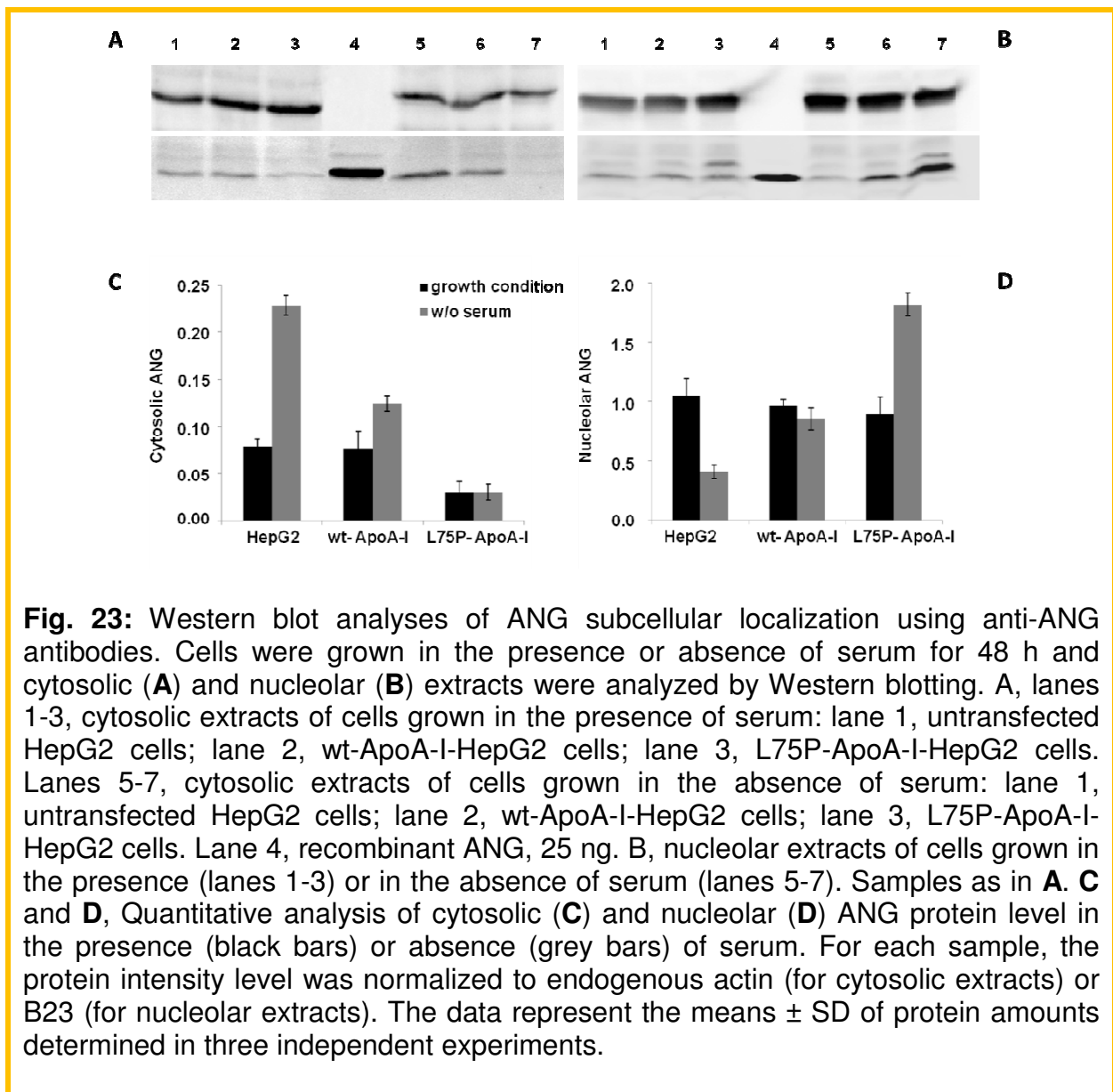


Fig. 22: Quantitative RT-PCR analysis. Cells were grown in the presence (black bars) or in the absence (grey bars) of serum for 48 h. Total RNA was extracted and analyzed with probes specific for ANG and actin mRNAs. Data shown are the mean \pm SD of triplicate determinations and the results were analyzed using the comparative Ct (threshold cycle) method normalized against the housekeeping gene actin. The range of expression levels was determined by calculating the standard deviation of the ΔCt (i.e. Ct of the target gene – Ct of the reference gene).

ANG subcellular localization was determined by Western blotting analyses of cytosolic and nucleolar extracts. We first examined protein ANG levels in the cytosol of cells grown under growth or stress conditions by using anti-ANG-antibodies (Fig. 23 A and C). Endogenous actin, measured with anti-actin antibodies, was used as an internal standard. Western blot analyses showed that, in growth conditions, ANG was

detected in both the cytosolic and nucleolar fractions of the three cell lines (Fig. 23 A and B, lanes 1-3). By densitometric analyses we observed that the amount of cytosolic ANG in untransfected cells was comparable to that of wt-ApoA-I-HepG2 cells, while it was significantly lower in the case of L75P-ApoA-I-HepG2 cells (Fig. 23 C). Western blotting of nucleolar extracts, followed by densitometric analyses, indicated no differences in nucleolar ANG levels among the three cell lines (Fig 23 B, lanes 1-3). B23 protein was used as an internal standard for nucleoli. Under stress conditions, ANG was no longer localized in nucleoli but was rather cytosolic in both untransfected and wt-ApoA-I-HepG2 cells, indicating that stress induces a shift of ANG distribution from nucleus to cytosol (Fig. 23 A and B, lanes 5-6).



This preferential localization of ANG in the nucleoli or in the cytosol, when cells are kept in growth or stress conditions, respectively, is consistent with recent data reported in literature [108]. Interestingly, in the case of the amyloidogenic variant, it

was not observed any shift of ANG from nucleoli to the cytosol (Fig. 23 A and B, lane 7), but ANG level in the nucleoli was found to be dramatically increased (Fig. 23 D).

Then the effects of serum starvation on cell viability was analyzed by performing the MTT reduction assay, as an indicator of metabolically active cells. Cells were grown in complete DMEM medium for 24 h, then incubated in serum-free medium for up to 96 h, in the presence or absence of 0.5 $\mu\text{g/ml}$ ANG. In Fig. 24, the results of time course experiments are shown. The values are the average of 3 independent experiments carried out with triplicate determinations. In the absence of serum, we observed a significant decrease of cell viability in a time-dependent manner, with L75P-ApoA-I-HepG2 cells the most sensitive to serum withdrawal (Fig. 24, white bars). When ANG was added to the complete culture medium, no significant differences in cell viability were observed for the three cell lines (Fig. 24, grey bars) with respect to the same cells grown in the absence of ANG. When instead ANG was added to the serum-free medium (Fig. 24, panel c, dashed bars), we observed a strong protective effect of ANG on L75P-ApoA-I-HepG2 cells, with no significant effects on wt-ApoA-I-HepG2 cells and untransfected cells.

To confirm the above findings, cells were stained with ethidium bromide (EB) and with acridine orange (AO) (Fig. 25). AO permeates intact cells staining all the nuclei (green), whereas EB enters cells only when the plasma membrane is damaged, thus staining only apoptotic nuclei (red). This method has been widely used to visually distinguish apoptotic cells [81].

Cells were grown in complete medium for 24 h and then grown in serum-free medium for 48 h. For untransfected HepG2, the percentage of EB-stained cells was $48.7 \pm 3.40\%$ and $20.7 \pm 3.17\%$, when determined in the absence or presence of serum, respectively (Fig. 25). The last percentage did not vary significantly ($23.6 \pm 0.19\%$) when ANG was added to the complete medium, whereas upon ANG addition to the serum-free medium the percentage of apoptotic cells slightly decreased to $41.6 \pm 2.41\%$ (Fig. 25), indicating a slight positive effect of ANG on cell viability. Similar results were observed for wt-ApoA-I-HepG2 cells, where the percentage of apoptotic nuclei was $49.0 \pm 3.03\%$ and $19.9 \pm 3.54\%$, in the absence and presence of serum, respectively (Fig. 25), and $17.9 \pm 1.44\%$ when ANG was added to the complete medium. The addition of ANG to serum-free medium did not change significantly the amount of apoptotic cells ($44.0 \pm 3.09\%$, Fig. 25).

Different results were obtained in the case of L75P-ApoA-I-HepG2 cells. A higher percentage of apoptotic cells was observed in growth conditions ($35.8 \pm 3.05\%$), suggesting that the presence of an amyloidogenic protein is harmful. When cells were grown in the absence of serum, a very high proportion of EB-stained cells was measured ($62.5 \pm 2.39\%$). Interestingly, ANG addition to the serum-free medium of L75P-ApoA-I-HepG2 cells significantly prevented apoptosis induced by serum withdrawal, as the percentage of apoptotic cells was reduced to $44.4 \pm 1.24\%$. On the other hand, according to the other two cell lines, when ANG was added to the complete medium of L75P-ApoA-I-HepG2 cells, no significant differences were observed with respect to cells grown in complete medium but in the absence of ANG ($29.8 \pm 1.46\%$ and $35.8 \pm 3.05\%$, respectively).

Thus, by two independent approaches we showed that ANG has an anti-apoptotic activity, similarly to foetal bovine serum, on L75P-ApoA-I-HepG2 cells.

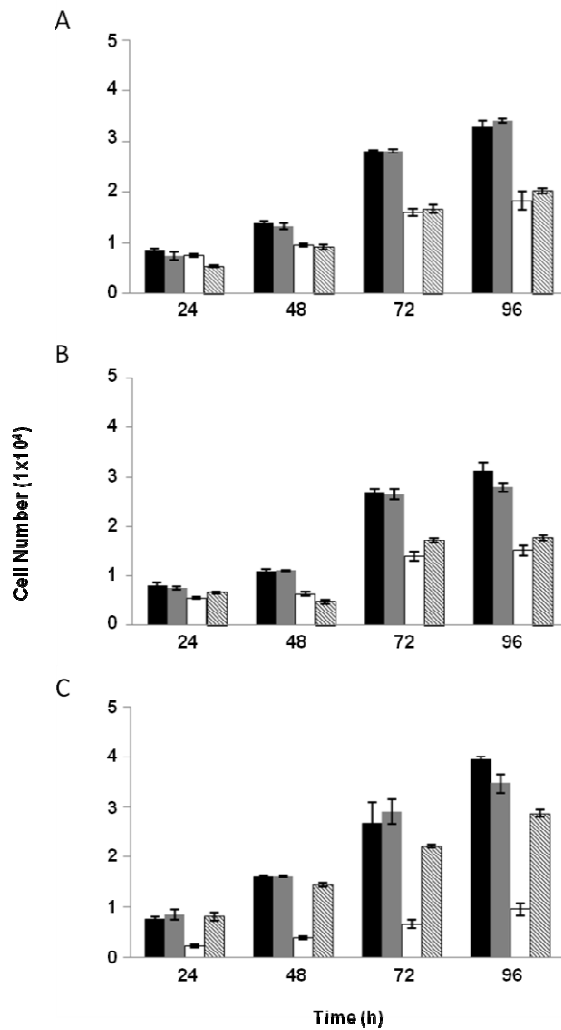


Fig. 24: Time-course of the effects of serum starvation on the viability of HepG2 cells in the presence of ANG by the MTT assay. Untransfected HepG2 (**A**), wt-ApoA-I-HepG2 (**B**), L75P-ApoA-I-HepG2 (**C**) cells were grown in complete medium in the absence (black bars) or presence (grey bars) of ANG (0.5 µg/ml), or in serum-free medium in the absence (white bars) or presence (dashed bars) of ANG for different lengths of time (24, 48, 72, 96 h). Cell number was calculated using a calibration curve obtained by counting the number of cells by the MTT assay. Error bars correspond to the SE values of three independent experiments. **P values** < 0.01.

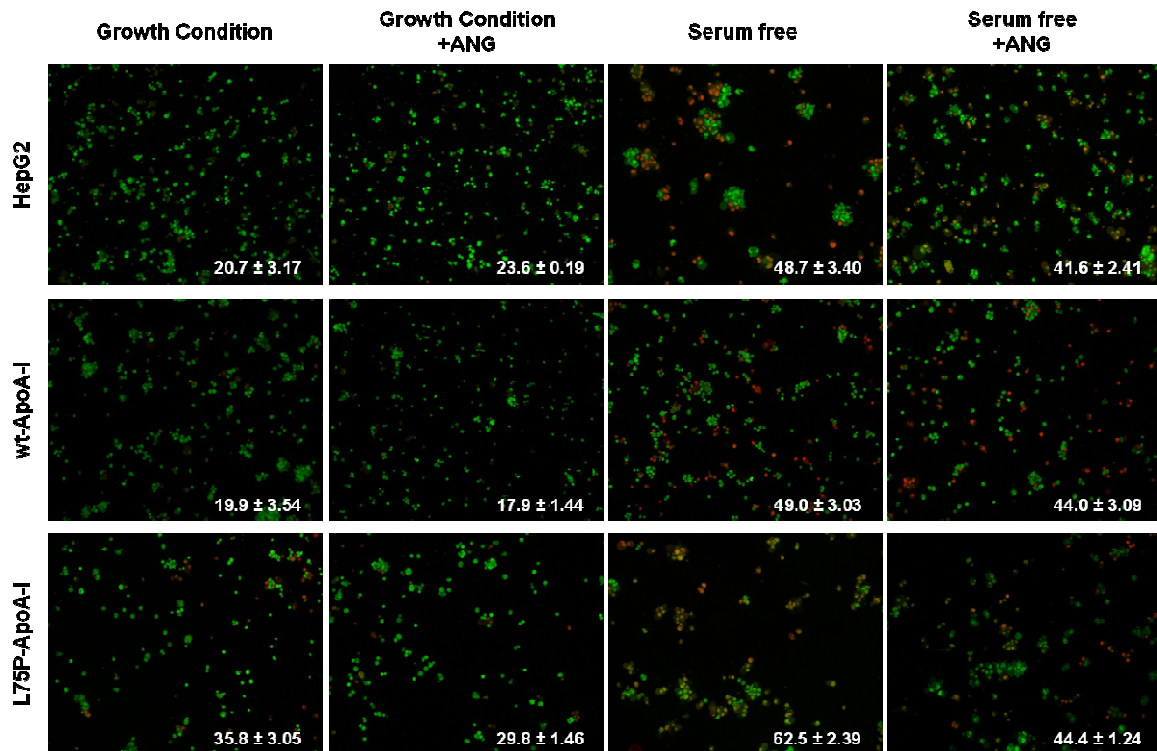


Fig. 25: Serum withdrawal-induced apoptosis in HepG2 cells in the presence or absence of ANG. Untransfected HepG2, wt-ApoA-I-HepG2, L75P-ApoA-I-HepG2 cells were grown in complete or serum-free medium in the presence or absence of 0.5 μ g/ml ANG for 48 h. Cells were collected and stained with ethidium bromide (red) and acridine orange (green) and applied to a microscope slide for imaging. Ethidium bromide-stained (apoptotic) cells were counted in a total of 750 cells from five randomly selected areas of each slide, and the percentage of apoptotic cells is shown at the bottom of each picture. The data shown are the means and SE of triplicates of a representative experiment of at least three repeats.

For a deeper inspection of the role of ANG in ApoA-I-related amyloidosis three ANG mutants were analyzed: R33A, K40Q and R66A. R33A is not able to translocate to the nucleus, K40Q is not active enzymatically and R66A is defective in binding to the receptor [117].

The effects of serum starvation on cell viability in the presence of these ANG mutants was analyzed by MTT reduction assays. Cells were grown in complete DMEM medium for 24 h, then grown in serum-free medium for up to 96 h, in the presence or absence of an ANG mutant (0.5 μ g/ml). In Figures 26, 27 and 28, the results of time-course experiments are shown. The values are the average of 3 independent experiments carried out with triplicate determinations.

When R33A mutant was added to the culture medium (complete or serum-free), no significant differences in cell viability were observed in untransfected, as well as in wt-ApoA-I-HepG2 cells (Fig. 26 A and B, grey and dashed bars). On the contrary, a strong protective effect of on L75P-ApoA-I-HepG2 cells was observed when tested in

the absence of serum, whereas the effect was not evident in the presence of serum (Fig. 26 C, dashed bars). Similar results were obtained with mutant K40Q (Fig. 27). When cells were treated with R66A mutant, the protective effect on serum-starved L75P-ApoA-I-HepG2 cells was found to be less evident than in the previous cases (Fig. 28C, dashed bars). For untransfected and wt-ApoA-I-HepG2 cells, a decrease of cell viability in the absence of serum was observed (Fig. 28 A and B, dashed bars). In conclusion, these experiments on a panel of ANG mutants, each defective for a single, specific ANG activity, add knowledge to the complex role of ANG in stress recovery and on its involvement in amyloid diseases. Taken together, our results suggest that, to elicit its protective role in cells under stress, ANG needs to be internalized into the cells, as the only mutant that fails in the recovery of cell viability is defective in binding to the receptor. On the contrary, ANG protective role seems do not involve its ribonucleolytic activity, nor its nuclear localization. Further experiments will be performed to elucidate the molecular basis of the protective role of ANG in ApoA-I related amyloidosis.

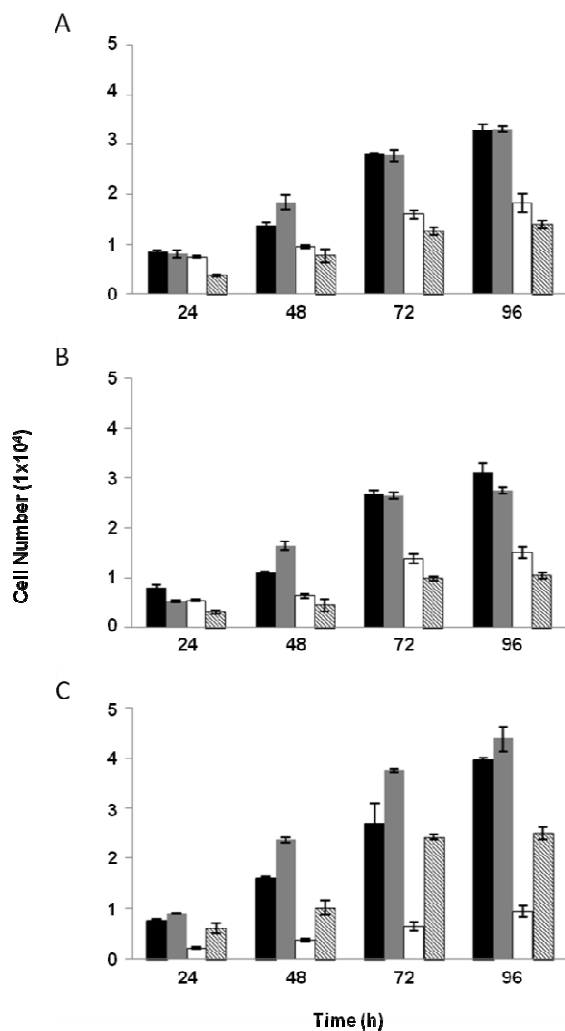


Fig. 26: Time-course of the effects of serum starvation on the viability of HepG2 cells in the presence of R33A ANG mutant by the MTT assay. Untransfected cells (**A**) and cells stably expressing wt-ApoA-I (**B**) or L75P-ApoA-I (**C**) were grown in complete medium in the absence (black bars) or presence (grey bars) of ANG (0.5 µg/ml), or in serum-free medium in the absence (white bars) or presence (dashed bars) of ANG for different lengths of time (24, 48, 72, 96 h). Cell number was calculated using a calibration curve obtained by counting increasing number of cells by the MTT assay. Error bars correspond to the SE values of three independent experiments. **P values < 0.01.**

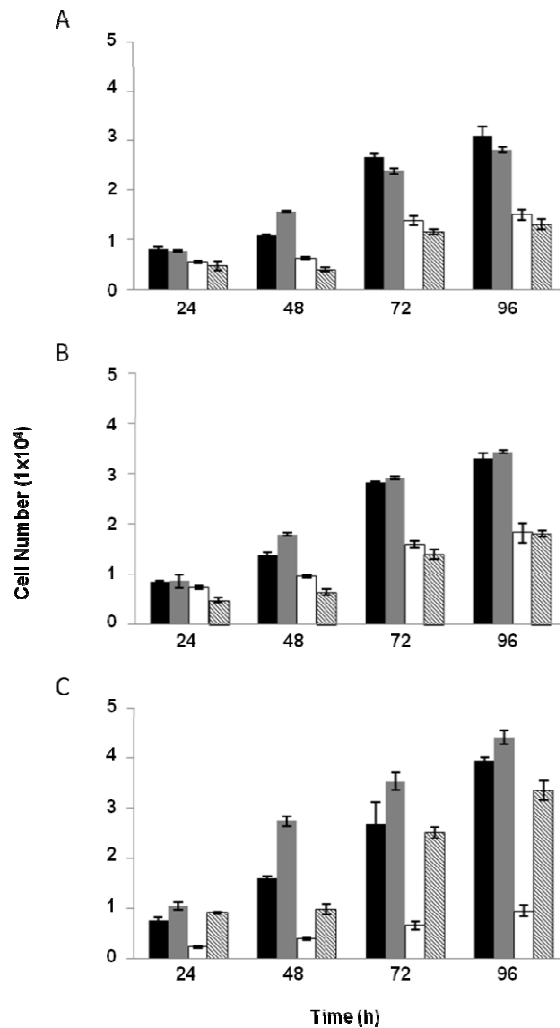


Fig. 27: Time-course of the effects of serum withdrawal on the viability of HepG2 cells in the presence of K40Q ANG mutant by the MTT assay. Untransfected cells (**A**) and cells stably expressing wt-ApoA-I (**B**) or L75P-ApoA-I (**C**) were treated as described in the legend of Fig. 26. Black and white bars represent cells incubated in complete or serum free medium, respectively. Grey and dashed bars refer to cells treated with of 0.5 µg/ml K40Q ANG mutant in the presence or absence of serum, respectively. Error bars correspond to the SE values of three independent experiments. **P values < 0.01.**

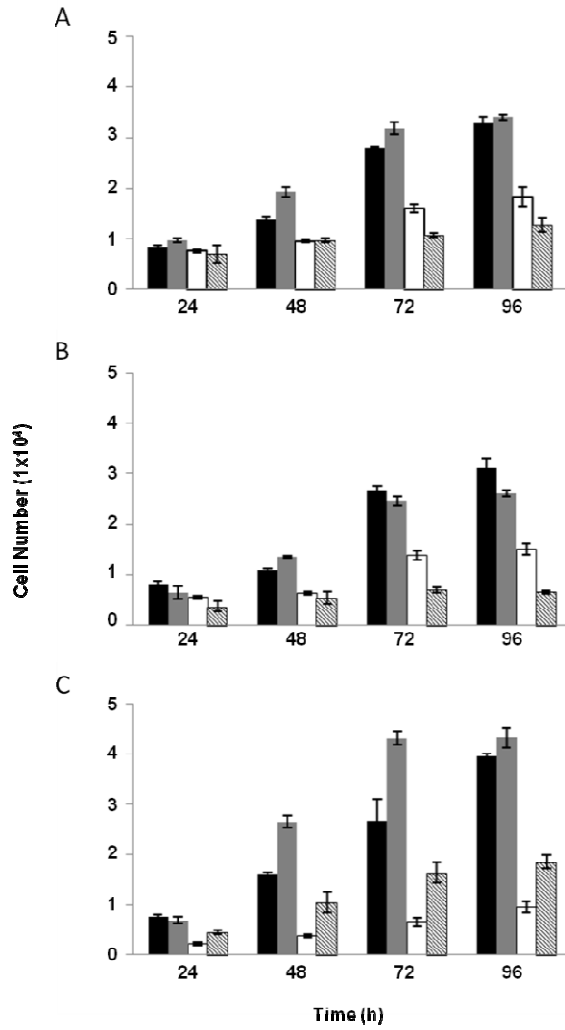


Fig. 28: Time-course of the effects of serum withdrawal on the viability of HepG2 cells in the presence of K40Q ANG mutant by the MTT assay. Untransfected cells (**A**) and cells stably expressing wt-ApoA-I (**B**) or L75P-ApoA-I (**C**) were treated as described in the legend of Fig. 26. Black and white bars represent cells incubated in complete or serum free medium, respectively. Grey and dashed bars refer to cells treated with of 0.5 $\mu\text{g/ml}$ K40Q ANG mutant in the presence or absence of serum, respectively. Error bars correspond to the SE values of three independent experiments. **P values** < 0.01.

DISCUSSION

An increasing number of human diseases is linked to protein aggregation and to the accumulation of protein deposits in different organs or tissues.

Almost 30 amyloidogenic proteins have been identified so far [9] and, despite the lack of any sequence homology or common structural determinants, they share a common fibrillogenic pathway which results in fibrils with the same architectural organization [10].

The elucidation of the cascade of biochemical events triggered by the exposure of cells to a fibrillogenic protein is of primary importance in the comprehension of the molecular bases of amyloid diseases. To this purpose, we focused our attention on ApoA-I related amyloidosis.

ApoA-I represents an intriguing case of a protein which, in its native form, plays a key role in the reverse cholesterol transport, as it acts as an antiatherogenic factor in humans. On the other hand, in the presence of one of the nineteen amyloidogenic mutations identified so far [58], ApoA-I is converted into the precursor of natively unfolded pathogenic fragments associated with familial systemic amyloidoses [52]. These fragments, corresponding to the N-terminal region of the native protein, are 90-100 residue long and accumulate in fibrillar deposits in peripheral organs leading to a progressive impairment of organ functions.

The molecular mechanism responsible for the release of the fibrillogenic polypeptide from a full-length amyloidogenic variant of ApoA-I remains largely unknown. However, recent findings allowed us to raise the hypothesis that the mutations located in ApoA-I N-terminal region are amyloidogenic as they favour from a structural point of view the proteolytic cleavage responsible for the release of the fibrillogenic polypeptide [78].

A general aim of this research project is that of using different cellular models to study both ApoA-I and its fibrillogenic polypeptide, not only to understand the molecular aspects of ApoA-I related amyloidosis, but also to discover mechanisms of action potentially common to different amyloidogenic proteins.

1. Studies on the fibrillogenic polypeptide [1-93]ApoA-I

1.1 The definition of the intracellular pathway of the fibrillogenic polypeptide

The intracellular pathway of [1-93]ApoA-I was analyzed in comparison to natural full-length ApoA-I in cardiac cells. Since in the case of ApoA-I associated amyloidoses the heart is a natural target for aggregate deposition *in vivo*, cardiomyoblasts were chosen as an experimental system.

We demonstrated that:

(i) the polypeptide partially co-localizes with ABCA1 on rat cardiomyoblasts cell membranes. By immunofluorescence analyses we demonstrated that this transporter is expressed in cardiomyoblasts and that the polypeptide partially co-localizes with ABCA1 on rat cardiomyoblasts cell membranes. Similar results were obtained for ApoA-I, in agreement with recent reports showing that the majority of cell-associated ApoA-I does not co-localize with ABCA1, although no internalization was observed in cells ABCA1^{-/-} [118].

(ii) We showed that the fibrillogenic polypeptide recognizes specific binding sites on cardiac cell membranes and that binding represents a key step for [1-93]ApoA-I internalization. The apparent affinity constant ($K_d = 5.90 \times 10^{-7} \text{ M}$) is similar to those previously reported for lipid-free full-length ApoA-I binding to different cell types [119, 120].

(iii) Following binding, the polypeptide is internalized in cardiomyoblasts. A comparative analysis of the internalization routes of the polypeptide and the full-length protein revealed that the polypeptide is internalized mostly by clathrin-mediated endocytosis and by lipid rafts, whereas a significant involvement of macropinocytosis could be excluded; ApoA-I is internalized *via* clathrin-coated pits and macropinocytosis, whereas internalization through lipid rafts was not observed.

Thus, evidence was provided that the pathogenic polypeptide translocates from the extracellular space, where fibrils form and grow, to the intracellular space. Considering that lipid rafts are rich in cholesterol, which is able to induce and stabilize [1-93]ApoA-I helical states [72], the polypeptide internalization mediated by lipid rafts may have a key role in the pathogenesis of the disease.

(iv) Upon internalization, no involvement of the retro-endocytosis pathway was observed for the fibrillogenic polypeptide, whereas ApoA-I was found to be associated to Rab4-labelled endosomal compartment, a station involved in ApoA-I recycling to the cell membrane.

(v) The fibrillogenic fragment is targeted to proteasomal and lysosomal stations for degradation, as at 24 hrs no intracellular fluorescent signals were detected, indicative of a massive degradation of [1-93]ApoA-I. The rapid degradation of the polypeptide is also in agreement with the absence of cytotoxic effects on cardiomyoblasts, at least in the experimental conditions tested.

Different results were obtained instead in the case of full-length ApoA-I, as the protein does not appear to be significantly degraded once internalized. However, we observed strong signals of co-localization of ApoA-I with lysosomes. Being these stations an intracellular reservoir of cholesterol, nascent lipoprotein particles may be formed at this level and then secreted in the extracellular space [121].

(vi) Unlike the unaggregated polypeptide, fibrils obtained *in vitro* have no access to the intracellular compartment.

The elucidation of key steps of the intracellular pathway and fate of ApoA-I fibrillogenic polypeptide reveals features common to other amyloidogenic proteins. In the case of transmissible spongiform encephalopathy, the misfolded form of APrP accumulates in the brain. It is known that, after being exported to the plasma membrane, PrPc is internalized and recycled back to the surface. It has been suggested that raft-enriched lipids represent the site of scrapie formation [122]. On the other hand, it is known that APrPsc undergoes proteasomal degradation and accumulates in lysosomes.

In the case of Parkinson's disease, α -synuclein accumulates inside the cells as fibrillar aggregates named Lewy bodies. However, although α -synuclein is a cytoplasmic protein, a small amount of the protein is secreted by the cells and is present in human body fluids. It has been demonstrated that non-fibrillar oligomeric aggregates, as well as fibrils are able to enter the cells through the endosomal pathway and to be degraded by lysosomes. This mechanism might protect neurons from exposure to potentially toxic α -synuclein [123]. However, it has to be noticed that newly synthesized α -synuclein monomers and dimers, but not protofibrils, can be degraded by the proteasome [124].

Along the internalization and intracellular pathway, common aspects are shared by [1-93]ApoA-I and amyloid β peptide ($A\beta$), responsible for Alzheimer's disease.

The most abundant forms of $A\beta$ are 40 and 42 residue long ($A\beta_{40/42}$), whose oligomeric species were found to rapidly bind and internalize in neuronal cells and accumulate in lysosomes. In contrast, aggregated polypeptides were found to associate with cells only weakly [125]. Furthermore, soluble $A\beta$ oligomers, but not monomers, inhibit proteasomal activity *in vitro* [126]. It has to be noticed that cellular mechanisms deputed to protein degradation, i.e. lysosomes, proteasome and autophagy, may be important targets for therapeutic approaches against amyloidoses. Since in several amyloid diseases the impairment of proteasomal activity has been pointed out, a promising therapeutic approach would be that of enhancing the activity of cellular mechanisms for protein clearance.

Based on the experimental data collected so far, a model representing the possible fate of [1-93]ApoA-I polypeptide in an *in vivo* context is proposed.

The continuous accumulation of the natively unfolded polypeptide in the cardiac tissue leads to a progressive, massive occupancy of the extracellular space by amyloid deposits, as observed in pathological hearts, from which the natural fibrillogenic polypeptide can be isolated. During the fibrillogenic process, a dynamic equilibrium between monomeric species and aggregated states has been proposed [127]. The results reported in this thesis provided evidence that, besides aggregation in the extracellular space, an alternative fate is available to the polypeptide, i.e. the interaction with target cells, internalization and subsequent degradation. Since the intracellular degradation pathway is precluded to fibrillar aggregates, the hypothesis can be raised that internalization and subsequent degradation of the unaggregated fibrillogenic polypeptide represent a protective mechanism against fibrillogenesis, able to balance [1-93]ApoA-I progressive aggregation and to slow down the fibrillogenic process. This phenomenon may be relevant in the slow progression and late onset of ApoA-I-associated amyloid pathology.

1.2 Towards the definition of two molecular partners of [1-93]ApoA-I

The definition of the molecular partners of the fibrillogenic polypeptide is a central issue in the comprehension of the disease molecular bases.

In collaboration with the research group of Prof. P. Pucci, Department of Chemical Sciences, a functional proteomic approach was followed to identify the polypeptide interactome. GST pull-down experiments, and protein identification by mass spectrometry were performed on cardiomyoblasts membrane extracts. This experimental approach provided a list of about 100 potential interactors of the fibrillogenic polypeptide and, among these, the ATP synthase β -chain and the protein nicastrin were selected to be analyzed in detail.

The validation of the selected putative interactors by independent approaches is an essential step of any functional proteomic experiment. Thus, co-immunoprecipitation (Co-IP) and fluorescent microscopy experiments have been performed.

Co-IP experiments have been performed using cardiomyoblasts lysates incubated with FITC-labelled [1-93]ApoA-I. The protein species immunoprecipitated with anti-FITC antibodies were analyzed by Western blotting using antibodies directed towards each of the selected interactors of the fibrillogenic polypeptide. Either anti-ATPase and anti-nicastrin antibodies recognized their respective antigens in the

immunoprecipitated sample, indicating that both proteins do represent cellular partners of [1-93]ApoA-I.

Immunofluorescence analyses performed using antibodies directed towards the β -chain of the ATP synthase complex allowed us to demonstrate the existence of an ectopic form of ATP synthase β -chain on the cell surface of cardiomyoblasts. Then, we demonstrated a significant co-localization of ATP synthase β -chain and [1-93]ApoA-I, strengthening the validation of ectopic ATPase as a specific target. Similarly, we demonstrated that the polypeptide co-localizes with nicastrin. These results indicate that both ATP synthase β -chain and nicastrin interact with the fibrillogenic polypeptide at the cell surface.

ATP synthase has been recently detected at the surface of different cell types, wide variety of tumor, as well as normal cells, where it is a high affinity receptor for ApoA-I. ApoA-I interacts with the endothelial ecto-F₁-ATPase to initiate a signaling pathway contributing to the anti-apoptotic and proliferative effects mediated by HDLs and ApoA-I on endothelial cells [92, 95]. In this scenario, the identification of ecto-ATP synthase as a partner of the fibrillogenic polypeptide of ApoA-I, that accumulates in the extracellular space where amyloid fibrils are generated, raises the question on which role this interaction may have during the fibrillogenesis, and/or the polypeptide internalization in target cells. Starting from these observations, it will be of great interest to analyze whether the fibrillogenic polypeptide is able to interfere with ApoA-I anti-apoptotic activity *via* ecto-F₁-ATPase, and which role the binding of the fibrillogenic polypeptide to this protein partner may have on the fate of the polypeptide inside or outside the cells.

Recently, a correlation was evidenced between AD and ectopic ATP synthase. It has been demonstrated that ATP synthase subunit α is a binding partner of the extracellular domain of APP and A β . Thus, modification of ATP synthase activity could result from binding of the extracellular domain of APP and A β to the α subunit. The extracellular domain of APP and A β interacts with ATP synthase subunit α and partially inhibits the extracellular generation of ATP by the ATP synthase complex. These observations demonstrate that A β competes with APP for binding to ATP synthase subunit α and that APP and A β regulate extracellular ATP levels in the brain, thus suggesting a novel mechanism in A β -mediated AD pathology [69]. Analogously, we demonstrated that ApoA-I fibrillogenic polypeptide, [1-93]ApoA-I, interacts directly or indirectly with ecto-F₁-ATPase. Therefore, we hypothesize a more general role played by this protein in amyloid diseases.

Nicastrin is an essential subunit of the γ -secretase complex, an endoprotease complex that catalyzes the intramembrane cleavage of integral membrane proteins such as Notch receptors and amyloid precursor protein (APP).

High levels of plasma cholesterol are known to be a risk factor for AD pathology since cholesterol is a well-established modulator of APP processing. The β -secretase cleavage of APP, which results in A β formation, mainly occurs in cholesterol rich lipid rafts, whereas the α -secretase activity seems to be favored in non rafts membranes. Cholesterol depletion inhibits the amyloidogenic pathway, leading to reduced A β levels and, in general, shifts APP processing toward preferential non-amyloidogenic pathway [128]. Moreover, it has been demonstrated that A β promotes the efflux of cellular cholesterol during its secretion. This process is mediated by ABCA1 and is accompanied by the formation of high density lipoprotein-like particles. This mechanism resembles that of apolipoprotein-mediated cholesterol efflux, although apolipoproteins interact with ABCA1 from the extracellular space [129], whereas the

A β –ABCA1 interaction appeared to occur within the plasma membrane or in the intracellular compartment [130].

Further experiments will be designed to verify whether the amyloidogenic polypeptide is able to interact directly with nicastrin and to deeply inspect a possible involvement of γ -secretase complex in [1-93]ApoA-I proteolytic release.

These observations suggest that common tracts are shared by different fibrillogenic polypeptides and that common pathways may be discovered. The identification of specific targets of a pathological protein or peptide is the pre-requisite to plan site-directed therapeutic intervention.

2. Studies on the full-length ApoA-I pathogenic variants

2.1. A cell model to produce full-length variants

Structural and functional analyses of the full-length variants of ApoA-I, in comparison to the wild-type protein, will greatly contribute to the understanding of the molecular bases of the pathology.

Nevertheless, all the patients analyzed so far were found to be heterozygous for the mutated gene, as both the wild-type and variant proteins are expressed. Moreover the variant protein was found in the plasma at lower levels than the wild-type.

Thus, being impracticable any approach to isolate the ApoA-I variant as a pure product from patient's tissues or plasma, heterologous expression systems are needed. With the exception of variants G26R and L178H produced in bacterial cells [99, 100], no reports are available to date on the production and isolation of ApoA-I amyloidogenic variants.

We set up a suitable cellular model consisting in stably transfected mammalian cells to express recombinant ApoA-I amyloidogenic variant L174S, responsible for amyloid deposition preferentially in the heart of patient. Stably transfected CHO-K1 clones were obtained to express the ApoA-I amyloidogenic variant, as well as the wild-type protein. Both recombinant proteins, efficiently secreted in the culture medium, albeit with different kinetics, were isolated from the cell medium following a one-step purification procedure. Both proteins were found to be associated to fatty acids, as expected for lipid binding proteins, although to our knowledge no evidence of ApoA-I interaction with fatty acids has been provided so far.

Two saturated and two monounsaturated fatty acids were associated to both proteins, with a higher lipid-to-protein molar ratio observed for the amyloidogenic variant. As it is known that long-chain saturated, monounsaturated and polyunsaturated fatty acids have a role in a number of cellular processes, e.g. trafficking and secretion of ApoA-I and B [131] and stimulation of triacylglycerol synthesis and secretion [132], our findings may have physiological implications.

Nevertheless, due to the low amount of the recombinant proteins isolated, extensive structure to function relationship studies cannot be performed. Thus, an alternative expression system is needed. Recently, we started to settle a prokaryotic expression system to obtain a higher amount of ApoA-I pathogenic variants, suitable for structural and functional analyses.

2.2. Effects of endogeneous ApoA-I full-length variants on cell vulnerability to stress and stress response

The survival of mammalian cells exposed to adverse environmental conditions requires a radical reprogramming of protein translation [133]. This is part of an integrated stress response that promotes survival of cells subjected to adverse environmental conditions [134]. Usually, stress-induced translational arrest of mRNAs encoding “housekeeping” proteins is triggered by a family of eIF2 α kinases that reduce the availability of eIF2 α –GTP–tRNA^{Met} ternary complexes required for translation initiation [135]. However, low-dose oxidative stress inhibits protein translation in cells expressing non-phosphorylatable eIF2 α , suggesting the existence of a phospho-eIF2 α –independent translation control pathway [112]. It has been reported that angiogenin (ANG) is involved in stress response by cleaving tRNAs, thus inhibiting protein translation and promoting cell survival [108]. ANG is a secreted RNase that was first identified as an angiogenic factor found in tumor cell conditioned medium [136]. ANG binds to receptors on the surface of endothelial cells that facilitate its internalization and transport to the nucleolus [137-139]. Remarkably, promotion of new blood vessel growth is dependent on ANG ribonuclease activity [140]. Although the RNA targets required for angiogenesis are unknown, *in vitro* studies have shown that tRNAs are preferred targets [141].

Few years ago, a mutated form of ANG was identified in patients affected by familial or sporadic amyotrophic lateral sclerosis (ALS) [116], representing the first loss-of-function gene mutation associated to the pathology. Later, it was demonstrated that ANG is able to protect against hypoxia-induced motor neuron degeneration to prevent motor neuron death induced by excitotoxicity and endoplasmic reticulum stress [142, 143]. Moreover, it has been observed that the secretion of ANG is enhanced by hypoxia, which indicated ANG as a component of a stress response program [144, 145]. Recently, ANG levels have been found to be reduced in PD transgenic mouse models in which α -syn is over-expressed [113] and in AD patients [114], suggesting a more general protective role of ANG in neurodegenerative disorders.

We found that reduced ANG levels occur in hepatic cells over-expressing an amyloidogenic variant of ApoA-I, L75P, responsible for systemic amyloidosis predominantly involving the liver, with respect to cells over-expressing wt-ApoA-I, or to untransfected cells. Interestingly, quantification of intracellular and extracellular ApoA-I levels by Western blotting analysis indicated that, differently from wt-ApoA-I, the L75P amyloidogenic variant is highly retained within the cells. Moreover, L75P-ApoA-I cells showed a high number of apoptotic nuclei with respect to wt-ApoA-I or untransfected hepatic cells. Similarly, Marchesi and co-workers observed that secretion of the amyloid proteins L75P and L174S-ApoA-I is down-regulated in transiently transfected cells [146]. Taken together, these results suggest that the impairment of ApoA-I variant secretion might be a first line of defence of the organism against the disease.

It has been demonstrated that ANG is able to protect cells from stress factors, such as oxidative stress or serum withdrawal [108, 116]. Taking advantage of an experimental system in which ANG levels and localization are altered, due to the presence of an amyloidogenic protein, we analyzed what happens when cells are exposed to stress conditions (serum starvation).

A significant difference in ANG intracellular localization was observed between wt and L75P-ApoA-I hepatic cells. In the absence of serum, ANG was mostly localized in the cytosolic compartment of wt-ApoA-I or untransfected cells, according to its role

in stress response [108]. Surprisingly, in the presence of the amyloidogenic variant, ANG was mostly localized in the nucleus. Moreover, L75P-ApoA-I cells showed a higher number of apoptotic nuclei and a significant impairment of cell viability with respect to controls. qRT-PCR experiments indicated that serum starvation causes an increase in ANG levels in both untransfected and wt-ApoA-I hepatic cells, while only a very slight increase was observed in the case of L75P-ApoA-I hepatic cells.

In conclusion, in the presence of an amyloidogenic variant, cell viability and ANG levels and localization are altered, suggesting a possible role of this protein in ApoA-I related amyloidosis. We reasoned that, if this hypothesis is correct, addition of exogenous ANG should be able to restore cell viability. MTT assays and ethidium bromide staining were performed in the presence of exogenous ANG in serum-starved cells. We found a strong anti-apoptotic effect of ANG on L75P-ApoA-I-HepG2 cells, with no significant effect on wt-ApoA-I-HepG2 cells or untransfected cells, indicating a protective role of ANG in cells expressing a pathogenic variant.

To understand how ANG exerts its protective effect, we used three ANG mutants: R33A, K40Q and R66A, each defective in one of the activities associated to ANG. R33A is not able to translocate to the nucleus, K40Q is not active enzymatically and R66A is unable to bind efficiently to the receptor [117]. Three distinct functional sites are responsible for ANG activities, all of them essential for ANG to have angiogenic and growth stimulating activities [147-149]. The loop region from K60 to N68 is the receptor-binding site that interacts with a to-be-identified cell surface receptor [147]; upon binding to the cell surface receptor, ANG is internalized and translocated to the nucleus [117], a process is mediated by a NLS located between M30 and G34 [148]. The ribonucleolytic activity of ANG, executed by the catalytic triad H13, K40, and H113 [149], is believed to function in stimulating ribosomal RNA (rRNA) transcription after ANG translocation to the nucleus.

We tested by MTT assays these loss-of-function ANG mutants and observed that the only the mutant defective in binding to the receptor (R66A) fails in the recovery of L75P-ApoA-I cells viability. On the contrary, ANG protective role seems do not involve its ribonucleolytic activity (K40Q), nor its nuclear localization (R33A). From the analysis of this set of ANG mutants, we hypothesized that ANG needs to be internalized into the cells to elicit its protective role in cells under stress conditions.

It seems that an alteration in ANG expression is likely a pathological consequence of L75P-ApoA-I over-expression, similarly to experimental observations in PD transgenic mice. It is still unclear how over-expression of amyloidogenic proteins can cause a decrease in ANG expression. In the case of α -synuclein, Kontopoulos hypothesized that this protein normally negatively regulates ANG expression in the brain, by affecting transcription *via* inhibition of histone acetylation [150]; therefore, α -synuclein over-expression could cause a reduction in ANG levels *via* this mechanism. The same mechanism of acetylation inhibition has been described for another neurodegenerative disease, involving the fibrillogenic protein ataxin-3 [151].

In conclusion, regardless whether or not reduced ANG levels play a role in PD or ApoA-I pathologies, the ability of exogenous ANG to reduce cell death suggests that increasing ANG levels could serve as a means to slow down degenerative processes in amyloidosis.

Further experiments will be performed to elucidate the molecular basis of the protective role of ANG in ApoA-I related amyloidosis.

BIBLIOGRAPHY

- [1] Anfinsen CB. Principles that govern the folding of protein chains. (1973) *Science*; 181:223-30
- [2] Murzin A.G. Biochemistry. Metamorphic proteins. (2008) *Science*; 320: 1725-6
- [3] Bukau B. Molecular chaperones and protein quality control. (2006) *Cell*; 125:443-51
- [4] Muchowsky P.J. and Wacker J.L. Modulation of neurodegeneration by molecular chaperones. (2005) *Nat. rev. Neurosci.*; 6: 11-22
- [5] Carrel L.W. and Lomas D.A. Conformational disease. (1997) *Lancet*; 350:1348
- [6] Stefani M. and Dobson C.M. Protein aggregation and aggregate toxicity: new insights into protein folding, misfolding diseases and biological evolution. (2003) *J. Mol. Med.*; 81: 678–699
- [7] Westermark P. et al. Amyloid: toward terminology clarification. Report from the Nomenclature Committee of the International Society of Amyloidosis. (2005) *Amyloid*;12:1-4
- [8] Agorogiannis E. I. et al. Protein misfolding in neurodegenerative diseases (2004) *Neuropathology and Applied Neurobiology*; 30: 215-224
- [9] Eriksson M., et al. Hereditary apolipoprotein AI-associated amyloidosis in surgical pathology specimens: identification of three novel mutations in the APOA1 gene. (2009) *The Journal of Molecular Diagnostics*; 11: 257-262
- [10] Relini A., et al. Monitoring the process of HypF fibrillization and liposome permeabilization by protofibrils. (2004) *Journal of Molecular Biology*; 338: 943-957
- [11] Uversky VN, Fink AL. Conformational constraints for amyloid fibrillation: the importance of being unfolded. (2004) *Biochim. Biophys. Acta*; 1698:131–53
- [12] Gebbink M. F., et al. Amyloids:a functional coat for microorganisms. (2005) *Nat Rev Microbiol*; 3: 333-341
- [13] Berson J. F., et al. Proprotein convertase cleavage liberates a fibrillogenic fragment of a resident glycoprotein to initiate melanosome biogenesis. (2003) *J. Cell. Biol*; 161: 521-533
- [14] Harper D. C., et al. Premelanosome amyloid-like fibrils are composed of only golgi-processed forms of Pmel17 that have been proteolytically processed in endosomes. (2008) *J. Biol. Chem.*; 283: 2307-2322
- [15] Serpell L.C., et al. The protofilament substructure of amyloid fibrils. (2000) *J. Mol. Biol.*; 300:1033–39
- [16] Sunde M., Blake C. The structure of amyloid fibrils by electron microscopy and X-ray diffraction. (1997) *Adv. Protein Chem.*; 50:123–59
- [17] Bauer H.H., et al. Architecture and polymorphism of fibrillar supramolecular assemblies produced by in vitro aggregation of human calcitonin. (1995) *J. Struct. Biol.*; 115:1–15;
- [18] Saiki M., et al. Higher-order molecular packing in amyloid-like fibrils constructed with linear arrangements of hydrophobic and hydrogen-bonding side-chains. (2005) *J. Mol. Biol.*; 348:983–98 14.
- [19] Pedersen J.S., et al. The changing face of glucagon fibrillation: structural polymorphism and conformational imprinting. (2005) *J. Mol. Biol.*; 355:501–23

- [20] Stefani M. Protein misfolding and aggregation: new examples in medicine and biology of the dark side of the protein world. (2004) *Biochimica et Biophysica Acta*; 1739: 5-23
- [21] Zrovnik E. Amyloid-fibril formation. Proposed mechanisms and relevance to conformational disease. (2002) *Eur. J. Biochem*; 269: 3362-3371
- [22] Relini A., et al. Ultrastructural organization of ex vivo amyloid fibrils formed by the apolipoprotein A-I Leu174Ser variant: an atomic force microscopy study. (2004) *Biochimica et Biophysica Acta*; 1690: 33-41
- [23] Snow A. D., et al. A close ultrastructural relationship between sulfated proteoglycans and AA amyloid fibrils. (1987) *Lab. Invest*; 57: 687-698
- [24] Snow A. D., et al. Cationic dyes reveal proteoglycans structurally integrated within the characteristic lesions of Alzheimer's disease (1989) *Acta Neuropathol*; 78: 113-123
- [25] Alexandrescu A.T. Amyloid accomplices and enforcers. (2005) *Protein Science*; 14: 1-12
- [26] Pepys M. B., et al. Amyloid P component. A critical review. (1997) *Int. J. Exp. Clin. Invest*; 4: 274-295
- [27] Pepys M. B. Pathogenesis, diagnosis and treatment of systemic amyloidosis. (2001) *Philos. Trans. R. Soc. Lond. B*; 356: 203-211
- [28] Chiti F., Dobson C.M. Protein misfolding, functional amyloid, and human disease (2006) *Annu. Rev. Biochem.*; 75: 333-66
- [29] Naiki H., et al. Establishment of a kinetic model of dialysis-related amyloid fibril extension in vitro. (1997) *Amyloid*; 4:223–32
- [30] Serio T.R., et al. Nucleated conformational conversion and the replication of conformational information by a prion determinant. (2000). *Science*; 289:1317–21
- [31] Goldsbury C.S.; et al. Studies on the in vitro assembly of a beta 1-40: implications for the search for a beta fibril formation inhibitors. (2000) *Journal of Structural Biology*; 130: 217-231
- [32] Stefani M.; et al. Protein aggregation and aggregate toxicity: new insights into protein folding, misfolding diseases and biological evolution. (2003) *Journal of Molecular Medicine*;81: 678-699
- [33] Abedini A., Raleigh D.P. A critical assessment of the role of helical intermediates in amyloid formation by natively unfolded proteins and polypeptides. (2009) *Prot. Eng. Des. Sel.*; 22: 453-459
- [34] Weinreb P.H.et al. NACP, a protein implicated in Alzheimer's disease and learning, is natively unfolded. (1996) *Biochemistry*; 35(43): 13709-13715
- [35] Uversky V.N. Natively unfolded proteins: a point where biology waits for physics. (2002) *Protein Science*; 11(4): 739-756
- [36] Fielding C.J., Fielding P.E. Molecular physiology of reverse cholesterol transport. (1995) *Lipid Re*; 36(2): 211-228
- [37] Pastore L. et al. Helper-dependent adenoviral vector-mediated long-term expression of human apolipoprotein A-I reduces atherosclerosis in apo E-deficient mice. (2004) *Gene*; 327(2): 153-60
- [38] Brouillette C.G. et al. Structural models of human apolipoprotein A-I: a critical analysis and review. (2001) *Biochim Biophys Acta*; 1531:4-46
- [39] Briton E.A. Oral estrogen replacement therapy in postmenopausal women selectively raises levels and production rates of lipoprotein A-I and lowers hepatic lipase activity without lowering the fractional catabolic rate. (1996) *Arter Thromb. Vasc. Biol.*; 16:431-440

- [40] Mooradian A.D. Ascorbic acid and alpha-tocopherol down-regulate apolipoprotein A-I gene expression in HepG2 and Caco-2 cell lines. (2006) *Metabol*; 55:159-167
- [41] Duong P. T. et al. Characterization and properties of pre beta-HDL particles formed by ABCA1-mediated cellular lipid efflux to apoA-I. (2008) *J. Lipid Res.*; 49(5): 1006–1014
- [42] Adorni M.P. et al. The roles of different pathways in the release of cholesterol from macrophages. (2007) *J Lipid Res.*; 48(11): 2453-2462
- [43] Mulya A. et al. Minimal lipidation of pre-beta HDL by ABCA1 results in reduced ability to interact with ABCA1. (2007) *Arterioscler Thromb Vasc Biol.*; 27(8): 1828-1836
- [44] Sacks F.M. et al. Selective delipidation of plasma HDL enhances reverse cholesterol transport in vivo. (2009) *J. Lipid Res.*; 50(5): 894-907
- [45] Rye K.A. et al. Evidence that cholesteryl ester transfer protein-mediated reductions in reconstituted high density lipoprotein size involve particle fusion. (1997) *J Biol Chem.*; 272(7): 3953-3960
- [46] Liang H.Q. et al. Remodelling of reconstituted high density lipoproteins by lecithin: cholesterol acyltransferase. (1996) *J Lipid Res.*; 37(9): 1962-1970
- [47] Lusa S. et al. The mechanism of human plasma phospholipid transfer protein-induced enlargement of high-density lipoprotein particles: evidence for particle fusion. (1996) *Biochem. J.*; 313 (Pt 1): 275-282
- [48] Rya R.O. et al. Human apolipoprotein A-I liberated from high-density lipoprotein without denaturation. (1992) *Biochemistry*; 31(18): 4509-4514
- [49] Clay M.A. et al. Cholesteryl ester transfer protein and hepatic lipase activity promote shedding of apo A-I from HDL and subsequent formation of discoidal HDL. (1992) *Biochim. Biophys. Acta*; 1124(1): 52-58
- [50] Acton S. et al. Identification of scavenger receptor SR-BI as a high density lipoprotein receptor. (1996) *Science*; 271(5248): 518-520
- [51] Cavigiolio G. et al. Exchange of apolipoprotein A-I between lipid-associated and lipid-free states: a potential target for oxidative generation of dysfunctional high density lipoproteins. (2010) *J Biol Chem.*; 285(24): 18847-18857
- [52] Obici L. et al. Structure, function and amyloidogenic propensity of apolipoprotein A-I. (2006) *Amyloid*; 13(4): 191-205
- [53] Glass C.K. et al. Tissue sites of degradation of apoprotein A-I in the rat. (1983) *J. Biol Chem.*; 258(11): 7161-7167
- [54] Borhani D.W. et al. Crystal structure of truncated human apolipoprotein A-I suggests a lipid-bound conformation. (1997) *Proc Natl Acad Sci U S A.*; 94(23): 12291-12296
- [55] Silva R.A. et al. A three-dimensional molecular model of lipid-free apolipoprotein A-I determined by cross-linking/mass spectrometry and sequence threading. (2005) *Biochemistry*; 44(8): 2759-2769
- [56] Sorci-Thomas M.G., Thomas M.J. The effects of altered apolipoprotein A-I structure on plasma HDL concentration. (2002) *Trends Cardiovasc. Med.*; 12:121-28
- [57] Wiesgraber K.H. et al. A-I-milano apoprotein. Isolation and characterization of a cysteine-containing variant of the A-I apoprotein from human high density lipoproteins. (1980) *J. Clin. Invest.*; 66:901-907
- [58] Rowczenio D. et al. Amyloidogenicity and clinical phenotype associated with five novel mutations in apolipoprotein A-I. (2011) *Am. J. Pathol* 179 (4): 1978-87
- [59] Bellotti V. et al. The workings of the amyloid diseases. (2007) *Ann Med* 39:200-7

- [60] Amarzguioui, M. et al. Extensive intimal apolipoprotein A1-derived amyloid deposits in a patient with an apolipoprotein A1 mutation. (1998) *Biochem Biophys Res Commun.* 242, 534-539
- [61] Di Gaetano S. et al. Recombinant amyloidogenic domain of ApoA-I: analysis of its fibrillogenic potential. (2006) *Biochem. Biophys. Res. Commun.*; 351: 223-8
- [62] Andreola A. et al. Conformational switching and fibrillogenesis in the amyloidogenic fragment of apolipoprotein a-I. (2003) *J Biol Chem.*; 278: 2444-2451
- [63] Obici L. et al. The new apolipoprotein A-I variant leu(174) --> Ser causes hereditary cardiac amyloidosis, and the amyloid fibrils are constituted by the 93-residue N-terminal polypeptide. (1999) *Am J Pathol.*; 155(3): 695-702
- [64] Fantini J., Yahi N., Molecular insights into amyloid regulation by membrane cholesterol and sphingolipids: common mechanisms in neurodegenerative diseases. (2010) *Expert Rev Mol Med.*; doi: 10.1017/S1462399410001602
- [65] Shanmugam G. Jayakumar R. Structural analysis of amyloid beta peptide fragment (25-35) in different microenvironments. (2004) *Biopolymers*; 76: 421-434
- [66] Kakio A. et al. Interaction between amyloid beta-protein aggregates and membranes. (2004) *Pept Sci.*; 10(10): 612-621
- [67] Hou X. et al. Binding of amyloidogenic transthyretin to the plasma membrane alters membrane fluidity and induces neurotoxicity. (2005) *Biochemistry*; 44(34): 11618-11627
- [68] Kazlauskaitė J. et al. Structural changes of the prion protein in lipid membranes leading to aggregation and fibrillization. (2003) *Biochemistry*; 42(11): 3295-3304
- [69] Fernandez-Escamilla A.M. et al. Prediction of sequence-dependent and mutational effects on the aggregation of peptides and proteins. (2004) *Nat Biotechnol.*; 22(10): 1302-1306
- [70] Frank P.G., Marcel Y. L. Apolipoprotein A-I: structure-function relationships. (2000) *J. Lipid Res.*; 41: 853–872
- [71] Tanaka M. et al. Contributions of the N- and C-terminal helical segments to the lipid-free structure and lipid interaction of apolipoprotein A-I. (2006) *Biochemistry*; 45: 10351-10358
- [72] Monti D.M. et al. Effects of a lipid environment on the fibrillogenic pathway of the N-terminal polypeptide of human apolipoprotein A-I, responsible for in vivo amyloid fibril formation. (2010) *Eur Biophys J.*; 39(9): 1289–1299
- [73] Lee S.J. et al. A detergent-insoluble membrane compartment contains A beta in vivo. (1998) *Nat Med.*; 4(6): 730-734
- [74] Ehalt R. et al. Amyloidogenic processing of the Alzheimer beta-amyloid precursor protein depends on lipid rafts. (2003); *J Cell Biol.*;160: 113-123
- [75] Kakio A. et al. Formation of a membrane-active form of amyloid beta-protein in raft-like model membranes. (2003) *Biochim. Biophys. Res. Commun.*; 303(2): 514-518
- [76] Vedhachalam C. et al. Mechanism of ATP-binding cassette transporter A1-mediated cellular lipid efflux to apolipoprotein A-I and formation of high density lipoprotein particles. (2007) *J. Biol. Chem.*; 282: 25123-25130
- [77] Zhu M., Fink A.L. Lipid binding inhibits alpha-synuclein fibril formation. (2003) *J Biol. Chem.*; 278(19): 16873-16877
- [78] Raimondi S. et al. Effects of the known pathogenic mutations on the aggregation pathway of the amyloidogenic peptide of apolipoprotein A-I. (2011) *J. Mol Biol.*; 407 (3): 465-76

- [79] Mei X., Atkinson D. Crystal structure of C-terminal truncated apolipoprotein A-I reveals the assembly of high density lipoprotein (HDL) by dimerization. (2011) *J Biol. Chem.*; 286: 38570-82
- [80] Muramatsu M., et al. Quantitative aspects of isolation of nucleoli of the Walker carcinosarcoma and liver of the rat. (1963) *Cancer Res.*; 25:693-697
- [81] Ribble D. et al. A simple technique for quantifying apoptosis in 96-well plates. *BMC Biotechnol.* (2005); 6:12
- [82] Georgeaud V., et al. Identification of an ApoA-I ligand domain that interacts with high-affinity binding sites on HepG2 cells. (2000) *Biochem Biophys Res Commun.*; 267: 541-5
- [83] Denis M. et al. ATP-binding cassette A1-mediated lipidation of apolipoprotein A-I occurs at the plasma membrane and not in the endocytic compartments. (2008) *J Biol Chem.*; 283: 16178-86
- [84] Vedhachalam C. et al. ABCA1-induced cell surface binding sites for ApoA-I. (2007) *Arterioscler Thromb Vasc Biol.*; 27: 1603-9
- [85] Eckman C.B., Eckman E.A. An update on the amyloid hypothesis. (2007) *Neurol Clin.*; 25: 669-82
- [86] Cavelier C. et al. Lipid efflux by the ATP-binding cassette transporters ABCA1 and ABCG1. (2006) *Biochim Biophys Acta*; 1761: 655-66
- [87] Azuma Y. et al. Retroendocytosis pathway of ABCA1/apoA-I contributes to HDL formation. (2009) *Genes to Cells.*; 14: 191-204
- [88] Monti M. et al. Functional proteomics. (2005) *Clin Chim Acta*; 375: 140-150
- [89] Kocher T., Superti-Furga G. Mass spectrometry-based functional proteomics: from molecular machines to protein networks. (2007) *Nat Methods*; 4: 807-815
- [90] Vantourout P., et al. Ecto-F₁-ATPase: a moonlighting protein complex and an unexpected apoA-I receptor. (2010) *World J. Gastroenterol.*; 16(47): 5925-5935
- [91] Radojkovic C., et al. Stimulation of cell surface F₁-ATPase activity by apolipoprotein A-I inhibits endothelial cell apoptosis and promotes proliferation. (2009) *Arterioscler. Thromb. Vasc. Biol.*; 29: 1125-1130
- [92] Laurent O. M., et al. Ectopic beta-chain of ATP synthase is an apolipoprotein A-I receptor in hepatic HDL endocytosis. (2003) *Nature*; 421: 75-79
- [93] Jacquet S., et al. The nucleotide receptor P2Y₁₃ is a key regulator of hepatic high-density lipoprotein (HDL) endocytosis. (2005) *Cell. Mol. Life Sci.*; 62: 2508-2515
- [94] Fabre A. C. S., et al. Cell surface adenylate kinase activity regulates the F(1)-ATPase/P2Y (13)-mediated HDL endocytosis pathway on human hepatocytes. (2006) *Cell. Mol. Life Sci.*; 63(23): 2829-2837
- [95] Howard A.D., et al. The β -subunit of ATP synthase is involved in cellular uptake and resecretion of apoA-I but does not control apoA-I-induced lipid efflux in adipocytes. (2011) *Mol. Cell. Biochem.*, 348: 155-164
- [96] Yu G.; et al. Nicastrin modulates presenilin-mediated notch/glp-1 signal transduction and betaAPP processing. (2000) *Nature*; 407: 48-54
- [97] Robbie E.; et al. The secreted protein discovery initiative (SPDI), a large-scale effort to identify novel human secreted and transmembrane proteins: a bioinformatics assessment. (2003) *Genome Res.*; 13: 2265-2270
- [98] Kimberly W.T.; et al. Gamma-secretase is a membrane protein complex comprised of presenilin, nicastrin, Aph-1, and Pen-2. (2003) *Proc. Natl. Acad. Sci. U.S.A.*; 100: 6382-6387
- [99] Lagerstedt J.O. et al. Mapping the structural transition in an amyloidogenic apolipoprotein A-I. (2007) *Biochemistry*; 46: 9693-9699

- [100] Petrlova J. et al. The fibrillogenic L178H variant of apolipoprotein A-I forms helical fibrils. (2012) *Journal of Lipid Res.*; 53(3): 390-8
- [101] Strydom D.J. et al. Amino acid sequence of human tumor derived angiogenin. (1985) *Biochemistry*; 24(20): 5486-94
- [102] Tsuji T. et al. Angiogenin is translocated to the nucleus of HeLa cells and is involved in ribosomal RNA transcription and cell proliferation. (2005) *Cancer Res*; 65: 1352-1360
- [103] Xu Z. P. et al. Identification and characterization of an angiogenin-binding DNA sequence that stimulates luciferase reporter gene expression. (2003) *Biochemistry*; 42: 121-128
- [104] Xu Z. P. et al. The nuclear function of angiogenin in endothelial cells is related to rRNA production. (2002) *Biochem Biophys Res Commun* 294, 287-292
- [105] Moss T. At the crossroads of growth control: making ribosomal RNA. (2004) *Curr Opin Genet Dev*; 14: 210-217
- [106] Ibaragi S. et al. Angiogenin-stimulated Ribosomal RNA Transcription Is Essential for Initiation and Survival of AKT-induced Prostate Intraepithelial Neoplasia. (2009) *Mol Cancer Res*; 7: 415-424
- [107] Yoshioka N. et al. A therapeutic target for prostate cancer based on angiogenin-stimulated angiogenesis and cancer cell proliferation. (2006) *Proc Natl Acad Sci USA* 103: 14519-14524
- [108] Yamasaki S. et al. Angiogenin cleaves tRNA and promotes stress-induced translational repression. (2009) *J Cell Biol* 185, 35-42
- [109] Fu H. et al. Stress induces tRNA cleavage by angiogenin in mammalian cells. (2009) *FEBS Lett* 583: 437-442
- [110] Emara M. M. et al. Angiogenin-induced tRNA-derived stress-induced RNAs promote stress-induced stress granule assembly. (2010) *J Biol Chem* 285: 10959-10968
- [111] Ivanov P. et al. Angiogenin-Induced tRNA Fragments Inhibit Translation Initiation. (2011) *Mol Cell* 43, 613-623
- [112] McEwen E. et al. Heme-regulated inhibitor kinase-mediated phosphorylation of eukaryotic translation initiation factor 2 inhibits translation, induces stress granule formation, and mediates survival upon arsenite exposure. (2005) *J Biol Chem* 280: 16925–16933
- [113] Steidinger T. U. et al. A neuroprotective role for angiogenin in models of Parkinson's disease. (2011) *Journal of Neurochemistry*; 116: 334-341
- [114] Kim Y.N. and Kim D.H. Decreased serum angiogenin level in Alzheimer's disease. (2012) *Progress in Neuro-Psychopharmacology & Biological Psychiatry* 38: 116–120
- [115] Bai J. and Cederbaum A. I. Cycloheximide Protects HepG2 Cells from Serum Withdrawal- Induced Apoptosis by Decreasing p53 and Phosphorylated p53 Levels. (2006) *Journal of Pharmacology and Experimental Therapeutics*; 319 (3): 1435-1443
- [116] Li S. et al. Angiogenin prevent serum withdrawal-induced apoptosis of P19 embryonal carcinoma cells. (2010) *FEBS J*; 277 (17): 3575-3858
- [117] Moroianu J. and Riordan J. F. Nuclear translocation of angiogenin in proliferating endothelial cells is essential to its angiogenic activity. (1994) *Proc. Natl. Acad. Sci. USA*; 91: 1677-1681
- [118] Zha X. et al. Endocytosis is enhanced in Tangier fibroblasts: possible role of ATP-binding cassette protein A1 in endosomal vesicular transport. (2001) *J Biol Chem*. 276: 39476–83

- [119] Barbaras R. et al. Specific binding of free apolipoprotein A-I to a high-affinity binding site on HepG2 cells: characterization of two high-density lipoprotein sites. (1994) *Biochemistry*; 33: 2335–40
- [120] Rohrer L. et al. Binding, internalization and transport of apolipoprotein A-I by vascular endothelial cells. (2006) *Biochim Biophys Acta*; 1761: 186–94
- [121] Oram J.F. The ins and outs of ABCA. (2008) *J Lipid Res.*; 49: 1150-1151
- [122] Sarnataro D. et al. PrP(C) association with lipid rafts in the early secretory pathway stabilizes its cellular conformation. (2004) *Mol Biol Cell.*; 15(9): 4031-4042
- [123] Lee H.J. et al. Assembly-dependent endocytosis and clearance of extracellular alpha-synuclein. (2008) *Int J Biochem Cell Biol.*; 40(9): 1835-1849
- [124] Zhang N.Y. et al. alpha-Synuclein protofibrils inhibit 26 S proteasome-mediated protein degradation: understanding the cytotoxicity of protein protofibrils in neurodegenerative disease pathogenesis. (2008) *J Biol Chem.*; 283(29): 20288-20298
- [125] Bateman D.A. and Chakrabarty A. Cell surface binding and internalization of $a\beta$ modulated by degree of aggregation. (2011) *Int J Alzheimers Dis.*: 2011: 962352
- [126] Tseng B.P. et al. A β inhibits the proteasome and enhances amyloid and tau accumulation. (2008) *Neurobiol Aging.*; 29(11): 607-1618
- [127] Carulla N. et al. Molecular recycling within amyloid fibrils. (2005) *Nature*; 436: 554–8
- [128] Grimm M.O.W. The role of APP proteolytic processing in lipid metabolism. (2012) *Exp Brain Res*; 217(3-4): 365-75
- [129] Yokoyama S. Assembly of high density lipoprotein by the ABCA1/apolipoprotein pathway. (2005) *Curr Opin Lipidol*; 16: 269–279
- [130] Umeda T. et al. Regulation of cholesterol efflux by amyloid beta secretion. *Journal of Neuroscience Research* 2010; 88: 1985-94
- [131] Wang H. et al. Apolipoprotein secretion and lipid synthesis: regulation by fatty acids in newborn swine intestinal epithelial cells. (1997) *Am J Physiol*; 272: G935–G942
- [132] Yao Y. et al. Regulation of triacylglycerol and phospholipid trafficking by fatty acids in newborn swine enterocytes. (2002) *Am J Physiol Gastrointest Liver Physiol*; 282: G817–G824
- [133] Yamasaki S. and Anderson P. Reprogramming mRNA translation during stress. (2008) *Curr Opin Cell Biol* 20: 222–226.
- [134] Ron D. and Walter P. Signal integration in the endoplasmic reticulum unfolded protein response. (2007) *Nat Rev Mol Cell Biol*; 8(7): 519-29
- [135] Anderson P. and Kedersha N. Stress granules: the Tao of RNA triage. (2008) *Trends Biochem. Sci.* 33: 141–150
- [136] Fett J.W. et al. Isolation and characterization of angiogenin, an angiogenic protein from human carcinoma cells. (1985) *Biochemistry*; 24:5480–5486
- [137] Hu G.F. et al. A putative angiogenin receptor in angiogenin-responsive human endothelial cells. (1997) *Proc. Natl. Acad. Sci. USA*; 94: 2204–2209
- [138] Hatzi E. and Badet J. Expression of receptors for human angiogenin in vascular smooth muscle cells. (1999) *Eur. J. Biochem.*; 260: 825–832
- [139] Wiedlocha A. Following angiogenin during angiogenesis: a journey from the cell surface to the nucleolus. (1999) *Arch. Immunol. Ther. Exp. (Warsz.)*; 47: 299–305
- [140] Shapiro R. and Vallee B.L. Human placental ribonuclease inhibitor abolishes both angiogenic and ribonucleolytic activities of angiogenin. (1987) *Proc. Natl. Acad. Sci. USA.*; 84: 2238–2241

- [141] Saxena S.K. et al. Angiogenin is a cytotoxic, tRNA-specific ribonuclease in the RNase A superfamily. (1992) *J. Biol. Chem.*; 267: 21982–21986
- [142] Sebastia J. et al. Angiogenin protects motoneurons against hypoxic injury. (2009) *Cell Death Differ.*; 16: 1238–1247
- [143] Kieran D. et. Control of motoneuron survival by angiogenin. (2008) *J Neurosci.*; 28: 14056–14061
- [144] Hartmann A. et al. Hypoxia-induced up-regulation of angiogenin in human malignant melanoma. (1999) *Cancer Res*; 59: 1578–1583
- [145] Nakamura M. et al. Hypoxic conditions stimulate the production of angiogenin and vascular endothelial growth factor by human renal proximal tubular epithelial cells in culture. (2006) *Nephrol Dial Transplant*; 21: 1489–1495
- [146] Marchesi M. et al. The intracellular quality control system down-regulates the secretion of amyloidogenic apolipoprotein A-I variants: a possible impact on the natural history of the disease. (2011) *Biochim Biophys Acta.*; 1812(1): 87-93
- [147] Hallahan T.W. et al. Dual site model for the organogenic activity of angiogenin. (1991) *Proc Natl Acad Sci USA* 88: 2222–2226
- [148] Moroianu J, Riordan JF. 1994a. Identification of the nucleolar targeting signal of human angiogenin. *Biochem Biophys Res Commun* 203: 1765–1772.
- [149] Shapiro R, Vallee BL. 1989. Site-directed mutagenesis of histidine-13 and histidine-114 of human angiogenin. Alanine derivatives inhibit angiogenin-induced angiogenesis *Biochemistry* 28:7401–7408
- [150] Kontopoulos E. et al α -synuclein acts in the nucleus to inhibit histone acetylation and promote neurotoxicity. (2006) *Human Molecular Genetics*; 15 (20): 3012–3023
- [151] Li F. et al. Ataxin-3 is a histone-binding protein with two independent transcriptional corepressor activities. (2002) *J. Biol. Chem.*; 277: 45004–45012

List of publications inherent to the Doctorate research activity of Dr. Rita Del Giudice

Publications:

- Arciello A., De Marco N., Del Giudice R., Guglielmi F., Pucci P., Relini A., Monti D.M., Piccoli R. Insights into the fate of the N-terminal amyloidogenic polypeptide of ApoA-I in cultured target cells. *J. Cell. Mol. Med.* 2011 Dec; 15(12):2652-63
- Monti D.M., Di Gaetano S., Del Giudice R., Giangrande C., Amoresano A., Monti M., Arciello A., Piccoli R. Apolipoprotein A-I amyloidogenic variant L174S, expressed and isolated from stably transfected mammalian cells, is associated to fatty acids. *Amyloid* 2012 Mar; 19 (1): 21-7

Published contributes to Meetings:

- R. Del Giudice, A. Arciello, D. M. Monti, N. De Marco, R. Piccoli. Amyloidoses associated to apolipoprotein A-I: the intriguing case of a natively unfolded protein fragment. 36th FEBS Congress "Biochemistry for Tomorrow's Medicine", Torino, 25-30 June 2011. *Special Issue on FEBS Journal.* 278: 125 ISSN 1742-4658.

Communications:

- Arciello, D. M. Monti, N. De Marco, R. Del Giudice and R. Piccoli. Binding, internalization and intracellular route of the fibrillogenic fragment of ApoA-I in cardiomyoblasts. 55th National Meeting of the Italian Society of Biochemistry and Molecular Biology (SIB), Milano, 14-17 September 2010.
- R. Del Giudice, A. Arciello, D. M. Monti, N. De Marco, P. Pucci, R. Piccoli. Internalizzazione e percorso intracellulare del frammento fibrillogenico di ApoA-I in cardiomioblasti. Giornate Scientifiche del Polo delle Scienze e delle Tecnologie per la Vita (Università degli Studi di Napoli "Federico II"), Napoli, 25-26 Novembre 2010.
- D. M. Monti, C. T. Supuran, R. Del Giudice, A. Sandomenico, A. Arciello, A. Di Fiore, V. Alterio, G. De Simone, S. M. Monti. Insights into Carbonic Anhydrase VII functional role. The 9th International Conference on Carbonic anhydrase (CA). Antalya (Turkey), 11-15 April 2012, p. 22
- D. M. Monti, R. Del Giudice, A. Sandomenico, A. Arciello, C. T. Supuran, A. Di Fiore, V. Alterio, G. De Simone, S. M. Monti. Human Carbonic Anhydrase VII protects cells from oxidative damage . 13th Naples workshop on bioactive peptides- Conformation and activity in peptides: relationships and interactions. Naples, 7-10 June 2012, p. 110

- R. Del Giudice, A. Arciello, D. M. Monti, A. Amoresano and R. Piccoli. Amyloidoses associated to Apolipoprotein A-I: analysis of the molecular bases of the disease. 56th National Meeting of the Italian Society of Biochemistry and Molecular Biology (SIB), Chieti, 26-29 September 2012.

Research activity in Scientific Institutions abroad

From July to October 2012, the research activity of Dr. Del Giudice has been carried out at the Molecular Oncology Research Institute (MORI), Tufts Medical Center, Boston, MA, USA.



ACKNOWLEDGMENTS

First of all, I would like to express my deepest gratitude to my supervisor, Prof. Renata Piccoli, for allowing me to work in her lab. She has been a fundamental guide and has supported me throughout my thesis with her knowledge.

I am very grateful to Prof. Guo-fu Hu for giving me the opportunity to work in his lab. I have really appreciated his comments and suggestions to make my work more complete and productive.

I would like to thank the Hu's lab members for their critical discussions during lab meetings.

I wish to thank the "Savin Hill company" for allowing me to spend an unforgettable summer in Boston. Thank you Ivy, Kirill, Alex, Chris, Esther and, of course, Carmen, for all the joyful moments we spent together.

There are no words to express my immense gratitude to Dr. Daria Monti and Angela Arciello, who have always guided, encouraged and supported me in all these years. In particular, I'm deeply grateful to Daria, who shared with me part of the best moments of my PhD, as the time we spent together in Boston.

I wish to express my thanks to Dr. Elio Pizzo for all the times he helped me with the HPLC and the lyophilizer.

How can I forget to thank Carmen, Sara and Giusiana. You are my best friends and I won't thank you enough for having been by my side during these years, especially during the most difficult moments, when I've thought to give up.

I would like to thank all the members of the SFP lab, in particular Chiara and Gennaro for all the moments of relax we spent together, during the endless days spent in lab.

I wish to thank all my lab colleagues, especially Francesco, for helping me during the busiest days in the lab.

Finally, I would like to express all my gratitude to my parents for the constant support and for have always believed in me. In particular I thank my Daddy, because I know that for him I will be always the best scientist in the world.

Insights into the fate of the N-terminal amyloidogenic polypeptide of ApoA-I in cultured target cells

Angela Arciello^{a, b}, Nadia De Marco^a, Rita Del Giudice^a, Fulvio Guglielmi^a, Piero Pucci^{c, d}, Annalisa Relini^{b, e}, Daria Maria Monti^{a, b, *}, Renata Piccoli^{a, b}

^a Department of Structural and Functional Biology, University of Naples Federico II, School of Biotechnological Sciences, Naples, Italy

^b Istituto Nazionale di Biostrutture e Biosistemi (INBB), Rome, Italy

^c Department of Organic Chemistry and Biochemistry, University of Naples Federico II, Naples, Italy

^d Ceinge Biotechnologie Avanzate, Naples, Italy

^e Department of Physics, University of Genoa, Genoa, Italy

Received: September 14, 2010; Accepted: January 6, 2011

Abstract

Apolipoprotein A-I (ApoA-I) is an extracellular lipid acceptor, whose role in cholesterol efflux and high-density lipoprotein formation is mediated by ATP-binding cassette transporter A1 (ABCA1). Nevertheless, some ApoA-I variants are associated to systemic forms of amyloidosis, characterized by extracellular fibril deposition in peripheral organs. Heart amyloid fibrils were found to be mainly constituted by the 93-residue N-terminal fragment of ApoA-I, named [1–93]ApoA-I. In this paper, rat cardiomyoblasts were used as target cells to analyse binding, internalization and intracellular fate of the fibrillogenic polypeptide in comparison to full-length ApoA-I. We provide evidence that the polypeptide: (i) binds to specific sites on cell membrane ($K_d = 5.90 \pm 0.70 \times 10^{-7}$ M), where it partially co-localizes with ABCA1, as also described for ApoA-I; (ii) is internalized mostly by clathrin-mediated endocytosis and lipid rafts, whereas ApoA-I is internalized preferentially by clathrin-coated pits and macropinocytosis and (iii) is rapidly degraded by proteasome and lysosomes, whereas ApoA-I partially co-localizes with recycling endosomes. *Vice versa*, amyloid fibrils, obtained by *in vitro* aggregation of [1–93]ApoA-I, were found to be unable to enter the cells. We propose that internalization and intracellular degradation of [1–93]ApoA-I may divert the polypeptide from amyloid fibril formation and contribute to the slow progression and late onset that characterize this pathology.

Keywords: apolipoprotein A-I • amyloidosis • cardiomyoblasts • binding • internalization

Introduction

Apolipoprotein A-I (ApoA-I), the major component of high-density lipoproteins (HDL), is known to play a central role in cholesterol efflux from cells and transport to the liver [1], a crucial process to prevent cellular lipid overload as well as atherosclerosis. Epidemiological studies have demonstrated that plasma levels of HDL, and their major constituent ApoA-I, are inversely correlated with the risk of atherosclerosis [2]. Nevertheless, the molecular

mechanism of the atheroprotective action of ApoA-I, as well as HDL biogenesis, is not fully understood. ApoA-I may act as an extracellular receptor of cellular cholesterol and phospholipids. ApoA-I lipidation to form nascent HDL particles is a process that involves ATP-binding cassette transporter A1 (ABCA1) [3–5], that mediates cholesterol efflux to ApoA-I. ApoA-I is also known to internalize to the endosomes, an intracellular reservoir of cholesterol, to bind lipids and to be resecreted to the medium as HDL [6]. Despite intense research activity suggesting a direct association between ApoA-I and ABCA1 [7], whether or not ABCA1 is to be considered as an ApoA-I receptor is still ambiguous. ApoA-I association to cell surface might not involve direct binding to ABCA1; rather, ABCA1 would induce modifications of lipid distribution at the membrane facilitating ApoA-I docking [3].

Despite its protective role against hypercholesterolemia and cardiovascular diseases, ApoA-I is associated to systemic

*Correspondence to: Daria Maria MONTI,
Department of Structural and Functional Biology,
University of Naples Federico II,
Complesso Universitario di Monte S. Angelo,
via Cinthia 4, 80126 Napoli, Italy.
Tel.: 39-081-679150
Fax: 39-081-679233
E-mail: mdmonti@unina.it

amyloidoses when specific mutations occur in the 243-residue sequence of ApoA-I. Amyloidoses, conformational diseases related to protein misfolding, have been associated to over 40 different peptides and proteins identified so far [8]. Mutations and/or environmental conditions able to destabilize the protein native conformation kinetically favour aggregate nucleation [9] leading to fibrils that accumulate in amyloid deposits in tissues and organs [8].

Sixteen variants of ApoA-I are responsible for systemic amyloidoses characterized by aggregate deposition in peripheral organs, such as heart, liver or kidneys [1, 10, 11]. Amyloid fibrils isolated *ex vivo* were found to be mainly constituted by N-terminal fragments of ApoA-I, 90–100 residue long, released by a still unidentified protease. In particular, the fragment corresponding to sequence 1–93 was found to be the main constituent of cardiac fibrils extracted from patients harbouring variant L174S ApoA-I [10] and affected by a severe systemic amyloidosis predominantly involving the heart. The 93-residue fibrillogenic domain of ApoA-I, extracted from amyloid deposits of a patient who underwent a heart transplant for end-stage heart failure, was found to be a natively unfolded protein in water at neutral pH [12]. Acidic conditions (pH 4) were able to switch on a complex fibrillogenic pathway, consisting of extensive structural rearrangements of the polypeptide, that shifts from a random coil structure to an unstable helical conformation, and then aggregates into a β -sheet based polymeric structure [12].

We produced a recombinant version of ApoA-I 1–93 fragment, denoted as [1–93]ApoA-I, as a pure and stable product, following a strategy aimed at protecting the recombinant polypeptide from intracellular degradation [13]. Conformational analyses revealed that recombinant [1–93]ApoA-I, as the native polypeptide, undergoes conformational transitions and fibrillogenesis, leading to the formation of typical amyloid fibrils on a time scale comparable with that of the natural polypeptide [13].

Nothing is known about the mechanism leading to the release of the fibrillogenic polypeptide from a full-length amyloidogenic variant of ApoA-I, or in which context the proteolytic cleavage does occur. Nevertheless, the hypothesis can be raised that the fibrillogenic polypeptide is released at the site of fibrils deposition, where it accumulates in the extracellular space of target tissues. Here, aggregation in fibrillar structures occurs favoured by molecular crowding and the unfolded structure of the polypeptide. It has been demonstrated that the N-terminal region of full-length ApoA-I is involved in lipid membrane binding [14]. Recently, we suggested that lipids have a key role in [1–93]ApoA-I aggregation [15], as cholesterol, a natural ApoA-I ligand, was found to induce and stabilize helical conformers, slowing down the aggregation process. Moreover, zwitterionic, positively and negatively charged liposomes were found to affect [1–93]ApoA-I conformation by inducing the formation of helical species [15]. Hence, it is conceivable that, although the fibrillogenic polypeptide accumulates in the extracellular space of cardiac cells, it interacts with cell membranes as does the full-length protein.

Here we report binding, internalization and intracellular fate of [1–93]ApoA-I in cultured cardiomyoblasts, in comparison to the full-length protein. Our results show for the first time that the

fibrillogenic fragment of ApoA-I is able to recognize specific binding sites on cell membrane, to be internalized in target cells and to be degraded following an intracellular route only partially coincident with that of full-length ApoA-I.

Materials and methods

Proteins and reagents

All reagents, wild-type ApoA-I, fluorescein isothiocyanate (FITC)-insulin and transferrin (Tf) were from Sigma-Aldrich (St Louis, MO, USA). LysoTracker Red was from Molecular Probes (Invitrogen, Carlsbad, CA, USA). Anti-human ApoA-I polyclonal antibodies were purchased from DAKO (Glostrup, Denmark); anti- β -catenin antibody from Santa-Cruz Biotechnology (Heidelberg, Germany); anti-ABCA1 polyclonal antibodies and the chemiluminescence detection system (SuperSignal[®] West Pico) from Pierce Biotechnology (Rockford, IL, USA); goat anti-rabbit and antimouse antibodies, conjugated with Texas red or with Bodipy fluorescein were from Invitrogen. [1–93]ApoA-I polypeptide was expressed and purified as previously described [15], omitting the neutralization step with ammonium hydroxide. Pure [1–93]ApoA-I was lyophilized and stored at -70°C until use.

Fibrillar aggregates were obtained by incubating [1–93]ApoA-I for 2 weeks at 37°C at 0.3 mg/ml protein concentration in 12 mM sodium phosphate buffer, pH 6.4 containing 20% (v/v) trifluoroethanol (TFE). By centrifugation, insoluble aggregates of [1–93]ApoA-I (pellet) were separated from the unaggregated, soluble polypeptide (supernatant). To quantify aggregated [1–93]ApoA-I, the amount of the soluble polypeptide was determined spectrophotometrically and subtracted from the total amount of [1–93]ApoA-I before aggregation. The pellet was dried under N_2 to remove TFE and resuspended in cell medium to reach the appropriate protein concentration [16]. The suspension of the aggregated species was tested for cytotoxicity.

Cell culture, transfection and Western blot analyses

Rat embryos heart myoblasts H9c2 and human hepatic carcinoma HepG2 cells were purchased from American Type Culture Collection (ATCC). Cells were cultured in DMEM (Sigma-Aldrich), supplemented with 10% foetal bovine serum (HyClone; Thermo Scientific, Logan, UT, USA) and antibiotics, in a 5% CO_2 humidified atmosphere at 37°C . The growth medium of H9c2 cells was implemented with 2 mM L-glutamine and 2 mM sodium pyruvate. Expression vectors for enhanced green fluorescent protein (GFP) tagged Rab4 [17] and enhanced red fluorescent protein (RFP) tagged Rab5 [18] were kindly provided by Dr Marino Zerial (Max-Planck-Institute, Dresden, Germany). H9c2 cells were transiently transfected with either expression vector by the use of METAFECTENE reagent according to the manufacturer's instructions (Biontex-USA, San Diego, CA, USA). After 24 hrs, transfected cells were incubated with the appropriate protein and analysed. To prepare cell lysates, HepG2 and H9c2 cells were scraped off in phosphate-buffered saline (PBS), centrifuged at $1000 \times g$ for 10 min. and resuspended in lysis buffer (1 mM MgCl_2 , 0.25% SDS, 1% Triton X-100 in 10 mM Tris-HCl, pH 7) containing protease inhibitors. After 30 min. incubation on ice, lysates were centrifuged at $14,000 \times g$ for 30 min. at 4°C . Supernatants were diluted in loading buffer containing 8 M urea and analysed, without boiling, by 10% polyacrylamide SDS-PAGE electrophoresis. Protein concentration was determined by Bradford assay.

Atomic force microscopy (AFM) analysis

[1–93]ApoA-I was incubated as described above to generate fibrillar aggregates. Following incubation, the whole sample was diluted 10 times using Milli-Q water; 10 μ l aliquots of the diluted sample were deposited on freshly cleaved mica and dried under mild vacuum. Tapping mode AFM measurements were performed in air using a Dimension 3100 scanning probe microscope equipped with a G scanning head (maximum scan size 100 μ m) and driven by a Nanoscope IIIa controller (Digital Instruments-Bruker AXS GmbH, Karlsruhe, Germany). Images were acquired in tapping mode in air using single beam uncoated silicon cantilevers (type OMCL-AC160TS, Olympus, Tokyo, Japan). The drive frequency was typically 300 kHz and the scan rate was between 0.8 and 1.0 Hz. The size of aggregates was measured from the heights in cross-section in the topographic AFM images.

Binding assays

Proteins under test (100 μ g) were labelled with 1 mCi carrier-free Na^{125}I (Amersham; GE Healthcare Bio-Sciences AB, Uppsala, Sweden) using Iodobeads (Pierce), according to the manufacturer's instructions. Labelled proteins were desalted on PD10 columns (Amersham) equilibrated in PBS. The specific activity was about 1.5 $\mu\text{Ci}/\mu\text{g}$. Cells were seeded in 24-well plates at a density of 5×10^4 /well. After 24 hrs, 200 μ l of binding buffer (25 mM Hepes, pH 7.5, 1 mg/ml bovine serum albumin in DMEM), containing increasing concentrations of the labelled protein under test, were added to the cells. Following 2 hrs incubation at 4°C, cells were washed three times with PBS containing 0.1% bovine serum albumin. Bound radioactivity (total binding) was removed by treating cells with 0.7 ml of cold 0.6 M NaCl in PBS for 2 min. on ice and measured with a γ counter (Packard Instrument Co. Inc., Meriden, CT, USA). Non-specific binding was determined by incubating the cells with the labelled protein in the presence of a 40-fold molar excess of the unlabelled protein. Specific binding was calculated by subtracting non-specific binding from total binding. Affinity constant values (K_d) were calculated according to the Scatchard equation.

Cytotoxicity assays

Cells were seeded in 96-well plates (100 μ l/well) at a density of 5×10^3 /well. After 24 hrs, [1–93]ApoA-I, dissolved in 12 mM sodium phosphate buffer, pH 6.4 (1 mg/ml) and centrifuged to remove insoluble material, was added to the medium to a final concentration of 5 or 10 μM . To test fibrillar aggregates, [1–93]ApoA-I was incubated as described above, and insoluble species were resuspended in cell medium at a final concentration of 5 or 10 μM and added to the cells. Cells were then grown for 72 hrs at 37°C. Cell viability was assessed by the 3-(4,5-dimethylthiazol-2-yl)-2,5-diphenyltetrazolium bromide (MTT) assay. MTT reagent, dissolved in DMEM without phenol red (Sigma-Aldrich), was added to the cells (100 μ l/well) to a final concentration of 0.5 mg/ml. After 4 hrs at 37°C, the culture medium was removed and the resulting formazan salts were dissolved by the addition of isopropanol containing 0.1 N HCl (100 μ l/well). Absorbance values of blue formazan were determined at 570 nm using an automatic plate reader (Microbeta Wallac 1420, Perkin Elmer). Cell survival was expressed as the percentage of viable cells in the presence of the protein under test, with respect to control cells grown in the absence of the protein. The occurrence of plasma membrane damage was determined by measuring the release of lactate dehydrogenase (LDH) in the culture medium [19].

Fluorescence studies

Immediately prior to be tested, proteins were dissolved or dialysed in 0.1 M sodium carbonate, pH 9.0, to a final concentration of 1 mg/ml. Proteins (500 μ g) were conjugated to FITC, following the manufacturer's protocol (Sigma-Aldrich). A Sephadex G25 column, equilibrated in PBS, was used to separate the unreacted FITC from the conjugate. The same procedure was used to label proteins with rhodamine. Fluorescent fibrillar aggregates of [1–93]ApoA-I were obtained by incubating the FITC-labelled polypeptide as described for the unlabelled polypeptide. Insoluble aggregates were resuspended in cell medium and tested as described below. Cells were seeded on glass cover slips in 24-well plates and grown to semi-confluency. Cells were incubated for the indicated times in complete medium with fluorescent proteins or compounds at the following concentrations: [1–93]ApoA-I (3 μM), ApoA-I (1 μM), dextran (5 mg/ml), Tf (0.5 mg/ml), insulin (0.1 mg/ml). Lysosomes were labelled by adding LysoTracker Red (1:500) to living cells at 37°C. After 40 min., cells were treated with 1 μ g/ml Hoechst 33342 for 10 min. at 37°C and washed with PBS. When required, surface bound proteins were stripped with 1 M Hepes, pH 7.5, containing 0.5 M NaCl (Hepes/NaCl) for 5 min. Cells were then fixed for 10 min. at RT with 4% paraformaldehyde in PBS.

To inhibit clathrin-dependent endocytosis, cells were pre-incubated with either 100 μM monodansylcadaverine (MDC) for 30 min. or with 300 μM sucrose for 15 min. As a control, cells were incubated under the same conditions but in the absence of the inhibitors. Cells were then incubated for 6 hrs with the fluorescent protein under test. For immunofluorescence analyses, cells were permeabilized with 0.5% Triton X-100 in PBS (5 min.). Cells were then incubated for 30 min. with 3% goat serum in PBS to saturate non-specific binding sites. Afterwards, cells were incubated overnight at 4°C with anti-ABCA1 antibodies (1:200), or anti- β -catenin antibody (1:200), and then rinsed with 0.1% Triton X-100 in PBS. Finally, cells were incubated 1 hr in the darkness with fluorescent goat anti-rabbit or antimouse IgG (1:500). Slides were washed with 0.1% Triton X-100 in PBS and then with PBS, and mounted in 50% glycerol in PBS. Samples were examined using a Leica 6000 UV microscope and a Leica TCS SP5 confocal microscope, equipped with a Leica application suite software (Leica Microsystems GmbH, Wetzlar, Germany). All images were taken under identical conditions.

Protein degradation analyses

To inhibit proteasome activity, cells were pre-treated for 4 hrs at 37°C with 2.5 μM Z-Leu-Leu-Leu-al (MG132), or with 10 μM N-Ac-Leu-Leu-norleucinal (ALLN). Cells were then incubated with the fluorescent protein for the indicated times. Intralysosomal catabolism was inhibited by treating cells with 20 mM ammonium chloride or 100 μM chloroquine. As a control, cells were incubated under the same conditions but in the absence of the inhibitors.

Results

[1–93]ApoA-I binding to cardiomyoblasts

The ability of [1–93]ApoA-I to recognize specific binding sites on cell surface was investigated by performing binding assays of ^{125}I -

labelled [1–93]ApoA-I to rat cardiomyoblasts (H9c2) and human hepatocytes (HepG2). These cell lines are of interest, as in ApoA-I associated amyloidoses the heart is a natural target for aggregate deposition *in vivo*, whereas the liver is the major source of ApoA-I. The binding curves shown in Fig. 1A and B were obtained incubating cardiomyoblasts or hepatocytes, respectively, for 2 hrs at 4°C

with increasing concentrations of the iodinated polypeptide, in the absence (total binding) or presence (non-specific binding) of a 40-fold molar excess of the unlabelled polypeptide. Specific binding was calculated by subtracting the values relative to non-specific binding from total binding. The data points represent the average of three independent experiments carried out in triplicate determinations. The linearization of the binding data (specific binding) was performed according to the Scatchard equation to obtain the linear plots shown in the insets of Fig. 1. The apparent affinity constants (K_d) were determined and found to be $5.90 \pm 0.70 \times 10^{-7}$ M and $1.78 \pm 0.26 \times 10^{-7}$ M for H9c2 and HepG2, respectively. These results indicate that the fibrillogenic fragment is able to bind with high affinity to specific sites on cell surface of both cell lines.

To test the effects of the fibrillogenic polypeptide on cell viability, cardiomyoblasts were incubated for 72 hrs in the presence of 5 or 10 μ M freshly prepared [1–93]ApoA-I. MTT reduction assays were performed to test metabolically active cells. No inhibition of cell viability was observed in treated cells with respect to untreated cells (Fig. 1C). Furthermore, we tested membrane destabilization of treated cells by measuring LDH release into the culture medium. No significant LDH release was observed upon treatment with [1–93]ApoA-I (data not shown). Finally, the absence of apoptotic nuclei in treated cells (Fig. 1C) confirmed that the fibrillogenic polypeptide, at least in our experimental conditions, is not cytotoxic for cardiomyoblasts.

Endocytosis of [1–93]ApoA-I in cardiomyoblasts

To test whether the fibrillogenic polypeptide of ApoA-I undergoes endocytosis upon interaction with cardiomyoblasts plasma membrane, we labelled [1–93]ApoA-I, as well as full-length ApoA-I, with FITC. H9c2 cells were incubated for different lengths of time either with the polypeptide or with the full-length protein. Cells were then treated with high salt buffer (Hepes/NaCl) to remove proteins specifically bound to the extracellular side of plasma membrane. Following membrane permeabilization with Triton X-100, anti- β -catenin antibody was added to the cells to label the

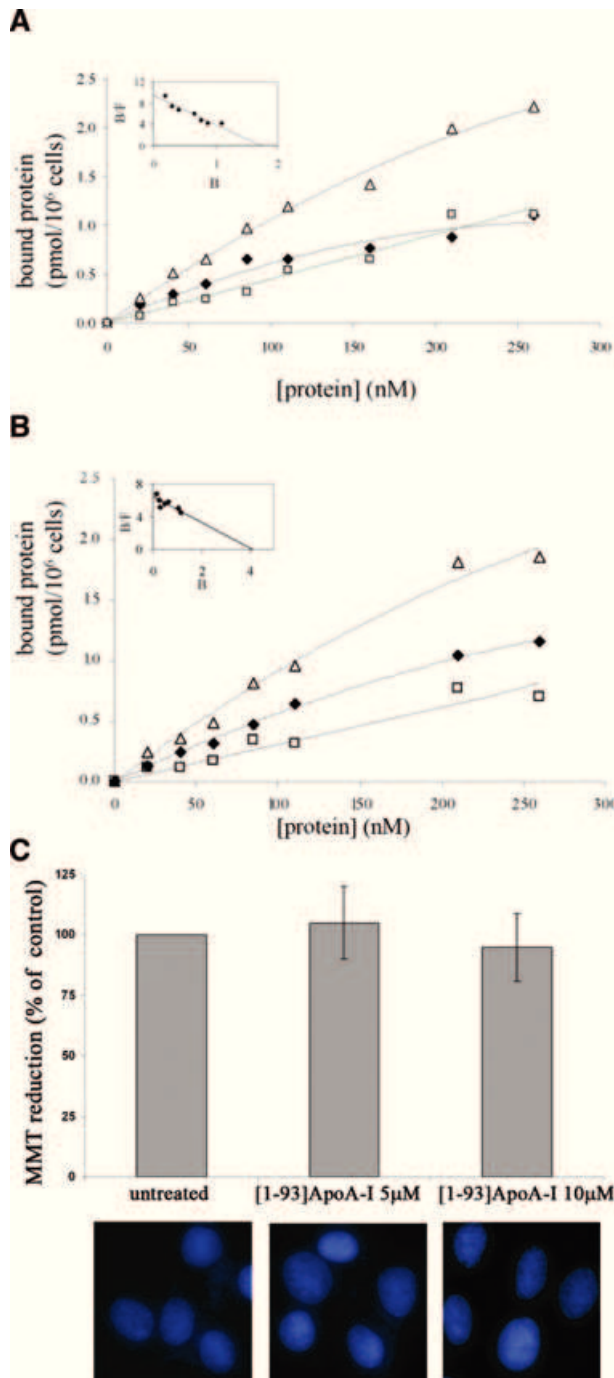
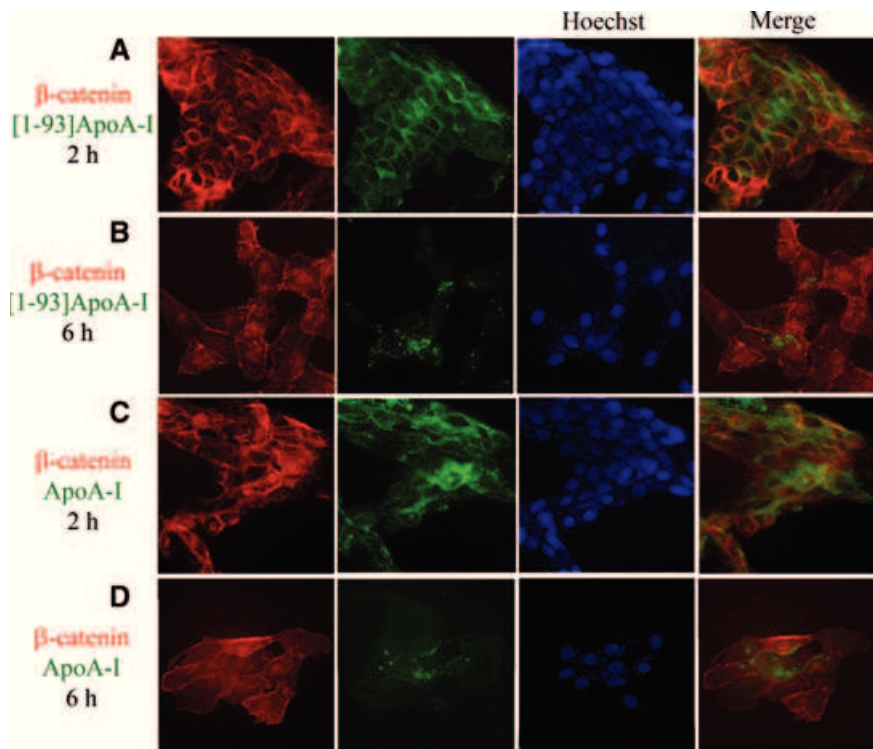


Fig. 1 Binding of [1–93]ApoA-I to cultured cells and its effects on cell viability. Binding curves were obtained incubating H9c2 cells (A) or HepG2 cells (B) for 2 hrs at 4°C with increasing concentrations of iodinated [1–93]ApoA-I, in the absence (Δ, total binding) or in the presence (□, non-specific binding) of a 40-fold molar excess of the unlabelled polypeptide. Specific binding values (◆) were obtained by subtracting the values relative to non-specific binding from those of total binding. The linearization of specific binding curves was obtained according to the Scatchard equation (insets of A and B). B: pmoles of protein bound to 1×10^6 cells; F: concentration of the unbound protein. (C) MTT reduction assay and Hoechst staining of H9c2 cells untreated or treated with 5 μ M or 10 μ M [1–93]ApoA-I. Error bars indicate standard deviations obtained from four independent experiments. All images have been acquired at the same magnification.

Fig. 2 Endocytosis of [1–93]ApoA-I and full-length ApoA-I in H9c2 cells. Cells were grown on cover slips, incubated 2 hrs (A) or 6 hrs (B) with 3 μ M FITC-[1–93]ApoA-I (green) and immunofluorescently stained for β -catenin (red). (C) and (D), cells incubated 2 or 6 hrs, respectively, with 1 μ M FITC-ApoA-I (green) and immunostained for β -catenin (red). Nuclei were stained with Hoechst (blue). Cells were analysed by epifluorescence microscopy.



membrane compartment. As shown in Fig. 2A, after 2 hrs incubation the polypeptide (green) mostly co-localizes with β -catenin (red), whereas after 6 hrs the polypeptide fluorescent signal was found to be mostly intracellular (Fig. 2B). Hence, the polypeptide binds to the membrane first and then is internalized in target cells. Similar results were obtained with labelled ApoA-I (Fig. 2C and D). Immunostaining was specific, as no fluorescent signals were observed in the absence of primary antibody (data not shown).

It is known that the plasma membrane is the main platform where lipidation of ApoA-I occurs [4], mediated by the ATP-binding cassette transporter A1 (ABCA1). This allows cellular free cholesterol and phospholipids to be transferred to ApoA-I leading to the biogenesis of nascent HDL. It has been demonstrated that ApoA-I is internalized in an ABCA1-dependent manner, because no internalization was observed in cells ABCA1^{-/-} [20]. To test whether ABCA1 is expressed in cardiomyoblasts, cell lysates were analysed by Western blotting with anti-ABCA1 antibodies. HepG2 lysates were used as a positive control, as high levels of this transporter have been found in the liver. As shown in Fig. 3A, an immuno-positive species, with an apparent molecular mass corresponding to that expected for ABCA1 (about 210 kDa), was present in cell extracts prepared from H9c2 (lane 2) and HepG2 (lane 1) cells. These results were confirmed by immuno-fluorescence analyses of H9c2 and HepG2 cells with anti-ABCA1 antibodies, which revealed immuno-positive signals in both cell lines (Fig. 3B and C). We observed that in H9c2 cells ABCA1 is localized both on the plasma membrane and in intracellular compartments, whereas

in HepG2 cells it is mainly located on the plasma membrane. Although data reported in the literature indicate that the transporter is mostly localized on cell plasma membrane [21, 22], consistently with its role in cellular lipid efflux, ABCA1 has been also observed in intracellular compartments [5, 23, 24].

Furthermore, to test whether the fibrillogenic polypeptide co-localizes with ABCA1, we incubated H9c2 cells with rhodamine-[1–93]ApoA-I for 2 hrs at 37°C. Cells were then fixed and incubated with anti-ABCA1 antibodies to label the transporter. We found little co-localization between [1–93]ApoA-I (red) and ABCA1 (green). Representative images are shown in Fig. 3D. Similar results were obtained with rhodamine-ApoA-I (Fig. 3E), in agreement with recent reports showing that the majority of cell-associated ApoA-I does not co-localize with ABCA1 [25]. Immunostaining was specific as no signals were detected in the absence of primary antibody (data not shown).

Internalization pathway of [1–93]ApoA-I

To learn about the mechanism of [1–93]ApoA-I uptake in cardiomyoblasts, we analysed different routes of endocytosis. First, the involvement of clathrin-coated pits was evaluated using Rab5 as a marker, as this protein regulates vesicular transport from the plasma membrane to the endosomes. We transiently expressed Rab5 fused to the RFP in H9c2 cells. Twenty-four hours after transfection, cells were incubated with the FITC protein under test

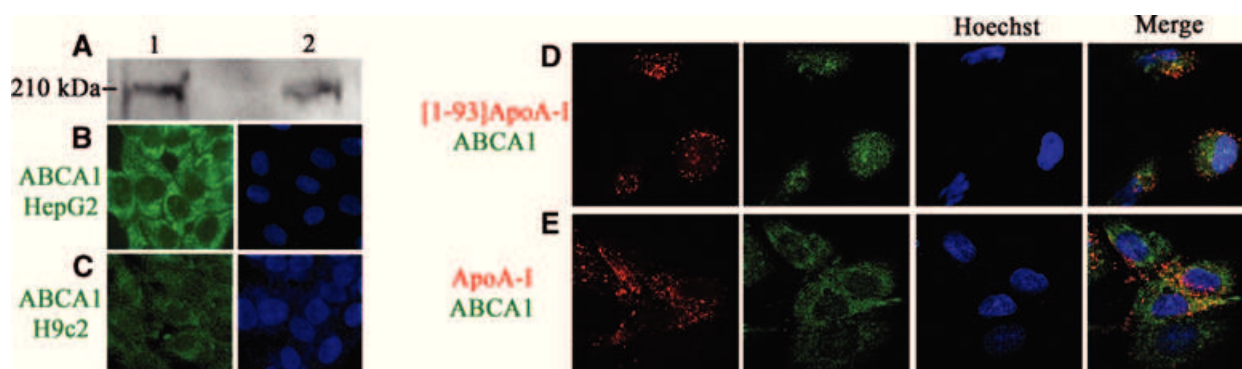


Fig. 3 ABCA1 expression and co-localization with [1–93]ApoA-I and ApoA-I. **(A)** Western blot analysis with anti-ABCA1 antibodies of cell lysates prepared from HepG2 cells (25 μ g total proteins, *lane 1*) and from H9c2 cells (50 μ g, *lane 2*). Immunostaining for ABCA1 (green) of HepG2 cells **(B)** and H9c2 cells **(C)**. Nuclei were stained with Hoechst (blue). **(D)** and **(E)**, co-localization of [1–93]ApoA-I and ApoA-I with ABCA1. H9c2 cells were incubated for 2 hrs either with 3 μ M rhodamine-[1–93]ApoA-I **(D)**, or with 1 μ M rhodamine-ApoA-I **(E)**, and immunostained for ABCA1 (green). Nuclei were stained with Hoechst (blue). Cells were observed by confocal microscopy.

for 6 hrs at 37°C, to allow internalization. As indicated in Fig. 4A, a significant, albeit partial, co-localization of internalized [1–93]ApoA-I (green) with RFP-Rab5 (red) was observed, indicating that a fraction of the internalized polypeptide is associated to early endosomes. Similar results were obtained when ApoA-I was tested (Fig. 4B), in line with recent findings [4, 5]. Additional experiments were performed with labelled transferrin (FITC-Tf), as a marker of the endocytic pathway. For both proteins we confirmed the results obtained with Rab5, because after 6 hrs incubation partial co-localization with FITC-Tf was observed (data not shown). To further confirm that both [1–93]ApoA-I and ApoA-I are internalized in H9c2 cells by clathrin-mediated endocytosis, we used specific inhibitors of this internalization pathway, such as MDC and sucrose. Upon pre-incubation of H9c2 cells with either MDC or sucrose, we observed that the amount of internalized polypeptide, and that of the full-length protein, appeared to be reduced (data not shown). Hence, endocytosis of both proteins is slowed down, although not fully blocked, by inhibitors of clathrin-mediated endocytosis. This indicates either that in our experimental conditions the endocytic pathway still functions, albeit less efficiently, or that endocytosis of [1–93]ApoA-I and ApoA-I does not occur solely *via* clathrin-coated pits.

Experiments were then performed to test internalization by lipid rafts. To do so, FITC insulin was used as a marker. H9c2 cells were incubated with rhodamine-[1–93]ApoA-I in the presence of FITC insulin for 4 hrs at 37°C. As shown in Fig. 4C, strong signals of co-localization of [1–93]ApoA-I (red) with insulin (green) were detected, indicating that [1–93]ApoA-I uptake occurs also by lipid rafts. On the other hand, when the same experiment was performed with rhodamine-ApoA-I, little co-localization was observed with FITC insulin (Fig. 4D).

As it has been demonstrated that ApoA-I is also internalized by macropinocytosis [4], we tested this internalization route for [1–93]ApoA-I. H9c2 cells were incubated with rhodamine-

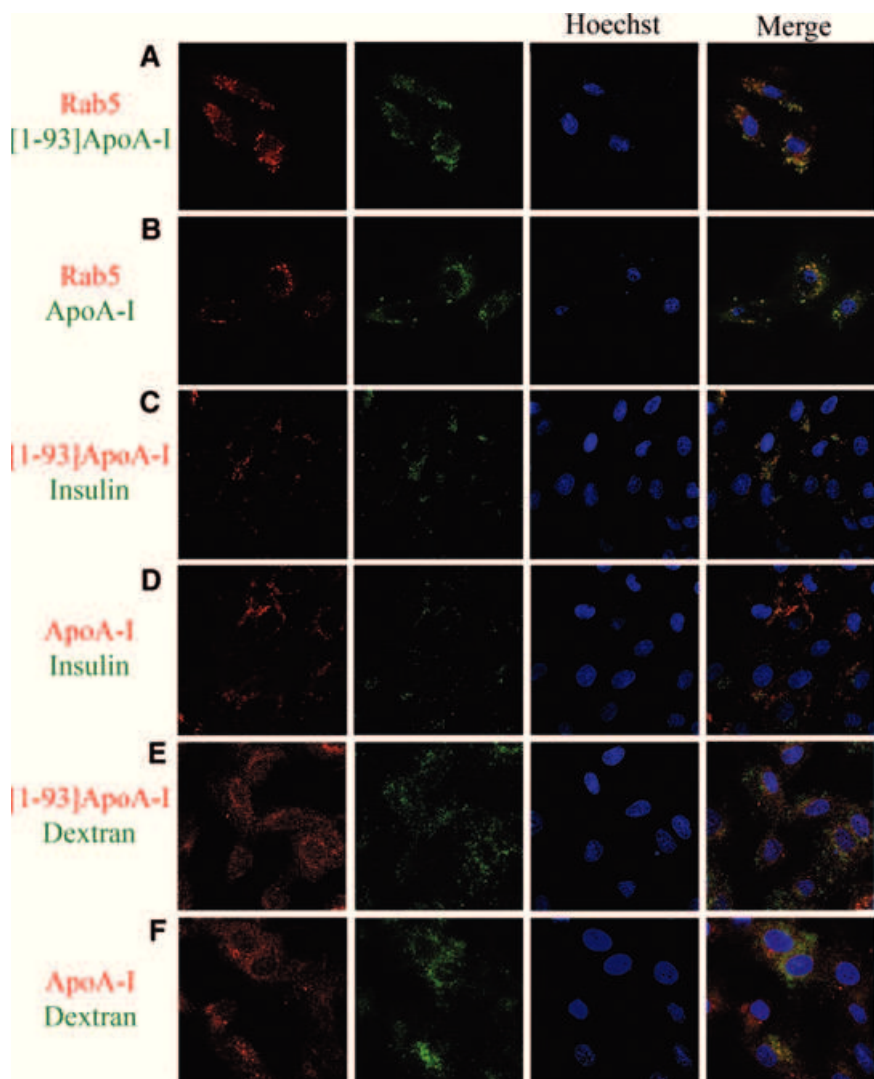
[1–93]ApoA-I in the presence of FITC dextran, a macropinocytosis marker, for 4 hrs at 37°C. As shown in Fig. 4E, little co-localization was observed between [1–93]ApoA-I (red) and dextran (green). On the contrary, clear signals of co-localization were detected for ApoA-I (Fig. 4F).

According to recent reports, ApoA-I, once internalized, is recycled back to the cell surface [3–5]. To investigate the retroendocytosis pathway, Rab4 was used as a marker, as it is located in vesicles directing protein recycling from early endosomes to the plasma membrane. We transiently transfected H9c2 cardiomyoblasts with a vector encoding Rab4 fused to the GFP. Twenty-four hours after transfection, cells were incubated with rhodamine-[1–93]ApoA-I, or ApoA-I, for 6 hrs at 37°C. As shown in Fig. 5A, [1–93]ApoA-I (red) does not co-localize with Rab4⁺ endosomal compartments (green), whereas significant signals of co-localization were observed for ApoA-I (Fig. 5B). Taken together, these results clearly indicate that the fibrillogenic polypeptide, once internalized in cardiomyoblasts, is not recycled to the cell membrane, whereas ApoA-I is shuttled back to the plasma membrane to be resecreted, as described for other cell lines [3–5].

Intracellular fate of [1–93]ApoA-I

Next, we analysed the fate of the internalized polypeptide in cardiomyoblasts. After a prolonged exposure to FITC-[1–93]ApoA-I (24 hrs), the complete disappearance of intracellular fluorescent signals associated to the polypeptide was observed (Fig. 6A and C), suggestive of polypeptide massive degradation. To investigate the degradation pathway, we used specific inhibitors of proteasomal and lysosomal activities. When cells were pre-incubated with the proteasome inhibitor MG132, we observed the persistence of [1–93]ApoA-I intracellular fluorescence at 24 hrs (Fig. 6B), indicative of proteasome involvement in [1–93]ApoA-I degradation.

Fig. 4 Analysis of the route of [1–93]ApoA-I and ApoA-I endocytosis in H9c2 cells by confocal microscopy. (A) and (B), clathrin-mediated endocytosis. H9c2 cells were transiently transfected with an expression vector for RFP-Rab5. After 24 hrs, cells were incubated 6 hrs at 37°C either with 3 μ M FITC-[1–93]ApoA-I (A) or with 1 μ M FITC-ApoA-I (B). (C) and (D), lipid rafts-mediated internalization. Cells were incubated 4 hrs at 37°C either with 3 μ M rhodamine-[1–93]ApoA-I (C), or with 1 μ M rhodamine-ApoA-I (D), in the presence of FITC insulin (0.1 mg/ml). (E) and (F), macropinocytosis. Cells were incubated 4 hrs at 37°C either with 3 μ M rhodamine-[1–93]ApoA-I (E), or with 1 μ M rhodamine-ApoA-I (F), in the presence of FITC dextran (5 mg/ml). Nuclei were stained with Hoechst (blue).



To test whether [1–93]ApoA-I is targeted to lysosomes, we incubated cells with FITC-[1–93]ApoA-I in the presence of ammonium chloride, an inhibitor of intralysosomal catabolism. Following incubation, lysosomes were labelled with LysoTracker red. As shown in Fig. 6D, a strong fluorescence signal associated to the polypeptide (green) was found to co-localize with lysosomes (red), suggesting that lysosomes play a role in [1–93]ApoA-I catabolism. Different results were obtained instead with full-length ApoA-I, as even at 24 hrs incubation with FITC-ApoA-I, the persistency of protein fluorescence within the cells was observed (Fig. 6E and G). This is in agreement with recent reports indicating that in different cell types ApoA-I is not significantly degraded [4]. Moreover, as shown in Fig. 6G, ApoA-I was found to co-localize with lysosomes, in line with reports indicating that lysosomes are an intracellular station of ApoA-I [3, 4]. In the presence of either MG132 or ammonium chloride, fluorescence signals associated to

ApoA-I did not significantly increase with respect to cells untreated with the inhibitors, as shown in Fig. 6F and H, respectively. Furthermore, by using different inhibitors, such as ALLN for the proteasome, and chloroquine for the lysosomes, we confirmed the data reported above (data not shown). Taken together, our results indicate that the inhibition of lysosomal or proteasomal activity does not significantly alter the amount of intracellular ApoA-I, whereas both pathways seem to be involved in the degradation of the fibrillogenic polypeptide.

Analysis of the uptake of [1–93]ApoA-I fibrils in cardiomyoblasts and the effects on cell viability

As it is conceivable that the accumulation of the fibrillogenic polypeptide in the extracellular space leads to fibrils deposition,

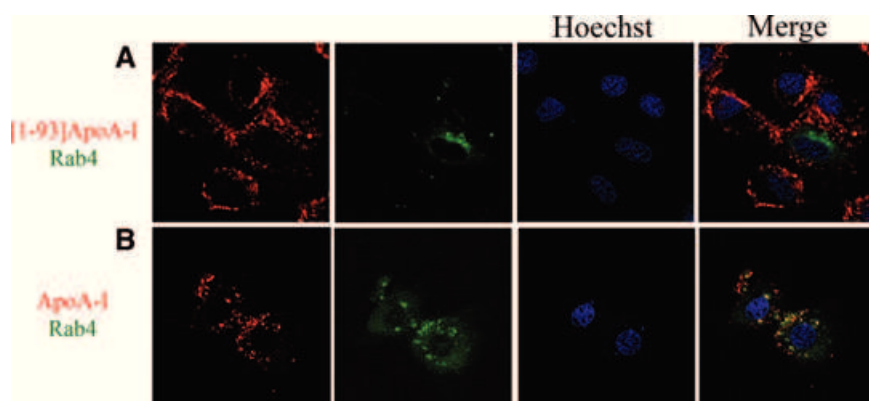


Fig. 5 Co-localization of [1–93]ApoA-I and ApoA-I with Rab4. H9c2 cells were transiently transfected with an expression vector for GFP-Rab4. After 24 hrs, cells were incubated 6 hrs at 37°C either with 3 μ M rhodamine-[1–93]ApoA-I (A) or with 1 μ M rhodamine-ApoA-I (B). Nuclei were stained with Hoechst (blue). Cells were observed by confocal microscopy.

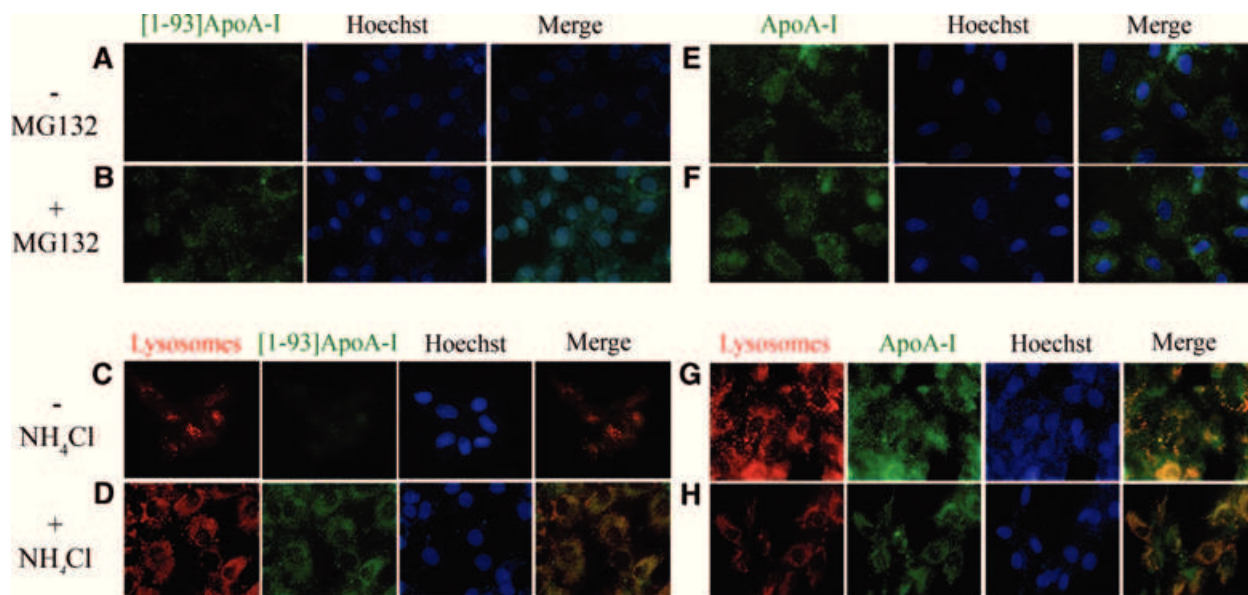


Fig. 6 Analysis of the degradation pathway of [1–93]ApoA-I and ApoA-I in H9c2 cells by epifluorescence microscopy. (A)–(D) [1–93]ApoA-I degradation. Cells were incubated 24 hrs at 37°C with 3 μ M FITC-[1–93]ApoA-I in the absence (A, C) or in the presence of MG132 (2.5 μ M) (B), or ammonium chloride (100 μ M) (D). (E)–(H), ApoA-I degradation. Cells were incubated for 24 hrs at 37°C with 1 μ M FITC-ApoA-I, in the absence (E and G) or in the presence of MG132 (F), or ammonium chloride (H). Lysosomes were stained with LysoTracker red. Nuclei were stained with Hoechst (blue).

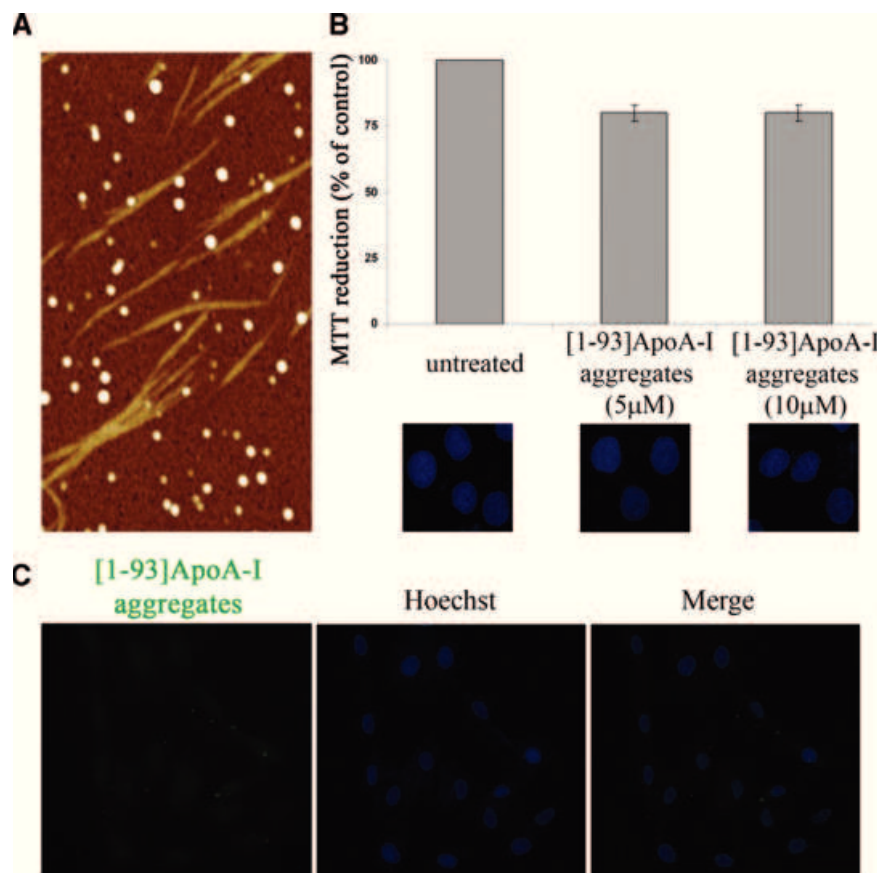
[1–93]ApoA-I fibrils were obtained by incubating the polypeptide for 2 weeks at pH 6.4 in the presence of the co-solvent TFE. AFM analysis of the incubated sample showed the presence of fibrils with height of 2.4 ± 0.1 nm and length between 0.4 and 1.5 μ m (Fig. 7A). Fibrils coexist with prefibrillar aggregates, including annular protofibrils, which form a network in the image background; spheroidal aggregates of variable size (height between 3 and 15 nm) are also present.

To test the effects of fibrils on cell viability, cardiomyoblasts were incubated for 72 hrs in the presence of 5 or 10 μ M aggregated [1–93]ApoA-I (insoluble species). No inhibition of cell viability was observed by MTT assays in treated cells with respect to

untreated cells (Fig. 7B). This was confirmed by the absence of apoptotic nuclei in treated cells (Fig. 7B).

To verify whether the fibrillar material is able to enter the cells, we produced fluorescent fibrils by incubating FITC-labelled [1–93]ApoA-I under the conditions previously described. H9c2 cells were incubated for 6 hrs with fluorescent fibrils (insoluble species) and then treated with HEPES/NaCl buffer to remove polypeptide molecules specifically bound to the extracellular side of the plasma membrane. No fluorescent signals associated to [1–93]ApoA-I fibrils were observed by epifluorescence microscopy analysis, demonstrating that no significant internalization of fibrils occurs in cardiomyoblasts (Fig. 7C).

Fig. 7 Analysis of [1–93]ApoA-I fibrils. **(A)** Tapping mode AFM image (height data) of aggregated [1–93]ApoA-I. Upon incubation in the aggregating conditions, the whole sample was observed. Fibrils coexist with prefibrillar aggregates; spheroidal aggregates are also found. Scan size 3.0 μm , Z range 10 nm. **(B)** Effects of [1–93]ApoA-I fibrils on cell viability. MTT reduction assay and Hoechst staining of H9c2 cells, untreated or treated with 5 μM or 10 μM [1–93]ApoA-I fibrils, are shown. Error bars indicate standard deviations obtained from three independent experiments. Nuclei images have been acquired at the same magnification. **(C)** Analysis of internalization of [1–93]ApoA-I fibrils in H9c2 cells. Cells were incubated for 6 hrs with 3 μM FITC-labelled [1–93]ApoA-I fibrils and analysed by epifluorescence microscopy. Nuclei were stained with Hoechst (blue).



Discussion

ApoA-I represents the intriguing case of a protein which, in its native form, plays a key role in cholesterol homeostasis, as it acts as an extracellular acceptor of lipids. Nevertheless, by specific mutations ApoA-I is converted into the precursor of natively unfolded pathogenic fragments associated with familial systemic amyloidoses [1]. N-terminal fragments of ApoA-I, 90–100 residue long, accumulate in tissues and organs of patients carrying one of the 16 amyloidogenic mutations identified so far in ApoA-I gene [1, 10, 11]. The molecular mechanism responsible for ApoA-I associated amyloid diseases remains largely unknown. However, recent findings allowed us to raise the hypothesis that the mutations located in ApoA-I N-terminal region are amyloidogenic as they favour the proteolytic cleavage responsible for the release of the fibrillogenic polypeptide [26].

As the heart is one of the targets of ApoA-I amyloid aggregate deposition in patients affected by the disease, rat cardiomyoblasts (H9c2 cell line) were selected for *in vitro* analyses. In this study, we demonstrated that the fibrillogenic polypeptide is able to specifically bind to cardiomyoblasts, as well as to human hepatocytes. The apparent affinity constants ($K_d = 5.90 \pm 0.70 \times 10^{-7}$ M and $1.78 \pm 0.26 \times 10^{-7}$ M for H9c2 and HepG2, respectively) were

found to be comparable to those previously reported for lipid-free ApoA-I binding to HepG2 cells ($K_d = 0.84 \times 10^{-7}$ M) [27], and to aortic endothelial cells ($K_d = 0.8 \times 10^{-7}$ M) [28]. These results are also consistent with the finding that region 62–77 of ApoA-I is a membrane binding domain of lipid-free ApoA-I, because the corresponding synthetic peptide binds with high affinity ($K_d \sim 10^{-7}$ M) to HepG2 cells [29]. Our data are also reinforced by the finding that region 1–43 is involved in ApoA-I lipid binding [14].

As ABCA1 transporter plays a central role in ApoA-I membrane binding and lipidation [3–5], we analysed the presence of this transporter in H9c2 cells. Immunofluorescence analyses demonstrated that ABCA1 is expressed in cardiomyoblasts, where it was found to partially co-localize with both full-length ApoA-I and its fibrillogenic polypeptide, supporting the hypothesis that ApoA-I and [1–93]ApoA-I share common determinants for membrane association. Low co-localization between ApoA-I and ABCA1 is in agreement with the general view that only a small fraction of membrane bound ApoA-I appears to co-localize with ABCA1 [25]. To explain these observations, a model was recently proposed [4, 30], in which the interaction of a small fraction of lipid-free ApoA-I to ABCA1 is sufficient to activate ABCA1 lipid translocase activity, which in turn promotes the formation of specialized lipid domains, acting as high affinity binding sites for ApoA-I [30].

Therefore, although ApoA-I binding occurs in an ABCA1-dependent manner, most of ApoA-I molecules bind to lipids rather than to ABCA1 itself [4].

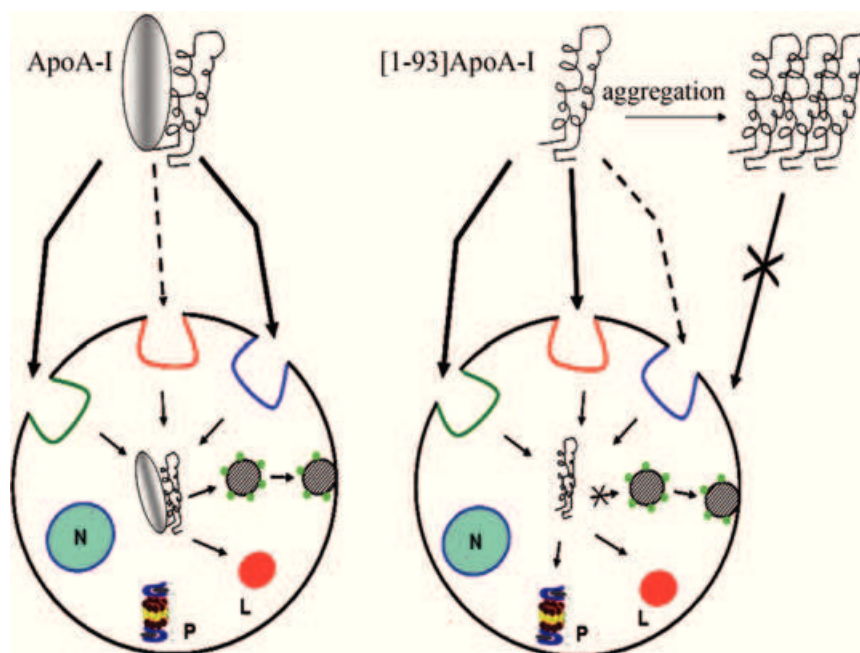
We demonstrated that ApoA-I fibrillogenic polypeptide is able to enter cardiac cells, as shown by fluorescence analyses. Our results support roles for both clathrin- and lipid raft-mediated pathways in [1–93]ApoA-I internalization, with very little contribution of macropinocytosis. Upon internalization, no involvement of the retroendocytosis pathway was observed; rather, the fibrillogenic fragment is targeted to proteasomal and lysosomal stations for degradation, as at 24 hrs no intracellular fluorescent signals were detected. This is not surprising, considering that the largely unfolded structure of the fibrillogenic polypeptide is responsible for its susceptibility to proteolytic cleavages, as previously demonstrated by experiments of limited proteolysis [13]. Accordingly, to produce the recombinant form of the polypeptide in a prokaryotic expression system, it has been necessary to transiently fuse the polypeptide to a stable bacterial protein to avoid intracellular degradation [13]. The rapid degradation of the polypeptide is also in agreement with the absence of cytotoxic effects on cardiomyoblasts, at least in the experimental conditions tested.

Furthermore, in parallel experiments we provided evidence that full-length ApoA-I is internalized in cardiomyoblasts *via* clathrin-dependent endocytosis and macropinocytosis as predominant internalization routes, with very low signals of co-localization with lipid rafts. To our knowledge, this is the first evidence of ApoA-I internalization in cardiac cells. Moreover, although ApoA-I is known to interact with plasma membrane lipid rafts to control cholesterol export [31], this is the first time that lipid rafts involvement in

ApoA-I internalization has been analysed. Once internalized, ApoA-I associates to Rab4-labelled endosomal compartment, a station involved in ApoA-I recycling to the cell membrane in other cell lines [3–5, 23]. At 24 hrs, ApoA-I associated fluorescent signals are still observed in cardiomyoblasts and co-localize with lysosomes. It is noteworthy that lysosomes are best known for their role in degradation, although recent studies have shown that they may also fuse to the plasma membrane and release their content to the extracellular medium [32]. The question of the physiological role of ApoA-I in lysosomes remains controversial. In fact, some authors demonstrated that ApoA-I reaches lysosomes to be degraded [3, 4], but studies support the idea that ABCA1-bound ApoA-I traffics to late endosomal vesicles and/or to lysosomes. Being these stations intracellular cholesterol reservoirs, here nascent lipoprotein particles are formed and then secreted from the cell [33–35].

In conclusion, the data reported here reveal that ApoA-I fibrillogenic fragment, the main constituent of amyloid fibrils, binds to target cells, is internalized and rapidly degraded. The internalization routes, intracellular pathways and degradation mechanisms of full-length ApoA-I and its fibrillogenic polypeptide are not fully coincident, as schematically depicted in Scheme 1.

We surmise that the intracellular fate of the polypeptide may be relevant in the development of the pathology. The continuous accumulation of the natively unfolded polypeptide in the cardiac tissue leads to a progressive, massive occupancy of the extracellular space by amyloid deposits, as observed in pathological hearts, from which the natural fibrillogenic polypeptide can be isolated [10]. During the fibrillogenic process, a dynamic equilibrium between monomeric species and aggregated states has been proposed [36]. Here we provided evidence that, besides aggregation in



Scheme 1 Schematic representation of internalization routes and intracellular fates of [1–93]ApoA-I and ApoA-I in H9c2 cells. Lipid rafts are coloured in red; clathrin-coated pits in green; macropinocytosis in blue. Rab4 vesicles are represented by green circles. N: nucleus; P: proteasome; L: lysosomes.

the extracellular space, an alternative fate is available to the polypeptide, *i.e.* the interaction with target cells, internalization and subsequent degradation. This would subtract unaggregated molecules of [1–93]ApoA-I from the equilibrium directing the polypeptide towards a non-pathological route. Relevant results were obtained when the analyses were extended to the polypeptide in the fibrillar state. Typical amyloid fibrils were obtained *in vitro*, as demonstrated by AFM analysis. Evidence was provided that, unlike the unaggregated polypeptide, fibrils have no access to the intracellular compartment. Thus, the intracellular degradation pathway is precluded to fibrillar aggregates. Hence, the hypothesis can be raised that internalization and subsequent degradation of the unaggregated fibrillogenic polypeptide represent a protective mechanism against fibrillogenesis, able to balance [1–93]ApoA-I progressive aggregation and to slow down the fibrillogenic process. This phenomenon may be relevant in the slow progression and late onset of ApoA-I-associated amyloid pathology.

Acknowledgements

We thank Prof. Chiara Campanella for helpful discussions, Dr. Marino Zerial (Max-Planck-Institute, Germany) for generously providing fluorescent Rab proteins constructs and Dr. Amanda Penco for help in AFM measurements. Confocal microscopy investigations were carried out at the CISME (Interdepartmental Centre of Electronic Microscopy) of the University of Naples Federico II. This work was supported by MIUR, Ministero dell'Università e della Ricerca Scientifica, Italy (PRIN 2007, Project N. 2007XY59ZJ_003; PRIN 2008, Project N. 20083ERXWS_002).

Conflict of interest

The authors confirm that there are no conflicts of interest.

References

1. **Obici L, Franceschini G, Calabresi L, et al.** Structure, function and amyloidogenic propensity of apolipoprotein A-I. *Amyloid*. 2006; 13: 1–15.
2. **Gordon DJ, Rifkind BM.** High-density lipoprotein—the clinical implications of recent studies. *N Engl J Med*. 1989; 321: 1311–6.
3. **Cavelier C, Lorenzi I, Rohrer L, et al.** Lipid efflux by the ATP-binding cassette transporters ABCA1 and ABCG1. *Biochim Biophys Acta*. 2006; 1761: 655–66.
4. **Denis M, Landry YD, Zha X.** ATP-binding cassette A1-mediated lipidation of apolipoprotein A-I occurs at the plasma membrane and not in the endocytic compartments. *J Biol Chem*. 2008; 283: 16178–86.
5. **Azuma Y, Takada M, Shin HW, et al.** Retroendocytosis pathway of ABCA1/apoA-I contributes to HDL formation. *Genes to Cells*. 2009; 14: 191–204.
6. **Mukherjee S, Zha X, Tabas I, et al.** Cholesterol distribution in living cells: fluorescence imaging using dehydroergosterol as a fluorescent cholesterol analog. *Biophys J*. 1998; 75: 1915–25.
7. **Chroni A, Liu T, Fitzgerald ML, et al.** Cross-linking and lipid efflux properties of apoA-I mutants suggest direct association between apoA-I helices and ABCA1. *Biochemistry*. 2004; 43: 2126–39.
8. **Chiti F, Dobson CM.** Protein misfolding, functional amyloid, and human disease. *Annu Rev Biochem*. 2006; 75: 333–66.
9. **Eckman CB, Eckman EA.** An update on the amyloid hypothesis. *Neurol Clin*. 2007; 25: 669–82.
10. **Obici L, Bellotti V, Mangione P, et al.** The new apolipoprotein A-I variant Leu¹⁷⁴→Ser causes cardiac amyloidosis, and the fibrils are constituted by the 93-residue N-terminal polypeptide. *Am J Pathol*. 1999; 155: 695–702.
11. **Eriksson M, Schönland S, Yumlu S, et al.** Hereditary apolipoprotein A1-associated amyloidosis in surgical pathology specimens: identification of three novel mutations in the APOA1 gene. *J Mol Diagn*. 2009; 11: 257–62.
12. **Andreola A, Bellotti V, Giorgetti S, et al.** Conformational switching and fibrillogenesis in the amyloidogenic fragment of apolipoprotein A-I. *J Biol Chem*. 2003; 278: 2444–51.
13. **Di Gaetano S, Guglielmi F, Arciello A, et al.** Recombinant amyloidogenic domain of ApoA-I: analysis of its fibrillogenic potential. *Biochem Biophys Res Commun*. 2006; 351: 223–8.
14. **Tanaka M, Dhanasekaran P, Nguyen D, et al.** Contributions of the N- and C-terminal helical segments to the lipid-free structure and lipid interaction of apolipoprotein A-I. *Biochemistry*. 2006; 45: 10351–8.
15. **Monti DM, Guglielmi F, Monti M, et al.** Effects of a lipid environment on the fibrillogenic pathway of the N-terminal polypeptide of human apolipoprotein A-I, responsible for *in vivo* amyloid fibril formation. *Eur Biophys J*. 2010; 39: 1289–99.
16. **Campioni S, Mannini B, Zampagni M, et al.** A causative link between the structure of aberrant protein oligomers and their toxicity. *Nat Chem Biol*. 2010; 6: 140–7.
17. **Sönnichsen B, De Renzis S, Nielsen E, et al.** Distinct membrane domains on endosomes in the recycling pathway visualized by multicolor imaging of Rab4, Rab5, and Rab11. *J Cell Biol*. 2000; 149: 901–14.
18. **Rink J, Ghigo E, Kalaidzidis Y, et al.** Rab conversion as a mechanism of progression from early to late endosomes. *Cell*. 2005; 122: 735–49.
19. **Gharibyan AL, Zamotin V, Yanamandra K, et al.** Lysozyme amyloid oligomers and fibrils induce cellular death via different apoptotic/necrotic pathways. *J Mol Biol*. 2007; 365: 1337–49.
20. **Zha X, Genest J Jr, McPherson R.** Endocytosis is enhanced in Tangier fibroblasts: possible role of ATP-binding cassette protein A1 in endosomal vesicular transport. *J Biol Chem*. 2001; 276: 39476–83.
21. **Fitzgerald ML, Mendez AJ, Moore KJ, et al.** ATP-binding cassette transporter A1 contains an NH₂-terminal signal anchor sequence that translocates the protein's first hydrophilic domain to the exoplasmic space. *J Biol Chem*. 2001; 276: 15137–45.
22. **Orsó E, Broccardo C, Kaminski WE, et al.** Transport of lipids from golgi to plasma membrane is defective in tangier disease patients and Abc1-deficient mice. *Nat Genet*. 2000; 24: 192–6.
23. **Neufeld EB, Stonik JA, Demosky SJ Jr, et al.** The ABCA1 transporter modulates

- late endocytic trafficking: insights from the correction of the genetic defect in Tangier disease. *J Biol Chem.* 2004; 279: 15571–8.
24. **Neufeld EB, Remaley AT, Demosky SJ, et al.** Cellular localization and trafficking of the human ABCA1 transporter. *J Biol Chem.* 2001; 276: 27584–90.
25. **Vedhachalam C, Ghering AB, Davidson WS, et al.** ABCA1-induced cell surface binding sites for ApoA-I. *Arterioscler Thromb Vasc Biol.* 2007; 27: 1603–9.
26. **Raimondi S, Guglielmi F, Giorgetti S, et al.** Effects of the known pathogenic mutations on the aggregation pathway of the amyloidogenic peptide of Apolipoprotein A-I. *J Mol Biol.* 2011; doi: 10.1016/j.jmb.2011.01.044
27. **Barbaras R, Collet X, Chap H, et al.** Specific binding of free apolipoprotein A-I to a high-affinity binding site on HepG2 cells: characterization of two high-density lipoprotein sites. *Biochemistry.* 1994; 33: 2335–40.
28. **Rohrer L, Cavalier C, Fuchs S, et al.** Binding, internalization and transport of apolipoprotein A-I by vascular endothelial cells. *Biochim Biophys Acta.* 2006; 1761: 186–94.
29. **Georgeaud V, Garcia A, Cachot D, et al.** Identification of an ApoA-I ligand domain that interacts with high-affinity binding sites on HepG2 cells. *Biochem Biophys Res Commun.* 2000; 267: 541–5.
30. **Vedhachalam C, Duong PT, Nickel M, et al.** Mechanism of ATP-binding cassette transporter A1-mediated cellular lipid efflux to apolipoprotein A-I and formation of high density lipoprotein particles. *J Biol Chem.* 2007; 282: 25123–30.
31. **Gaus K, Kritharides L, Schmitz G, et al.** Apolipoprotein A-1 interaction with plasma membrane lipid rafts controls cholesterol export from macrophages. *FASEB J.* 2004; 18: 574–6.
32. **Luzio JP, Pryor PR, Bright NA.** Lysosomes: fusion and function. *Nat Rev Mol Cell Biol.* 2007; 8: 622–32.
33. **Oram JF.** The ins and outs of ABCA. *J Lipid Res.* 2008; 49: 1150–1.
34. **Chen W, Sun Y, Welch C, et al.** Preferential ATP-binding cassette transporter A1-mediated cholesterol efflux from late endosomes/lysosomes. *J Biol Chem.* 2001; 276: 43564–9.
35. **Chen W, Wang N, Tall AR.** A PEST deletion mutant of ABCA1 shows impaired internalization and defective cholesterol efflux from late endosomes. *J Biol Chem.* 2005; 280: 29277–81.
36. **Carulla N, Caddy GL, Hall DR, et al.** Molecular recycling within amyloid fibrils. *Nature.* 2005; 436: 554–8.

Apolipoprotein A-I amyloidogenic variant L174S, expressed and isolated from stably transfected mammalian cells, is associated with fatty acids

Daria Maria Monti^{1,2}, Sonia Di Gaetano³, Rita Del Giudice¹, Chiara Giangrande⁴, Angela Amoresano⁴, Maria Monti^{4,5}, Angela Arciello^{1,2} & Renata Piccoli^{1,2}

¹Department of Structural and Functional Biology, University of Naples Federico II, School of Biotechnological Sciences, Naples, Italy, ²Istituto Nazionale di Biostrutture e Biosistemi (INBB), Rome, Italy, ³Institute of Biostructures and Bioimages, CNR, Naples, Italy, ⁴Department of Organic Chemistry and Biochemistry, University of Naples Federico II, Naples, Italy, and ⁵Ceinge Biotechnologie Avanzate, Naples, Italy

Sixteen variants of apolipoprotein A-I (ApoA-I) are associated with hereditary systemic amyloidoses, characterized by amyloid deposition in peripheral organs of patients. As these are heterozygous for the amyloidogenic variants, their isolation from plasma is impracticable and recombinant expression systems are needed. Here we report the expression of recombinant ApoA-I amyloidogenic variant Leu174 with Ser (L174S) in stably transfected Chinese hamster ovary-K1 cells. ApoA-I variant L174S was found to be efficiently secreted in the culture medium, from which it was isolated following a one-step purification procedure. Mass spectrometry analyses allowed the qualitative and quantitative definition of the amyloidogenic variant lipid content, which was found to consist of two saturated and two monounsaturated fatty acids. Interestingly, the same lipid species were found to be associated with the wild-type ApoA-I, expressed and isolated using the same cell system, with lower values of the lipid to protein molar ratios with respect to the amyloidogenic variant. A possible role of fatty acids in trafficking and secretion of apolipoproteins may be hypothesized.

Keywords: Amyloidosis, ApoA-I variants, apolipoprotein A-I, mass spectrometry, recombinant amyloidogenic proteins

Abbreviations: ApoA-I, apolipoprotein A-I; AApoA-I(L174S), ApoA-I variant carrying the mutation L174S; CAD, coronary artery disease; CHO, Chinese ovary hamster; ES-MS, electrospray mass spectrometry; GC-MS, gas chromatography mass spectrometry; HDL, high-density lipoproteins; RCT, reverse cholesterol transport

Introduction

The biological role of apolipoprotein A-I (ApoA-I), the main component of high-density lipoproteins (HDL), consists mostly in the removal of excess cell cholesterol from peripheral tissues and cholesterol transfer *via* the plasma to the liver, where it is either recycled back to plasma as a component of newly formed lipoproteins or is excreted from the body *via* bile [1]. This pathway, named reverse cholesterol transport (RCT), plays a key role in the prevention of atherosclerosis, so that plasma HDL levels correlate inversely with the incidence of coronary artery disease (CAD) [2].

ApoA-I is synthesized in the liver and intestine as a *pre-pro*-protein. The 18-residue *pre*-peptide is cleaved intracellularly by a signal peptidase during translocation in the endoplasmic reticulum to give a *pro*-protein, with a hexapeptide amino-terminal extension. The mature protein (28 kDa) is secreted in the plasma, mostly associated with lipids in spherical HDL [3], or in small amount in a lipid-free/lipid-poor state (5%–10%) [1,4]. In the RCT pathway, phospholipids and unesterified cholesterol bind to lipid-free/lipid-poor ApoA-I. At the cell membrane, this complex interacts with the ATP-binding cassette A1 that promotes HDL biogenesis [5]. From mature HDL, lipid-free/lipid-poor ApoA-I is released through the action of the scavenger receptor B type 1 [1] and triglycerides transferred to other HDL subclasses or degraded by specific lipases [3]. Thus, a dynamic process, not yet fully understood, consisting of lipidation, delipidation and relipidation of ApoA-I is critical in ApoA-I biological functions. To this regard, the conformational plasticity of ApoA-I is a functionally relevant feature for the complex mechanism of its biological action [6–8].

Besides its biological functions, ApoA-I is also associated with hereditary systemic amyloidoses, when specific mutations occur in *ApoA-I* gene. ApoA-I amyloidoses are dominantly inherited diseases characterized by extracellular fibrillar deposits mainly localized in the heart, liver, kidneys and testis. There are 16 variants of ApoA-I identified so far associated with the disease [1,9,10]. In all cases, amyloid fibrils isolated *ex vivo* were found to be mainly constituted by N-terminal fragments of ApoA-I, 90–100 residue long. In particular, variant carrying the substitution of Leu174 with Ser (L174S) is responsible for preferential deposition of amyloid fibrils in the heart. In all the specimens investigated so far, the main constituent of fibrils was found to be a 93-residue polypeptide whose sequence corresponds to the N-terminal region of the protein [9]. Nevertheless, the mechanism leading to the release of the fibrillogenic polypeptide from a full-length amyloidogenic variant of ApoA-I is still fully unknown. To shed light on the disease molecular mechanism, we produced a recombinant form of the fibrillogenic polypeptide [11–13]. Based on experimental and computational data, we recently proposed a model [14], suggesting that all ApoA-I mutations associated with amyloidoses increase the conformational flexibility of the protein chain in the loop region 83–96, thus permitting the proteolytic cleavage and the release of the amyloidogenic N-terminal polypeptide.

All the patients analyzed so far were found to be heterozygous for the mutated gene, thus expressing both the wild-type and the mutated form, with the latter circulating in plasma at lower levels than the wild-type [1]. Therefore, being impracticable any approach to isolate the ApoA-I variant as a pure product from patients tissues or plasma, heterologous expression systems are needed. Whereas a variety of prokaryotic and eukaryotic expression systems have been used to produce recombinant wild-type ApoA-I [15–17], to date only the amyloidogenic variant of ApoA-I carrying the mutation G26R has been isolated from bacterial cells [18]. Here, we report the expression of ApoA-I amyloidogenic variant L174S in stably transfected mammalian cells. The recombinant protein, efficiently secreted in the culture medium, was isolated following a one-step purification procedure. Mass spectrometry analyses revealed the association of four lipid species with the recombinant protein.

Methods

Materials

Chinese hamster ovary (CHO)-K1 cells were from ATCC (Manassas, VA, USA). All reagents, ApoA-I and anti-actin polyclonal antibodies were purchased from Sigma-Aldrich (St. Louis, MO, USA). Rabbit anti-ApoA-I polyclonal antibodies were purchased from Dako (Glostrup, Denmark). Protein concentration was determined by the Bradford assay. The chemiluminescence detection system (SuperSignal® West Pico, Thermo Fisher Scientific, Rockford, IL, USA) was from Pierce.

Cloning

Plasmid pBOShApoAIgIS, encoding human ApoA-I, was kindly provided by Prof. L. Pastore [19]. The cDNA encoding

ApoA-I variant L174S was obtained by overlap extension polymerase chain reaction mutagenesis using pBOShApoAIgIS as a template. Two couples of primers were used (a-b; c-d). a: 5'-GGG GTA CCG AAG GAG GTC CCC CAC GG-3'; b: 5'-CGC GGC GCT GCG CTG GCG CAG CTC-3'; c: 5'-CAG CGC AGC GCC GCG CGC CTT GAG-3'; d: 5'-GCT CTA GAT CTG AGC ACC GGG AAG GG-3'. The sequences underlined represent the mutagenic codons. The recombinant plasmid carrying the mutated sequence was denoted as pBOSApoAI(L174S). Automated DNA sequencing was performed by Eurofins-MWG (Bavaria, Germany).

Cell transfection

CHO-K1 cells were plated on 6-well culture dishes (1.5×10^5 cells/well) in Dulbecco's modified Eagle's medium (DMEM-F12, Sigma-Aldrich, St. Louis, MO, USA), supplemented with 10% fetal bovine serum (HyClone, Thermo Fisher Scientific, Logan, UT, USA) and antibiotics. After 24 hours, cells were co-transfected with pSVneo plasmid (0.15 μ g), conferring neomycin resistance, and the plasmid encoding either AApoA-I(L174S) or the wild-type protein (1.5 μ g). Transfections were performed using Lipofectine (Invitrogen, Carlsbad, CA, USA) as described by the manufacturer. After 48 hours, cells were grown in the presence of 0.5 mg/ml G418 to select stably transfected clones.

Analysis of ApoA-I expression and secretion

Transfected or untransfected CHO-K1 cells were plated on 6-well culture dishes (1×10^5 cells/well) in DMEM-F12. After 24 hours, the medium was replaced by HyQSFMCHO (Thermo Fisher Scientific) Author: city and country needed and cells were grown in the absence of serum for different lengths of time (24, 48, 72 hours). Cells were then counted using the trypan blue exclusion assay. Then, for each sample the cell-conditioned medium and the cell lysate were analyzed for the presence of the recombinant protein. To analyze intracellular proteins, 20 000 cells were lysed in 1% NP40 in *phosphate buffered saline* (PBS) containing protease inhibitors (Roche, Mannheim, Germany). Upon 30-minute incubation on ice, lysates were centrifuged at 14 000 g for 30 minutes at 4°C. Following the determination of protein content by the Bradford assay, 25 μ g of proteins were analyzed by 15% sodium dodecyl sulfate polyacrylamide gel electrophoresis (SDS-PAGE) followed by western blotting with anti-ApoA-I antibodies (1:500 dilution). Similarly, aliquots of conditioned medium corresponding to 20 000 cells were analyzed for the presence of the recombinant protein.

Isolation of the recombinant proteins

Transfected cells were plated at a density of 8×10^4 cells/cm² (corresponding to 2×10^5 cells/ml) in HyQSFMCHO serum-free medium for 72 hours (serum-free procedure). The cell-conditioned medium was collected and centrifuged at 1500 rpm for 15 minutes at room temperature to remove cell debris. NaCl (0.8 M final concentration) was added to the supernatant and the sample was centrifuged at 12 000 rpm for 15 minutes at 4°C to remove insoluble species, filtered and loaded on a hydrophobic chromatography column (1 ml, HiTrap Butyl-S FF, GE Healthcare, Uppsala, Sweden)

following the manufacturer's instructions. Briefly, after loading, the column was washed with 10 volumes of washing buffer (0.8 M NaCl in 50 mM sodium phosphate buffer pH 7) to remove unbound proteins; recombinant ApoA-I was then eluted with 20 volumes of 20% isopropanol in 10 mM sodium phosphate buffer. Fractions were analyzed by SDS-PAGE on 15% polyacrylamide gels followed by coomassie staining and western blotting with anti-ApoA-I antibodies.

For immuno-affinity chromatography, a matrix was generated by linking anti-ApoA-I antibodies to an N-hydroxysuccinimide-activated resin (HiTrap, GE Healthcare) following the manufacturer's instructions. The column (1 ml) was equilibrated in PBS. After loading, unbound proteins were removed by extensive washing (PBS, 10 volumes) and the recombinant protein was eluted in 0.1 M glycine/HCl buffer, pH 2.7.

Reverse phase high-performance liquid chromatography was performed on a Ultrapure C4 column (Vydac, Grace, IL) with a gradient of buffer B (95% acetonitrile, 5% formic acid in 0.05% trifluoroacetic acid) in buffer A (5% formic acid in 0.05% trifluoroacetic acid) using a PerkinElmer chromatographic system (Series 200, Shelton, CT, USA). Proteins were eluted in 100% buffer B.

Lipid extraction

Lipids were extracted from protein samples by adding an equal volume of chloroform. The procedure was repeated three times and the organic extracts were collected and dried. Lipids were then trimethylsilylated in 200 μ l of N, O-bis(trimethylsilyl)acetamide (TMSA) for 45 minutes at 80°C. Samples were dried under nitrogen, dissolved in 50 μ l of hexane, centrifuged to remove the excess of solid reagents and the supernatants (1/50 of total volume) analyzed by mass spectrometry.

Mass spectrometry analyses

For lipids determinations, gas chromatography mass spectrometry (GC-MS) analyses were performed using a 5390 MSD quadrupole mass spectrometer (Agilent Technologies, Santa Clara, CA, USA) equipped with a gas chromatograph by using a SPB-5 fused silica capillary column (30 m, 0.5 mm ID, 0.25 μ m ft) from Supelco (Sigma-Aldrich, St. Louis, MO, USA). The injection temperature was 250°C. The oven temperature was increased from 25°C to 90°C in 1 minute and held at 90°C for 1 minute before increasing to 140°C at 25°C/minute, to 200°C at 5°C/minute and finally to 300°C at 10°C/minute. Electron ionization mass spectra were recorded by continuous quadrupole scanning at 70 eV ionisation energy.

Protein analyses were performed by electrospray mass spectrometry (ES-MS) using a Quattro-Micro triple quadrupole mass spectrometer (Waters, Micromass, UK) as described in [14].

Results

Expression of the recombinant proteins

CHO-K1 cells were stably transfected either with plasmid pBOShApoAIgS, carrying the cDNA encoding wild-type ApoA-I, or with plasmid pBOSApoAI(L174S), carrying the cDNA encoding the amyloidogenic variant ApoA-I(L174S). Both recombinant proteins carried at their N-terminus the

ApoA-I signal peptide sequence. By growing the cells under antibiotic selection, single, stably transfected clones were isolated; for each recombinant protein a single clone was selected for analyses. After 72 hours cell growth, the conditioned medium was analyzed by western blotting with anti-human ApoA-I polyclonal antibodies. For both wild-type ApoA-I and AApoA-I(L174S) transfectants an immunopositive species with a molecular mass corresponding to that of ApoA-I was observed in the cell-conditioned medium (Figure 1A and 1B, lane 12).

To analyze the kinetics of expression and secretion of the recombinant proteins, time-course experiments were performed. Cells were grown in complete DMEM-F12 medium for 24 hours, then grown in serum-free medium (HyQSFMCHO) for up to 72 hours. After 24, 48 and 72 hours growth, cell lysates were prepared and analyzed by western blotting using anti-ApoA-I antibodies. Definite amounts of pure ApoA-I (from 25 to 200 ng) were analyzed by western blotting (Figure 1A and 1B, lane 1–4) to generate a reference plot correlating immunopositive signals to protein amount. As shown in Figure 1A and 1B (lanes 6–8), an immunopositive species corresponding to ApoA-I molecular weight (MW) was detected in the intracellular

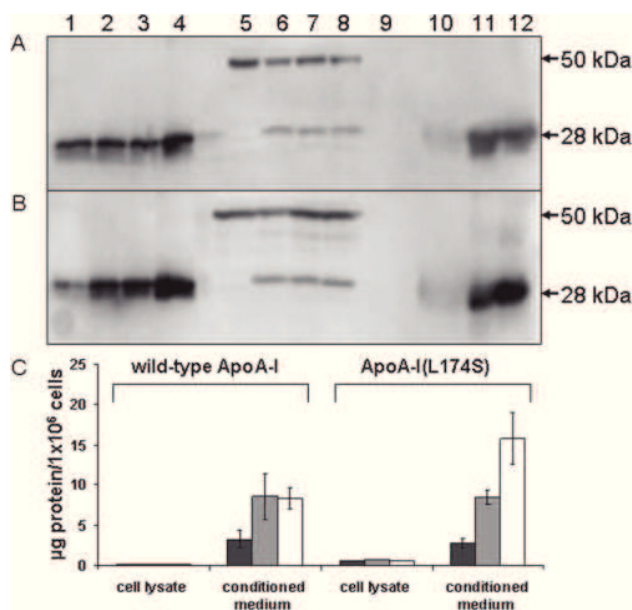


Figure 1. Analysis of intra- and extracellular levels of recombinant ApoA-I and AApoA-I(L174S) variant in CHO-K1 cells. A) Western blot analysis with anti-ApoA-I antibodies of wild-type ApoA-I. Lanes 1–4, increasing amounts of standard ApoA-I (25, 50, 100, 200 ng); lane 5, lysate of untransfected cells; lanes 6–8, lysates of stably transfected cells at 24, 48, 72 hours, respectively; lane 9, cell-conditioned medium of untransfected cells; lanes 10–12, cell-conditioned medium of transfected cells at 24, 48, 72 hours, respectively. The upper bands in lanes 5–8 refer to endogenous actin used as an internal standard. B) Western blot analysis with anti-ApoA-I antibodies of AApoA-I(L174S) variant. Samples as in A. C) Quantitative analysis of intra- and extracellular recombinant protein levels as a function of time (24 hours, black bars; 48 hours, grey bars; 72 hours, white bars). Protein amounts are expressed as μ g of protein/ 1×10^6 cells. The data represent the means \pm standard deviation of protein amounts determined in three independent experiments.

fraction of both transfected clones. Endogenous actin, measured with an anti-actin antibody, was used as an internal standard (lanes 5–8). No significant differences in protein amount during the time course were detected by densitometric analyses (Figure 1C). No immunopositive bands were detected in untransfected cells (Figure 1A and B, lane 5), indicating that no endogenous ApoA-I is expressed in CHO-K1 cells.

We then analyzed the cell-conditioned medium of CHO-K1 cells stably expressing wild-type ApoA-I (Figure 1A, lanes 10–12) and AApoA-I(L174S) variant (Figure 1B, lanes 10–12). Densitometric analyses (Figure 1C) indicated that the maximum level of extracellular wild-type ApoA-I was reached at 48 hours, with no significant differences at 72 hours. Instead, in the case of AApoA-I(L174S) the amount of the secreted protein at 72 hours was found to be higher than at 48 hours (Figure 1C). The overall data indicate that both proteins are efficiently secreted, although following different kinetics. We estimated that about 5.4 mg/l of wild-type ApoA-I and 4.5 mg/l of the amyloidogenic variant were secreted in 72 hours in the culture medium.

A comparison of the intra and extracellular amount of the recombinant proteins indicated that at any time of cell growth both proteins are mostly secreted by CHO-K1 cells. The intracellular amount of wild-type ApoA-I does not change significantly overtime, representing about 2%–3% of the total amount (inside plus outside). In the case of AApoA-I(L174S),

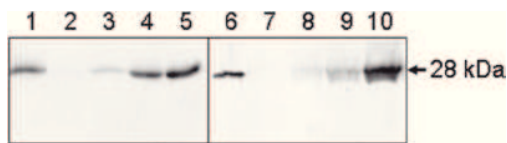


Figure 2. Western blot analysis of recombinant ApoA-I and AApoA-I(L174S) levels in the conditioned medium of CHO-K1 cells. Lanes 1 and 6, standard ApoA-I (25 ng); lanes 2 and 7, cell-conditioned medium of untransfected cells; lanes 3–5, cell-conditioned medium of cells stably expressing wild-type ApoA-I at 24, 48, 72 hours, respectively; lanes 8–10, cell-conditioned medium of cells stably expressing AApoA-I(L174S) at 24, 48, 72 hours, respectively.

instead, the intracellular fraction at 24, 48 and 72 hours represents about 17%, 8% and 4% of the total recombinant protein, respectively, according to the observation that protein secretion increases overtime.

Isolation of the recombinant proteins

In the procedure described above, cells were grown in a complete medium for 24 hours and then in serum-free medium. Nevertheless, in these conditions we noticed that traces of serum proteins contaminated the recombinant products, even after extensive cell wash to remove serum (data not shown). Therefore, to isolate the recombinant proteins, cells were plated in serum-free HyQSFMCHO medium and grown in the same medium (serum-free procedure). To evaluate protein expression levels, aliquots of cell-conditioned medium corresponding to 20 000 cells were withdrawn at 24, 48, 72 hours and analyzed by western blotting. As shown in Figure 2, both wild-type ApoA-I and L174S variant were found to be expressed and secreted by the cells, with the maximum expression level reached at 72 hours (lanes 3–5 and 6–8, respectively). We estimated that about 1.4 mg/l of each protein were secreted in 72 hours, a value lower than those obtained in the presence of serum.

To isolate the recombinant proteins, 72×10^6 cells expressing either the wild-type protein or the variant were grown in serum-free medium (360 ml). After 72 hours, the conditioned medium was centrifuged and loaded on a Butyl-S chromatographic column, upon addition of 0.8 M NaCl (final concentration). The eluted fractions were stained by coomassie blue (Figure 3A and C) and analyzed by western blotting with anti-ApoA-I antibodies (Figure 3B and D). The results indicated that a protein species, whose migration corresponds to that of ApoA-I, was present in both samples and found to be recognized by anti-ApoA-I specific antibodies (Figure 3B and D). The variant L174S was estimated to be more than 90% pure, whereas an additional protein species was observed in wild-type ApoA-I sample (Figure 3A). About 0.7 mg of variant AApoA-I(L174S) (~50% yield) and 0.3 mg of wild-type ApoA-I (~20% yield) were obtained from 1 l of cell-conditioned medium.

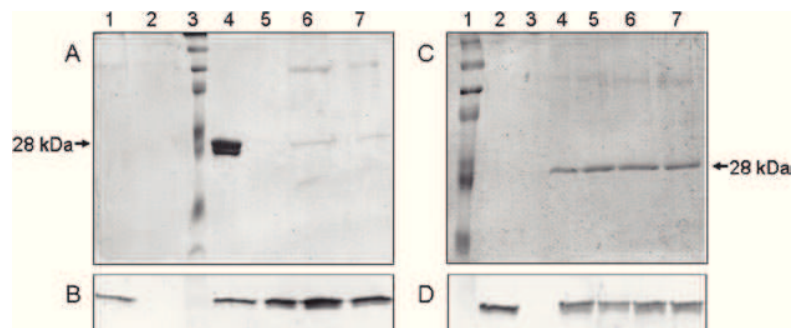


Figure 3. Analysis by sodium dodecyl sulfate polyacrylamide gel electrophoresis of wild-type ApoA-I and AApoA-I(L174S) after hydrophobic interaction chromatography. A) Coomassie staining of wild-type ApoA-I. Lane 1, cell-conditioned medium after 72 hours cell growth; lane 2, unbound protein species; lane 3, pre-stained markers; lane 4, standard ApoA-I (2 μ g); lanes 5–7, eluted fractions (2 μ g). B) Western blot analysis of wild-type ApoA-I. Samples as in A. C) Coomassie staining of AApoA-I(L174S). Lane 1, pre-stained markers; lane 2, cell-conditioned medium after 72 hours cell growth; lane 3, unbound protein species; lane 4, standard ApoA-I (2 μ g); lanes 5–7, eluted fractions (2 μ g). D) Western blot analysis of AApoA-I(L174S). Samples as in C.

The recombinant proteins were analyzed by ES-MS. The analysis of wild-type ApoA-I showed the occurrence of an equal amount of two protein components, whose molecular masses corresponded to the wild-type mature protein (MW 28091.8 ± 6.0 Da) and its unprocessed form containing the *pro*-peptide (MW 28969.6 ± 4.8 Da). Similarly, the molecular masses of the amyloidogenic variant of ApoA-I were 28938.5 ± 2.6 Da and 28055.4 ± 2.7 Da for the unprocessed and mature form, respectively. The latter values confirmed the presence of substitution of leucine for serine in the amyloidogenic variant.

Analysis of lipid content

Since ApoA-I has high affinity for lipid molecules, we analyzed the presence of lipids in the isolated recombinant protein samples. By GC-MS analysis, the lipid content of wild-type ApoA-I and amyloidogenic variant AApoA-I(L174S) was evaluated. Following liquid-liquid extraction of the lipid fraction, the mixture of lipids was modified to trimethylsilyl derivatives and directly analyzed by GC-MS.

Gas chromatograms obtained by monitoring the total ion current related to lipids as a function of time are shown Figure 4. Either for the wild-type protein (Figure 4A) and for its variant (Figure 4B), the presence of several analytes was revealed. All the analyses were performed as triplicates. Similarly, we identified the analytes present in control samples (not shown), represented by an unconditioned medium, as well as a conditioned medium from untransfected cells, both after hydrophobic chromatography. All the compounds were identified on the basis of the electron impact fragmentation spectra (not shown). Upon subtraction of species present also in the controls, a list of compounds specifically related to each recombinant protein was obtained (Figure 4C). Interestingly, for both recombinant proteins four species were found to be present, identified as: oleic acid (*cis*-9-octadecanoic acid, 18:1), stearic acid (octadecanoic acid, 18:0), *cis*-11-octadecanoic acid (18:1), tetradecanoic acid (14:0), with stearic acid as the most abundant.

To exclude that the identified lipids were selected by the hydrophobic chromatography through unspecific interactions with the resin, alternative procedures to isolate the recombinant proteins were used, such as immunoaffinity chromatography and reverse phase chromatography. The proteins isolated following these procedures were analyzed as described above. No differences in the lipid composition were detected with respect to those reported above (not shown). Similar results were obtained when samples eluted from the hydrophobic chromatography were extensively dialyzed (not shown).

As shown in Figure 4C, significant differences were appreciated in the relative amount of fatty acids in the mutant and the wild-type protein. A semiquantitative analysis revealed different lipid-to-protein molar ratios for the two proteins, with higher values associated with the variant protein with respect to the wild-type. Interestingly, the lipid-to-protein molar ratios calculated for the amyloidogenic variant were

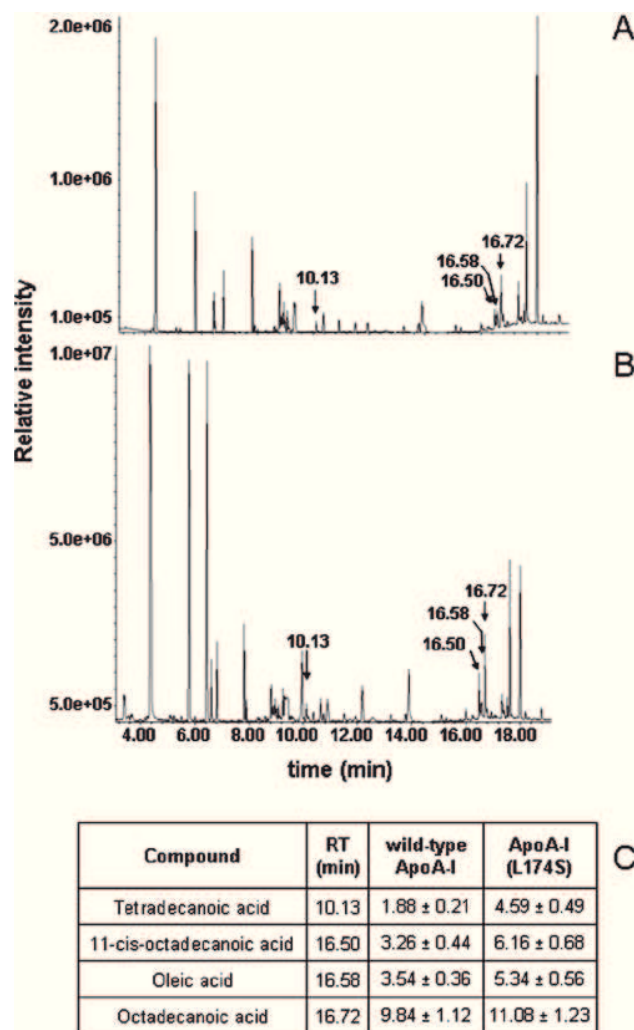


Figure 4. Gas chromatograms obtained by monitoring the total ion current as a function of time for wild-type ApoA-I (A) and AApoA-I(L174S) variant (B). The retention times of the four species associated with the recombinant proteins, indicated by an arrow, are reported. (C) Semi-quantitative data of the identified lipids are reported as lipid to protein molar ratio. The data represent the means \pm standard deviation of lipid to protein molar ratios determined in three independent experiments.

significantly higher (1.5- to 2.5-fold) than those determined for wild-type ApoA-I (Figure 4C). Only in case of stearic acid, the values calculated for the two proteins were comparable.

Discussion

ApoA-I amyloidogenic variant L174S, as well as the wild-type protein, were expressed in stably transfected CHO-K1 cells. Both recombinant proteins were found to be efficiently secreted in the culture medium, but with different kinetics. These observations are not in line with those reported by Marchesi et al. [20], who found that ApoA-I variants L75P and L174S were preferentially retained in the cell compartment of transiently transfected monkey kidney cells (COS-7), whereas

most of wild-type ApoA-I was secreted. These discrepancies may rely on the different experimental approaches used, as we performed a kinetic analysis of the intra and extracellular distribution of ApoA-I and its variant produced by stably transfected cell clones, whereas Marchesi et al. [20] analyzed protein distribution at a fixed time interval (48 hours) in transiently transfected cells.

We isolated the wild-type protein and its variant from the cell medium following a one-step purification procedure. Mass spectrometry analyses indicated that about 50% of both recombinant proteins were correctly processed in their mature form upon removal of the *pro*-peptide. We also defined the lipid content of the recombinant proteins and demonstrated that in both cases two saturated and two monounsaturated fatty acids were associated with the proteins. Interestingly, a higher lipid-to-protein molar ratio was observed for the amyloidogenic variant. As lipid binding proteins, ApoA-I and its amyloidogenic variants are expected to interact with a variety of lipids, although to our knowledge no evidence of ApoA-I interaction with fatty acids has been provided so far. It is known that long-chain saturated, monounsaturated and polyunsaturated fatty acids have a role in a number of cellular processes. A saturated fatty acid-rich diet has been associated with an increased incidence of CAD, whereas high intake of monounsaturated fatty acids was related to a protective effect [21,22]. Depending on fatty acids chain length and on degree of saturation, the cellular uptake of fatty acids was found to have marked effects on triacylglycerol and phospholipid trafficking in cultured enterocytes [23] and on trafficking and secretion of ApoA-I and B [24]. Oleic acid was found to be the fatty acid that most efficiently stimulated triacylglycerol synthesis and secretion, while in the presence of stearic acid phospholipids synthesis is efficiently induced [23].

Conclusions

The isolation of amyloidogenic forms of ApoA-I from patients is impracticable, as both the wild-type and variant proteins are expressed. Therefore, heterologous expression systems are needed. Nevertheless, with the exception of variant G26R, produced in bacterial cells [18], no reports are available to date on the production and isolation of ApoA-I amyloidogenic variants. Here, a recombinant form of the amyloidogenic variant L174S of ApoA-I, responsible for amyloid deposition preferentially in the heart of patients, was expressed in stably transfected mammalian cells and isolated. The recombinant ApoA-I amyloidogenic variant, as well as the wild-type protein, was found to be associated with fatty acids, for which a role in trafficking and secretion may be hypothesized.

Declaration of interest: This work was partially supported by Ministero della Istruzione, Università e Ricerca (MIUR), Italy, with PRIN 2009. The authors report no conflicts of interest. The authors alone are responsible for the content and writing of the article.

References

1. Obici L, Franceschini G, Calabresi L, Giorgetti S, Stoppini M, Merlini G, Bellotti V. Structure, function and amyloidogenic propensity of apolipoprotein A-I. *Amyloid* 2006;13:191–205.
2. Brunzell JD, Sniderman AD, Albers JJ, Kwiterovich PO Jr. Apoproteins B and A-I and coronary artery disease in humans. *Arteriosclerosis* 1984;4:79–83.
3. Rye KA, Barter PJ. Formation and metabolism of pre-beta-migrating, lipid-poor apolipoprotein A-I. *Arterioscler Thromb Vasc Biol* 2004;24:421–428.
4. Brouillette CG, Anantharamaiah GM, Engler JA, Borhani DW. Structural models of human apolipoprotein A-I: a critical analysis and review. *Biochim Biophys Acta* 2001;1531:4–46.
5. Duong PT, Weibel GL, Lund-Katz S, Rothblat GH, Phillips MC. Characterization and properties of pre beta-HDL particles formed by ABCA1-mediated cellular lipid efflux to apoA-I. *J Lipid Res* 2008;49:1006–1014.
6. Borhani DW, Rogers DP, Engler JA, Brouillette CG. Crystal structure of truncated human apolipoprotein A-I suggests a lipid-bound conformation. *Proc Natl Acad Sci U S A* 1997;94:12291–12296.
7. Silva RA, Hilliard GM, Fang J, Macha S, Davidson WS. A three-dimensional molecular model of lipid-free apolipoprotein A-I determined by cross-linking/mass spectrometry and sequence threading. *Biochemistry* 2005;44:2759–2769.
8. Mei X, Atkinson D. Crystal structure of C-terminal truncated apolipoprotein A-I reveals the assembly of high density lipoprotein (HDL) by dimerization. *J Biol Chem* 2011;286:38570–38582.
9. Obici L, Bellotti V, Mangione P, Stoppini M, Arbustini E, Verga L, Zorzoli I, et al. The new apolipoprotein A-I variant leu(174)-> Ser causes hereditary cardiac amyloidosis, and the amyloid fibrils are constituted by the 93-residue N-terminal polypeptide. *Am J Pathol* 1999;155:695–702.
10. Eriksson M, Schönland S, Yumlu S, Hegenbart U, von Hutten H, Gioeva Z, Lohse P, et al. Hereditary apolipoprotein AI-associated amyloidosis in surgical pathology specimens: identification of three novel mutations in the APOA1 gene. *J Mol Diagn* 2009;11:257–262.
11. Di Gaetano S, Guglielmi F, Arciello A, Mangione P, Monti M, Pagnozzi D, Raimondi S, et al. Recombinant amyloidogenic domain of ApoA-I: analysis of its fibrillogenetic potential. *Biochem Biophys Res Commun* 2006;351:223–228.
12. Monti DM, Guglielmi F, Monti M, Cozzolino F, Torrassa S, Relini A, Pucci P, et al. Effects of a lipid environment on the fibrillogenetic pathway of the N-terminal polypeptide of human apolipoprotein A-I, responsible for *in vivo* amyloid fibril formation. *Eur Biophys J* 2010;39:1289–1299.
13. Arciello A, De Marco N, Del Giudice R, Guglielmi F, Pucci P, Relini A, Monti DM, Piccoli R. Insights into the fate of the N-terminal amyloidogenic polypeptide of ApoA-I in cultured target cells. *J Cell Mol Med* 2011;15:2652–2663.
14. Raimondi S, Guglielmi F, Giorgetti S, Di Gaetano S, Arciello A, Monti DM, Relini A, et al. Effects of the known pathogenic mutations on the aggregation pathway of the amyloidogenic peptide of apolipoprotein A-I. *J Mol Biol* 2011;407:465–476.
15. Schmidt HH, Haas RE, Remaley A, Genschel J, Strassburg CP, Büttner C, Manns MP. *In vivo* kinetics as a sensitive method for testing physiologically intact human recombinant apolipoprotein A-I: comparison of three different expression systems. *Clin Chim Acta* 1997;268:41–60.
16. Mallory JB, Kushner PJ, Protter AA, Cofer CL, Appleby VL, Lau K, Schilling JW, Vigne JL. Expression and characterization of human apolipoprotein A-I in Chinese hamster ovary cells. *J Biol Chem* 1987;262:4241–4247.
17. Ryan RO, Forte TM, Oda MN. Optimized bacterial expression of human apolipoprotein A-I. *Protein Expr Purif* 2003;27:98–103.
18. Lagerstedt JO, Cavigiolio G, Roberts LM, Hong HS, Jin LW, Fitzgerald PG, Oda MN, Voss JC. Mapping the structural transition in an amyloidogenic apolipoprotein A-I. *Biochemistry* 2007;46:9693–9699.
19. Pastore L, Belalcazar LM, Oka K, Cela R, Lee B, Chan L, Beaudet AL. Helper-dependent adenoviral vector-mediated long-term expression of human apolipoprotein A-I reduces atherosclerosis in apo E-deficient mice. *Gene* 2004;327:153–160.
20. Marchesi M, Parolini C, Valetti C, Mangione P, Obici L, Giorgetti S, Raimondi S, et al. The intracellular quality control system down-regulates the secretion of amyloidogenic apolipoprotein A-I variants: a possible impact on the natural history of the disease. *Biochim Biophys Acta* 2011;1812:87–93.

21. Pérez-Jiménez F, Castro P, López-Miranda J, Paz-Rojas E, Blanco A, López-Segura F, Velasco F, et al. Circulating levels of endothelial function are modulated by dietary monounsaturated fat. *Atherosclerosis* 1999;145:351–358.
22. Nordøy A, Goodnight SH. Dietary lipids and thrombosis. Relationships to atherosclerosis. *Arteriosclerosis* 1990;10:149–163.
23. Yao Y, Eshun JK, Lu S, Berschneider HM, Black DD. Regulation of triacylglycerol and phospholipid trafficking by fatty acids in newborn swine enterocytes. *Am J Physiol Gastrointest Liver Physiol* 2002;282:G817–G824.
24. Wang H, Berschneider HM, Du J, Black DD. Apolipoprotein secretion and lipid synthesis: regulation by fatty acids in newborn swine intestinal epithelial cells. *Am J Physiol* 1997;272:G935–G942.